8-2012

THE NEW ROLE OF PROPROTEIN CONVERTASE SUBTILISIN/KEXIN TYPE 9: A CONNECTION OF PROPROTEIN CONVERTASE SUBTILISIN/KEXIN TYPE 9, APOLIPOPROTEIN B, and AUTOPHAGY

Hua Sun

THE NEW ROLE OF PROPROTEIN CONVERTASE SUBTILISIN/KEXIN TYPE 9: A CONNECTION OF PROPROTEIN CONVERTASE SUBTILISIN/KEXIN TYPE 9, APOLIPOPROTEIN B, and AUTOPHAGY

By

Hua Sun

APPROVED:

Ba-Bie Teng, Ph.D.

Supervisory Professor

Diane Bick, Ph.D.

Bingliang Fang, Ph.D.

Barrett Harvey, Ph.D.

Mikhail Kolonin, Ph.D.

APPROVED:

Dean, The University of Texas

Graduate School of Biomedical Sciences at Houston

THE NEW ROLE OF PROPROTEIN CONVERTASE SUBTILISIN/KEXIN TYPE 9: A CONNECTION OF PROPROTEIN CONVERTASE SUBTILISIN/KEXIN TYPE 9, APOLIPOPROTEIN B, and AUTOPHAGY

A

DISSERTATION

Presented to the Faculty of

The University of Texas

Health Science Center at Houston

and

The University of Texas

MD Anderson Cancer Center

Graduate School of Biomedical Sciences

in Partial Fulfillment

of the Requirements

for the Degree of

DOCTOR OF PHILOSOPHY

By

Hua Sun

Houston, Texas

August, 2012

ACKNOWLEDGEMENTS

I would like to thank the following people: my advisor, Dr. Ba-Bie Teng, for her extraordinary guidance over the past few years and for providing me the opportunity to study in her laboratory; the members of my advisory, examining and supervisory committees, Drs. Diane Bick, Bingliang Fang, Barrett Harvey, Mikhail Kolonin, Frank Marini and Rajagopal Ramesh for their valuable scientific input to my research project; Dr. C. Thomas Caskey, former director of Brown Foundation Institute of Molecular Medicine, for his support to my Ph.D. research over the past three years; Dr. Jagannadha Sastry, the director of the virology and gene therapy program of GSBS, for his support and supervising in the past 5 years; all my colleagues from Dr. Teng's group for their help with my research project; my colleagues from collaboration lab, Drs. Chuantao Jiang and Rowen Chang, for their great help and invaluable advice. Last, but certainly not least, I want to take this opportunity to give special thanks to my wife, Min Zhong, my son, Shining Sun, my mother, Mrs. Qiuyun Hua, and my father, Mr. Youshou Sun, for their inspiration and moral support.

The New Role of Proprotein Convertase Subtilisin/Kexin Type 9:

A Connection of Proprotein Convertase Subtilisin/Kexin Type 9,

Apolipprotein B, and Autophagy

Publication No.

Hua Sun

Supervisory Professor: Ba-Bie Teng, Ph.D.

Plasma low-density lipoprotein (LDL) levels are positively correlated with the incidence of coronary artery disease. In the circulation, the plasma LDL clearance is mainly achieved by the uptake via LDL receptor (LDLR). Proprotein convertase subtilisin/kexin type 9 (*PCSK9*) is a newly discovered gene, playing an important role in LDL metabolism. Gain-of-function mutations of *PCSK9* lead to hypercholesterolemia and loss-of-function mutations of *PCSK9* are associated with decrease of LDL cholesterol. The effects of PCSK9 on cholesterol levels are the consequence of a strong interaction between the catalytic domain of PCSK9 and epidermal growth factor-like repeat A (EGF-A) domain of LDLR on the cell surface of hepatocytes. This PCSK9/LDLR complex enters the cell via endocytosis, where both PCSK9 and LDLR are removed via the lysosome pathway, resulting in decreased levels of LDLR and accumulation of LDL in the plasma. However, whether this is the exclusive function of PCSK9 on LDL metabolism was challenged by us; we observed PCSK9 interacted with apolipoprotein B (apoB) and increased apoB production, irrespective of the LDLR.

ApoB is the primary structure protein of LDL particle and it also serves as the ligand for the LDL receptor. There is ample evidence showing that the levels of apoB are a better indicator for heart disease than either total cholesterol or LDL cholesterol levels. We used a second-generation adenoviral vector to overexpress PCSK9 (Ad-PCSK9) in wild-type C57BL/6 and LDLR deficient

mice (*Ldlr-/-* and *Ldlr-/-Apobec1-/-).* Our study revealed that overexpression of PCSK9 promoted the production and secretion of apoB in the form of very-low density lipoprotein (VLDL), which is the precursor of LDL, in the 3 mouse models studied (*C57BL/6J, Ldlr-/-, and Ldlr-/-Apobec1-/-).* The increased apoB production in mice was regulated at post-transcriptional levels, since there was no difference in apoB mRNA levels between mice treated with Ad-PCSK9 and control vector Ad-Null. By using pulse-chase experiment on primary hepatocytes, we showed that overexpression of PCSK9 increased the secretion of apoB, independent of LDLR.

In the circulation, we showed that PCSK9 was associated with LDL particles. By using 3 different protein–protein interaction assays of co-immunoprecipitation, mammalian two-hybrid system, and *in situ* proximity ligation assay, we demonstrated a direct protein–protein interaction between PCSK9 and apoB. The impact of this interaction inhibited the physiological removal process of apoB via autophagosome/lysosome pathway in an LDLR-independent fashion, resulting in increased production and secretion of apoB-containing lipoproteins. The significance of this process was shown in the *Pcsk9* knockout mice in the background of *Ldlr-/-Apobec1-/-* mice (triple knockout mice); in the absence of Pcsk9 (triple knockout mice) the levels of cholesterol, triacylglycerol, and apoB decreased significantly in comparison to that of *Ldlr-/-Apobec1-/-* mice. Taken together, our study demonstrated a direct intracellular interaction of PCSK9 with apoB, resulting in the inhibition of apoB degradation via the autophagosome/lysosome pathway independent of LDLR. This discovery provides a new concept of the importance of PCSK9 and suggests new approaches for the therapeutic intervention of hyperlipidemia.

TABLE OF CONTENTS

Results

LIST OF FIGURES

LIST OF TABLES

LIST OF ABBREVIATIONS

ApoA-I …….……apolipoprotein A-I

ApoB…….……...apolipoprotein B

Apobec1…….....apoB mRNA-editing enzyme catalytic polypeptide 1

ApoE……apolipoprotein E

CHD ……..coronary artery disease

DMEM…….....Dulbecco's Modified Eagle Medium

EARD……..…..……Endoplasmic reticulum (ER)-associated protein degradation

EBSS……..…Earle's Balanced Salts

ELISA……..Enzyme-linked immunosorbent assay

FAS……..……fatty acid synthase

FPLC……..……..…..fast protein liquid chromotograph

GADPH..…….. ……..... Glyceraldehyde 3-phosphate dehydrogenase

HBSS..……...……...……... …….……...Hank's Buffered Salt Solution

HMGCR……..3-hydroxy-3-methyl-glutaryl-CoA reductase

HNF1……..hepatocyte nuclear factor 1

HRP……..……...horseradish peroxidase

LDL……Low density lipoprotein

LDLR……...Low density lipoprotein receptor

mTOR……..mammalian target of rapamycin

PCSK9…….....Proprotein convertase subtilisin/kexin type 9

PERPP……..…post ER pre-secretory proteolysis

PI3K……..phosphoinositide 3 kinase

PLA……..……..…….……..….proximity ligation assays

qPCR…….....…quantitative polymerase chain reaction

RIPA……..radioimmunoprecipitation assay

SCD1…….stearoyl-CoA desaturase-1

SDS-PAGE……..……..……Sodium dodecyl sulfate polyacrylamide gel electrophoresis

SEAP…….…..……..secreted alkaline phosphatase

SREBP……..……....Sterol Regulatory Element-Binding Protein

TAG ……...……..……triacylglycerol

VLDL ……...……..……Very Low density lipoprotein

INTRODUCTION

1. PCSK9, a new target for cholesterol lowering drug

1.1 PCSK9 and its genetic variants

Proprotein convertase subtilisin/kexin type 9 (PCSK9) was initially discovered as a gene whose expression was up-regulated in the neural tissues. It belongs to the proteinase K subfamily of the subtilisin family (2). *PCSK9* gene is located on human chromosome 1p34.1−p32, and is recognized as the third major locus for autosomal dominant hypercholesterolemia (ADH) (3). The LDL receptor (LDLR) and apolipoprotein B (apoB) genes are the other 2 loci for ADH.

In 2003, Abifadel et al. studied 2 French families with the characteristics of ADH, who have no detectable mutations in *LDLR* or *apoB* genes. They were identified to carry the dominant point mutations (S127R and F216L) in *PCSK9* (4, 5). Later on, many other mutations on *PCSK9* were discovered. Most of these mutations are classified into 2 major functional categories: "gain-of-function mutations," which are associated with elevated level of LDL cholesterol and "loss-of-function mutations," which lead to lower level of LDL cholesterol (6) (Figure I-1). Some of these mutations have been intensively investigated. For example, a gain-of-function D374Y variant, which was found in Utah, Norway, and England cohorts, shows an increased affinity to LDLR (5, 7-9). On the other hand, loss-of-function variants of Y142L and C679X, which have high frequencies in African Americans, lead to very low cholesterol levels (10-13). So far more than 40 *PCSK9* gene mutations have been reported to be associated with either a gain or loss of function on PCSK9 activity (increase or decrease cholesterol levels) (14). These mutations are located through the 5′ UTR region to the C-terminal domain of the gene. It would be a challenge to characterize the structure/function of each variant on LDL cholesterol levels.

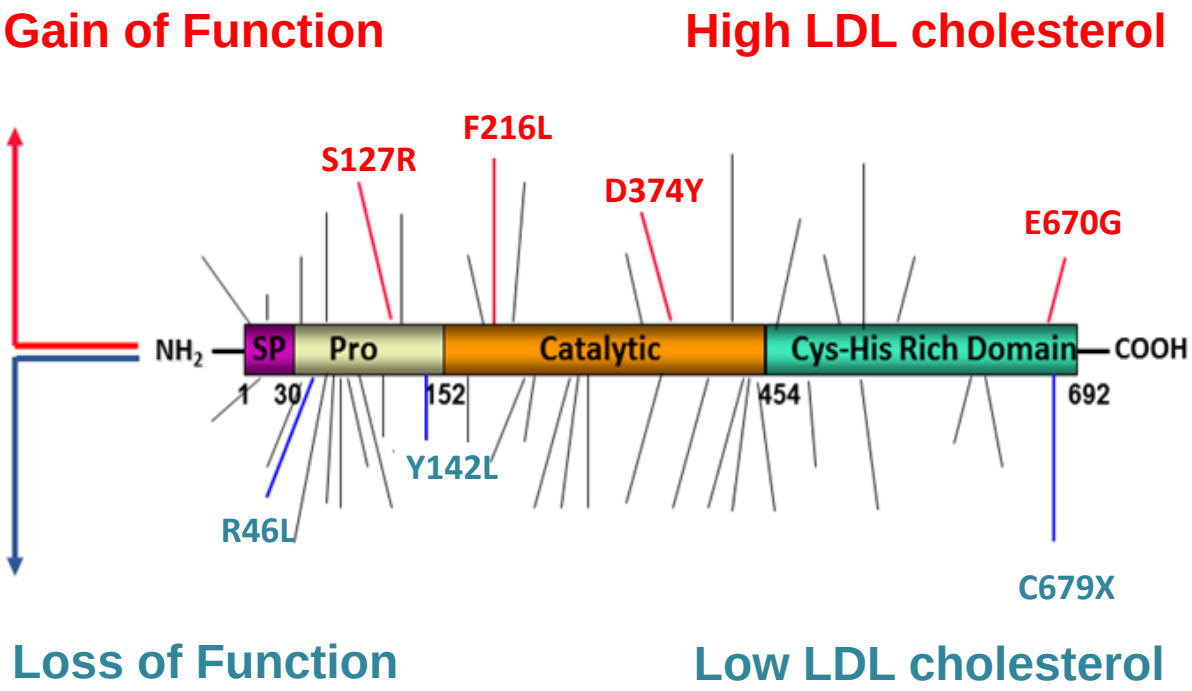

Figure I-1. Gain- and loss-of-function mutations of *PCSK9*.

Since 2003, more than 100 mutations of *PCSK9* have been reported. Gain-of-function mutations lead to high LDL cholesterol levels in plasma, which increases the risk of developing coronary heart diseases. On the other hand, loss-of-function mutations of *PCSK9* decrease plasma LDL cholesterol levels and prevent coronary heart disease. The graph is adapted from Seidah (1) with permission.

1.2. The action of PCSK9 on lipid metabolism

Over-expression of PCSK9 in mice either by adenoviral vector (15) or using transgenic method (16) resulted in significant reduction of hepatic LDLR protein and, in turn, increase of plasma LDL cholesterol levels. Similar effects were observed when mice were infused with purified PCSK9 protein (17, 18). By contrast, *Pcsk9-/-* mice have approximately 3-fold more hepatic LDLR levels than that of wild-type C57BL/6 mice and a 5-fold increase in LDL clearance (19). These findings have led to intense investigations of PCSK9 in the regulation of LDL cholesterol levels, and PCSK9 has emerged as promising therapeutic target for the treatment of hypercholesterolemia.

PCSK9, a 692-amino acid glycoprotein, is synthesized in the liver as a ~74 kDa enzyme precursor (zymogen) that undergoes autocatalytic processing, and thereby a pro-domain (14 kDa) is cleaved at the N-terminus at residue 152 (20). The pro-domain attaches noncovalently to the mature peptide that is secreted and then enters the circulation. The formation of this complex abrogates the catalytic activity of PCSK9, and so far no other substrates have been found except PCSK9 itself (21). Once in the circulation, this PCSK9 complex binds to the LDLR extracellular epidermal growth factor homology domain (EGF-A) on the hepatocyte surface (22, 23). The LDLR/PCSK9 complex is internalized via clathrin-coated pits and goes through endosome to lysosome for degradation. The binding affinity of PCSK9/LDLR in the endosome is very high, which prevents the dissociation of the complex and promotes the degradation of LDLR via lysosome (24), resulting in reduced numbers of the LDLR and hence, increased the plasma LDL-cholesterol levels (22, 25, 26) (Figure I-2). Studies demonstrated that gain-of-function mutation of PCSK9-D374Y, in which PCSK9 attains 50-fold higher affinity to LDLR and thus promotes LDLR degradation than that of the wild-type PCSK9 (5, 27). The pro-domain gain-of-function mutation of PCSK9-S127R interacts with the β-propeller of LDLR via van der Waals force, which also demonstrates a high affinity binding of PCSK9-S127R to LDLR (6). Moreover, the interaction of PCSK9 with LDLR in the endoplasmic reticulum compartment has also been reported (28).

The crystal structure of the interaction of PCSK9 catalytic domain and the EGF-A domain of LDLR has been reported (9, 29, 30). PCSK9 binds in a calcium-dependent manner to the first EGF-A of the EGF-A domain of the LDLR (23). The catalytic domain is the only part of PCSK9 molecule contacts with EGF-A of LDLR; the key residues of PCSK9 that interact with the EGF-A domain are Arg-194 and Asp-238. The residues of 367–381 form the surface for interaction. This region contains the Asp-374, which the gain-of-function mutation (D374Y) was reported in patients. The interface between PCSK9 and LDLR forms a hydrophobic surface and Phe-379 of PCSK9 is the center of it. Residues 153–155 on the N-terminus of the catalytic domain of PCSK9 also contribute to the interaction (29).

The integrity of LDLR EGF-A domain is very important for the maintenance of the receptor function. Several natural mutations in the EGF-precursor homology domain of LDLR that hinder receptor recycling are present in patients with FH (23, 24). The EGF-A and EGF-B tandem pair form an extended rod-like conformation stabilized by calcium binding and inter-domain hydrophobic packing interactions (25, 26). The interaction of EGF-A with the ligand-binding module R7 in LDLR confers a rigid conformation on this region of the LDLR across a wide pH range (27). This rigidity has been proposed to facilitate the acid-dependent closed conformation of the LDLR (28). The binding of PCSK9 towards EGF-A domain may disrupt the interaction between R7 and EGF-A domain, and leads to a reduced acid-dependent ligand release. It may finally promote the delivery of LDLR to the lysosome or prevent LDLR interaction with other proteins, which is required for LDLR recycling to the cell surface (23).

The structure of PCSK9 in complex with the LDLR EGF-A domain defines the potential therapeutic target sites for blocking agents that could interfere with this interaction *in vivo*, thereby increasing LDLR function and reducing plasma LDL-C levels.

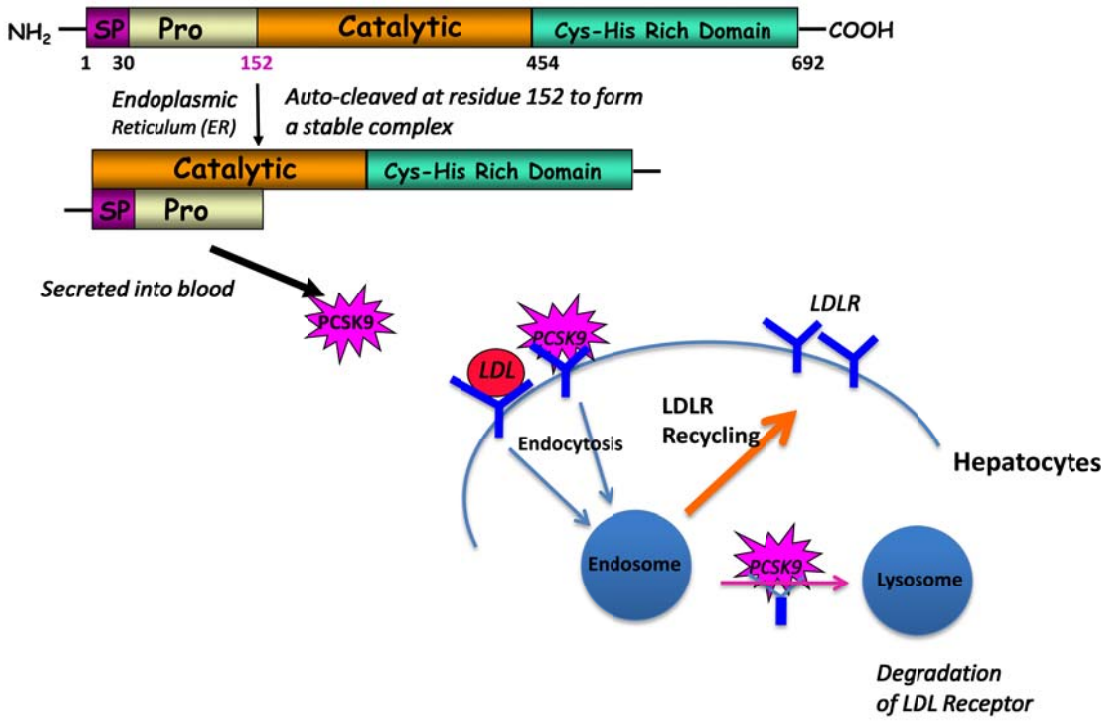

Figure I-2. The action of PCSK9.

PCSK9 undergoes auto-cleavage and is secreted as a mature complex. Circulatory PCSK9 binds to the LDLR on the hepatocytes' surface and leads it to degradation in the lysosome. The catalytic activity of PCSK9 is not required for the LDLR degradation.

1.3 The regulation and pharmacological modulation of PCSK9

PCSK9 is mainly synthesized in the liver, small intestine, and kidney (2, 15, 20). Like the LDLR, the levels of intracellular sterols regulate hepatic PCSK9 production; when the levels of cholesterol increase, the PCSK9 production decreases (31).

Both *PCSK9* gene expression and the PCSK9 levels in the circulation are affected by LDLR and enzymes in cholesterol biosynthesis such as HMG CoA synthase, HMG CoA reductase, or other factors that play roles in intracellular cholesterol homeostasis (32, 33). The regulation of PCSK9 by sterols is achieved by the increased binding of the sterol responsive element binding protein 2 (SREBP-2), a key transcriptional factor, to the sterol responsive element (SRE) in the promoter region of PCSK9 gene. This regulation is demonstrated when depleting the intracellular cholesterol pool, resulting in promoting the translocation of SREBP-2 from ER to nuclei to activate PCSK9 transcription (34, 35). *PCSK9* gene expression is also suppressed by glucagon, berberine, bile acids, or fasting (36, 37). All these regulations indicate the clinical significance of PCSK9, as it is recognized as an important cholesterol regulator.

SREBP regulates the transcription of PCSK9, LDLR, and enzymes involved in cholesterol and fatty acid biosynthesis pathways. SREBP belongs to the basic helix-loop-helix leucine zipper class of transcription factors. When cells have low levels of sterols, SREBP is cleaved and releases a water-soluble N-terminal domain, which translocates to the nucleus. This cleaved SREBP N-terminal domain then binds to the specific SRE sequences and up-regulates the enzymes involved in sterol biosynthesis. Increased sterol levels, in turn, inhibit the cleavage of SREBP, and therefore decrease the synthesis of sterol through this negative feedback loop.

Mammalian genomes have 2 separate *SREBP* genes (*SREBP1* and *SREBP2*). SREBP-1 produces 2 different isoforms, SREBP-1a and -1c. SREBP-1c is responsible for regulating genes for *de novo* lipogenesis. SREBP-2 regulates the genes of cholesterol biosynthesis. Thus, SREBPs are the main regulators for lipid metabolism.

Statin binds to HMG-CoA reductase, to inhibit the cholesterol biosynthesis. This inhibition decreases the levels of cholesterol, which activates the release of cleaved active form of SREBP-2. SREBP-2 activates the gene expressions of both LDLR and PCSK9. It is possible a balance between LDLR and PCSK9 governs whether statin is function beneficial for decreasing cholesterol levels. It has been shown that statin has no effect on patients with PCSK9-D374Y mutation (38). Patients with loss-of-function PCSK9 mutation of R46L, G106R, or R237W had increased LDLR and responded well to statin therapy (39). Thus a combination of statin with PCSK9 inhibitor therapy may be beneficial for a defined group of patients. The relationships of other cholesterol lowering drugs such as fenofibrates, bile acid binding resins, or ezetimibe with PCSK9 are not clear. With more clinical data become available on the PCSK9 levels in the patients treated with various cholesterol lowering drugs, the potential role of PCSK9 inhibitor acts as a synergistic medication would become very promising.

1.4 The therapeutic strategies to knockdown PCSK9 levels

Evidence demonstrates that *Pcsk9* knockout mice are viable with very low cholesterol levels (16, 19). Individuals carrying loss-of-function mutations of PCSK9 have low LDL-cholesterol and live a normal life (12, 19, 39, 40). Moreover, an epidemiological study of Atherosclerosis Risk in Communities (ARIC) shows many loss-of-function mutations in PCSK9 are associated with low coronary artery disease (decreased 88%) (10). Thus, therapeutics aiming to decrease PCSK9 levels is warranted.

There are several strategies that have been developed to regulate PCSK9 function. The most straightforward one is by using monoclonal antibodies to block the interaction between PCSK9 and LDLR in the circulation. Currently monoclonal antibodies produced from both Amgen and Regeneron are in Phase I clinical trials (41). These antibodies blocked the interaction of PCSK9 with LDLR, resulting to a significant reduction in LDL cholesterol levels for 3 days after antibody administration and the effect lasted for 7–10 days (42).

Mice treated with antisense oligonucleotides targeted at PCSK9 decreased triglyceride and cholesterol levels significantly (reduction of 65% and 53%, respectively) (43). Recently, a PCSK9 lipidoid nanoparticle (LNA) antisense oligonucleotide was shown to reduce the PCSK9 mRNA and serum PCSK9 protein by 85% and 55%, respectively, which resulted in a 50% reduction of circulating LDL cholesterol in nonhuman primates (44). PCSK9-specific siRNA almost completely eliminated the production of hepatic and plasma PCSK9 at day 3 after one treatment in nonhuman primates (45). Taken together, all these strategies shed some light on potential therapeutic application of PCSK9 in the treatment of hyperlipidemia.

2. Apolipoprotein B and Lipoproteins metabolism

2.1 VLDL, LDL, and HDL, their roles in atherosclerosis development

Lipoprotein particles are a group of protein and lipid assembled together serving as hydrophobic lipids transporter. According to their density and size, lipoprotein particles are generally classified as chylomicron, very low-density lipoprotein (VLDL), intermediate density- lipoprotein (IDL), low density-lipoprotein (LDL), and high density-lipoprotein (HDL). Triglyceride and cholesteryl ester are in the center core of lipoprotein particles, which are surrounded by a monolayer of phospholipids, unesterified cholesterol, and apolipoproteins. Each class of lipoprotein contains a different kind of apolipoproteins including apolipoprotein B (apoB), apoE, apoAI, apoAII, apoCI, apoCII, apoCIII, and apoD. VLDL, LDL, and HDL have been shown as important cardiovascular diseases (CVD) risk factors and many interventions have been developed to alter the levels of lipoprotein for the prevention and treatment of CVD (Figure I-3).

The metabolism of lipoprotein is very complicated. It begins from the absorption of fats in the small intestine. Enterocytes package the fats with apoB as chylomicron, and secrete to the circulation. Chylomicrons undergo lipolysis to become chylomicron remnants, which are taken up by the liver via chylomicron receptor. In the liver, VLDL is assembled and secreted to the circulation as apoB-containing triglyceride-rich lipoprotein particles. VLDL undergoes lipolysis to become IDL and LDL; there is a precursor-product relationship. The process of VLDL to LDL, which takes 2 to 10 h, is fast. LDL is cholesterol ester enrich lipoprotein particles. It has a normal half-life of 3 days before they are removed from plasma via LDLRs on the surface of hepatocytes. The internalized LDLs are degraded in the lysosomes, and the liberated cholesterol enters the cellular cholesterol pool. The LDL receptor recycles back to the cell membrane, and the number of LDLRs on the hepatocytes' surface determine the removing rate of plasma LDL (46).

HDL is the smallest and densest lipoprotein particles in the circulation. It is secreted from the liver as a nascent HDL disc containing apoAI and apoAII and phospholipids. HDLs are protective lipoprotein particles of cardiovascular diseases (although their protective role is

questioned recently). The major biological function of HDL is reverse cholesterol transport, a very important biological process in mammalians to remove excess cholesterol from periphery tissues, including the artery wall, back to the liver. Many enzymes and molecules participate in this process. ATP-binding cassette transporter A1 (ABCA1) initiates the process by mediating the efflux of cholesterol and phospholipids across extra- and intracellular membranes (47). Some other transporters, such as ATP-binding cassette sub-family G member 1 (ABCG1) and phospholipids transport protein (PLTP) are also involved in this lipid loading process (48, 49). In this process, the protein dominant nascent HDL particles gradually transform into larger, spherical HDL by being loaded with cholesterol and phospholipids. The free cholesterol is then converted by lecithin-cholesterol acyltransferase (LCAT) to cholesteryl ester, which is sequestered into the core of lipoprotein (50).

In the circulation, VLDL and LDL transfer triglyceride to HDL, in exchange for the CE via a transfer protein named cholesteryl ester transfer protein (CETP), also called plasma lipid transfer protein (51). CETP is positively associated with atherosclerosis. Recently, a small molecular agent named Torcetrapib has been designed to inhibit the activity of CETP; however, even though Torcetrapib treatment increases HDL levels by 60%, the cardiovascular endpoints were not achieved but had early death in patients (52). This study was terminated prematurely. New CETP inhibitors such as Dalceltrapid and Anacetrapid are continuously being investigated for long-term effects on coronary artery diseases development (53).

Atherosclerosis is a chronic inflammatory response to the accumulated lipids such as LDL in the artery wall. Although the main cause of atherosclerosis still remains unknown, high levels of LDL particles in the circulation is the most important and necessary initial event of atherosclerosis. In the intima of the artery wall, the LDLs are oxidized to ox-LDLs, which recruits macrophages and T lymphocytes to initiate immune responses. Macrophages uptake the ox-LDLs and convert into foam cells and eventually the atherosclerotic plagues.

Generally, in atherogenesis, VLDL and LDL are considered as the culprits of the disease while the HDL is considered as the protective factor. Most of the interventions are focused on achieving a low LDL cholesterol level, and a higher HDL level. Statins are the most successful class of drugs to lower LDL cholesterol. The main mechanism of action of statin is blocking cholesterol synthesis by competitively inhibiting HMG-CoA reductase. By doing so, lowered liver-cell cholesterol levels stimulate SREBP-2 transcriptional factor to translocate into nuclei and activate the transcription of LDLR, which uptake LDL from circulation (54, 55). Although statins have side effects such as rhabdomyolysis, their effects on lowering LDL-cholesterol are far better than other classes of lipid lowering drugs such as fibrates, or niacin, or bile acid sequestrants, or ezetimibe (56). Other drugs such as niacin and fibrates can increase HDL cholesterol levels. However, statins have little effect on HDL cholesterol levels.

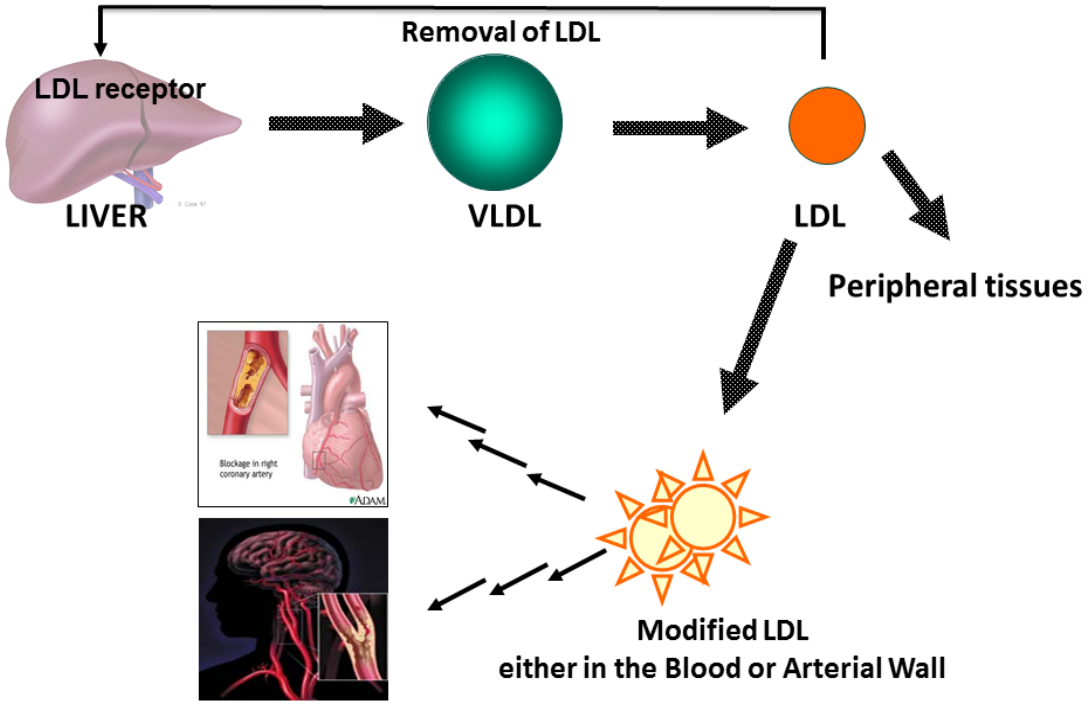

Figure I-3. The biosynthesis of LDL and its effects on atherosclerosis.

Liver produces VLDLs to deliver lipids for peripheral utilization. VLDLs gradually lose triglycerides in the peripheral tissues such as adipose and muscle, exchange their protein and lipid contents with other lipoproteins, and finally become cholesterol ester enriched particles; LDLs. The physiological function of LDL is to transport cholesterol to peripheral tissues, however, modified LDLs such as oxidized LDLs deposit in the arterial wall and initiate atherosclerosis. LDLs in the blood can also be removed via the LDLR on the surface of hepatocytes. The expression of the LDLR on the hepatocytes is critical for the regulation of LDL cholesterol levels in the circulation.

2.2. Apolipoprotein B, the structure protein of chylomicron, VLDL, and LDL

Apolipoprotein B (ApoB) is the major structural protein of chylomicron, VLDL, and LDL particles in vertebrates. In plasma, the clearance of LDL depends on the interaction of apoB with the LDLR in a ligand and receptor binding fashion (57) (Figure I-4A). Thus, apoB plays an essential role in apoB-containing lipoprotein homeostasis.

The human APOB gene (43 kb) resides on chromosome 2p and is expressed mainly in the hepatocytes and enterocytes (58). The apoB mRNA is translated into a full-length apoB-100 consisting of 4,536 amino acids in the liver. A truncated form of apoB, known as apoB-48, represents the N-terminal 48% of apoB-100 and is produced in the intestine by an RNA editing mechanism (59). The editing enzyme is known as the apoB mRNA-editing enzyme catalytic polypeptide 1 (Apobec1), which converts a C to a U to generate an in-frame stop codon (60) (Figure I-4B). In humans, apoB-100 is the obligatory structural protein for the assembly and secretion of hepatic VLDL. In rodents, the liver synthesizes and secretes both apoB-100 and apoB-48 containing VLDL, whereas mice that lack Apobec1 gene (*Apobec1-/-*), secrete only apoB-100 containing lipoproteins (61-63).

The plasma LDL cholesterol (LDL-C) level has been used as the primary risk factor of coronary heart diseases (CHD) for a long time. However, emerging findings suggest that other indicators such as non-HDL-C or apoB are much more accurate markers than LDL cholesterol levels, especially for patients with elevated triglycerides or with an LDL-C <100 mg/dL (64-66). ApoB has been reported by many studies to be strongly associated with CHD risk compared with other conventional measures (67-70). Furthermore, the ratio of apoB to apoAI is suggested to be a better predictor for disease risk than LDL cholesterol alone (71). Thus, apoB is a potential therapeutic target for the treatment of CHD.

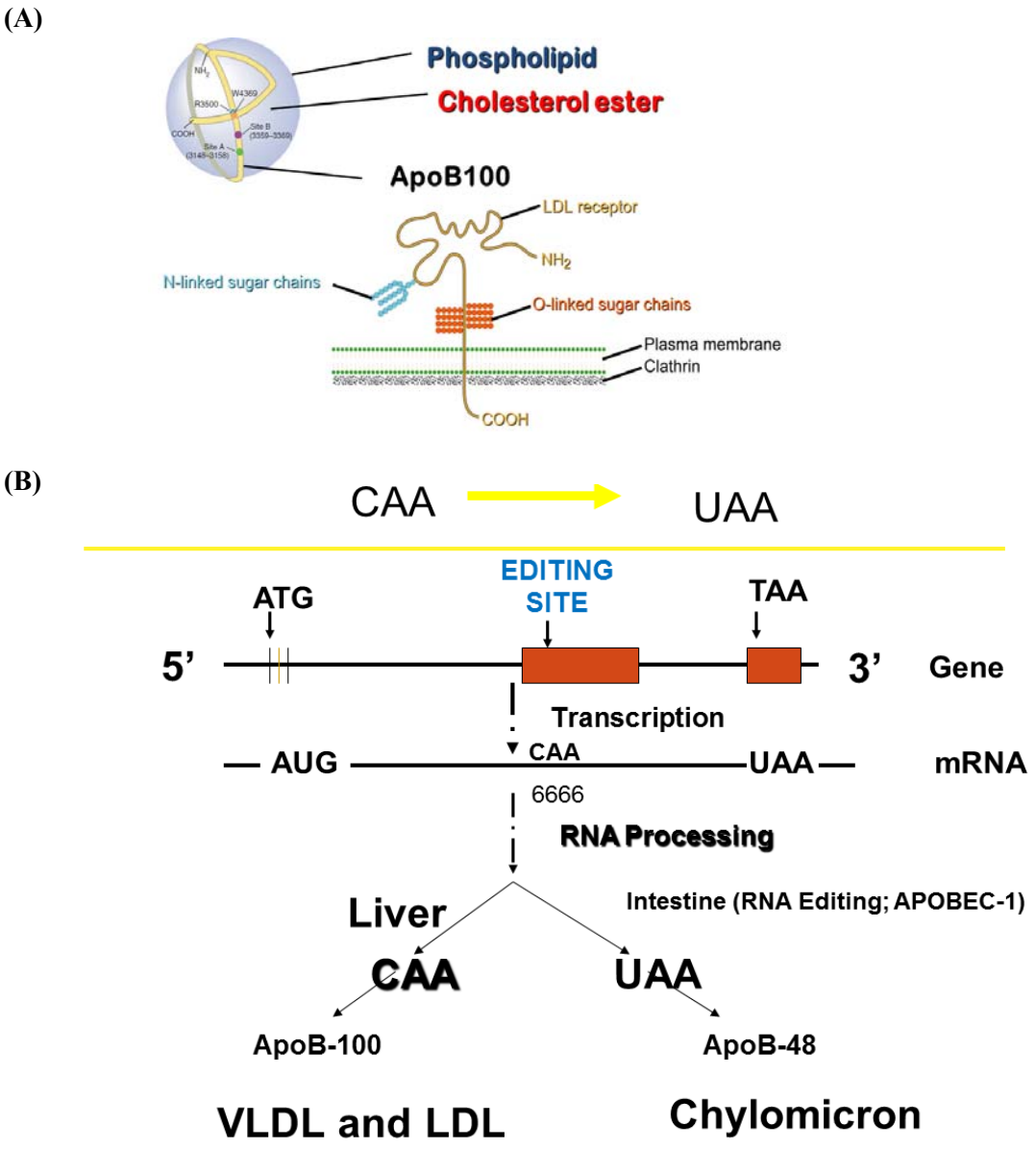

Figure I-4. ApoB structure and its mRNA editing.

(A) The organization of apoB100 on the low-density lipoprotein particle. ApoB100 (yellow band) spans the entire circumference of the LDL particle, which has phospholipid surface and cholesterol ester core. Sites A and B are the binding sites for its receptor: LDL receptor. (B) The mRNA editing of apoB. In the small intestine of all mammals, apobec-1 converts apoB mRNA cytidine-6666 to uridine, and forms a UAA stop codon. As a result, a truncated protein consisting of the N-terminal 48% of apoB is produced, namely apoB48. In rodents apobec1 is also expressed in liver, resulting in significant hepatic production of apoB48-containing lipoproteins.

2.3 The regulation of apoB and its degradation process

The apoB mRNA contains 28 exons and 29 introns. ApoB mRNA is constitutively expressed, and it is regulated at post-transcriptional level. The regulation of apoB translation is mainly through the mRNA sequence in the 5′UTR and the 3′UTR. The GC rich region in 5'UTR and AU rich region in 3′UTR change the stability of apoB mRNA and therefore affect apoB translation. Generally, the 5′UTR increases the translation of apoB while 3'UTR decreases the translation of apoB (72, 73). Insulin has been reported as a negative regulatory factor for apoB production. It may interact with a 64nt region of 5′UTR and attenuate apoB translation. A 110- kDa insulin sensitive factor binds to 5'UTR of apoB mRNA mediates apoB translation (74).

Microsomal triglyceride transfer protein (MTP) also plays a very important role in the regulation of apoB production. Individuals with a mutation of *Mtp* gene, which leads to dysfunction of MTP, have no apoB in the plasma (75). MTP is associated with N-terminal β-barrel and α-helix regions of apoB (76, 77). The role of MTP in VLDL production is unclear; MTP assists lipids and lipidated apoB in crossing the ER membrane and promote VLDL production and secretion (78). In the abscence of MTP, nascent apoB will be degraded.

The secretion of ApoB as VLDL is mainly regulated at post-transcriptional levels (79, 80). ApoB mRNAs are constitutively translated to apoB protein; however, most of the apoB are destined to degradation. There are 3 major ways for apoB degradation. The first one is that newly synthesized apoB can be internalized by LDLR or heparin sulfate proteoglycans when it arrives at cell surface. The second way is an ubiquitin-proteasome system that recycles all the apoB that failed to be lipidated as described above. Several protein chaperons, such as heat shock protein (HSP) 70, HSP 90, Hsp110, p97, and BiP participated in this process (81-88). The third one is called post-ER, pre-secretory proteolytic process (PERPP). This process has been suggested as an autophagic process (89).

In eukaryotes, autophagy is an evolutionarily conserved process to get rid of misfolded or long half-life proteins, or damaged organelles, or intracellular microorganism. Autophagy can

provide nutrients and energy by recycling extracellular materials when cells are exposed to various stresses. The autophagy process can be described as cytoplasmic cargo sequestered inside double-membrane vesicles to deliver materials to the lysosome for degradation.

In human Huh7 cell, lipid droplets associated with apoB100 molecules are detected in autophagosomes (90, 91). In McArdle RH-7777 (McA-RH7777) cell line, the apoB100 was also detected in autophagosomes, and increased apoB degradation was observed when the cells were treated with glucosamine to induce ER-stress. This degradation could be blocked by an inhibitor of autophagy: 3-methyl adenine (3-MA) (92). Thus, the autophagy process may represent an important regulatory pathway for apoB. We predicted that the reduction of autophagy degradation of apoB would accompany increased VLDL production. Further understating of the apoB degradation pathways may lead to the novel therapeutic strategies to lower VLDL production and reduce the risk of atherosclerosis.

3. The effect of PCSK9 on apoB production

Although it is well established that PCSK9 negatively regulates LDLR expression, whether or not PCSK9 has an impact on apoB production remains controversial and poorly understood. McA-RH7777 cells expressing the D374Y mutant of PCSK9 secrete an increased amount of apoB than that expressing either the wild-type PCSK9 or a non-functional mutant, S386A (5). An increased rate of apoB production was also observed in patients with the S127R mutation in PCSK9 (10). Overexpression of the wild-type PCSK9 or the S127R mutant in C57BL/6 and *Ldlr-/-* mice for 3 days, however, did not result in significant increase in apoB synthesis or production (11). Similar insignificant changes of plasma apoB levels were also observed in *C57BL/6* and *Ldlr-/-* mice over-expressing PCSK9 for 5 days (12). However, when the study was extended to 6 days after adenovirus injection, significant increased plasma cholesterol, triacylglycerol (TAG), and apoB were observed in *C57BL/6* mice, while overexpression of PCSK9 still had no effect on the *Ldlr-/-* mice (13). On the other hand, another group reported that overexpression of PCSK9 in *Ldlr-/-* mice for 7 days resulted in an approximately 2-fold increase in LDL-cholesterol and apoB (14). The apparent discrepancies among these experiments did not provide conclusive evidence for a causative effect of PCSK9 expression on apoB and apoB-containing lipoproteins. However, the increased apoB production in *Ldlr-/-* mice overexpressing PCSK9 (14) does suggest an LDLR-independent mechanism by which PCSK9 expression exerts an impact on apoB production. Thus, it is important to investigate whether PCSK9 plays a role in apoB production in a LDLR independent fashion. This was the central theme of this thesis.

STATEMENT OF OBJECTIVES

PCSK9 is a newly discovered protease mainly secreted by the liver. In the circulation, PCSK9 binds to LDLR on the surface of hepatocytes and leads to its degradation. Gain-of-function mutations in PCSK9 result in high plasma LDL cholesterol levels, whereas loss-of-function mutations cause increased numbers of LDL-receptor and are associated with reduced serum cholesterol (11). It is clear that the physiological function of PCSK9 is involved in LDL-receptor regulation. Mutations such as C679X that lead to no-functional PCSK9 in the body, not only reduce plasma cholesterol, but also are associated with a marked reduction in the incidence of coronary heart disease (10). All these findings have made PCSK9 an attractive target for cholesterol-lowering therapy for hypercholesterolemia. However, its role in lipid metabolism, especially in apoB, the most important lipoprotein in VLDL and LDL particles, remains controversial.

The purpose of the current study was to investigate the effects of PCSK9 on apoB and the mechanism by which PCSK9 regulates apoB and apoB-containing lipoproteins. This investigation will bring forth a better understanding of the physiological function of PCSK9 and its role in lipid metabolism. We hypothesized that overexpression of PCSK9 would lead to an increased plasma apoB containing lipoprotein levels as well as an increased apoB synthesis rate, irrespective of the presence of LDLR. It is anticipated that the proposed studies will result in understanding the relationship of PCSK9 and apoB and provide new insights to the mechanism of how PCSK9 regulates apoB. The study will provide evidence for the development of new cholesterol lowering therapeutic interventions.

The specific aims of this project are:

Specific Aim 1. **To elucidate the effect of PCSK9 expression on lipoprotein and apoB metabolism**.

We used a second-generation adenoviral vector to achieve a long-term (30 days) expression of PCSK9 in mice with or without the LDLR, including *C57BL/6J*, LDLR deficient mice of *Ldlr-/-*, and *LDb* (*Ldlr-/-Apobec1-/-*) mice. The second-generation adenoviral vector provides long-term gene expression with low toxicity, which is critical to the study on the effects of the overexpression on lipoprotein metabolism.

Specific Aim 2. **To delineate whether PCSK9 would interact with apoB.**

Wild-type PCSK9 and its gain-of-function mutations increase apoB containing lipoprotein secretion (27, 93). We hypothesized that PCSK9 would interact with apoB, resulting in overproduction of apoB. We used *in vitro* and *in vivo* assays to demonstrate the physical interaction of PCSK9 and apoB intracellularly.

Specific Aim 3. To investigate the impact of PCSK9 on apoB production.

ApoB is constitutively expressed in the hepatocytes. Most of the apoB is probably degraded via autophagosome/lysosomal pathway. We hypothesized that PCSK9 would regulate apoB production by altering the degradation pathway of apoB. We demonstrated the significant impact of the regulation of PCSK9 on apoB production in a LDLR independent fashion.

MATERIALS AND METHODS

1. Animal studies

C57BL/6, Pcsk9-/- and *Ldlr-/-* mice were purchased from Jackson Laboratory (Bar Harbor, ME). *LDb (Ldlr-/-Apobec1-/-*) mice were generated in Teng's laboratory as described previously (18-20). *Ldlr-/- Apobec1-/-Pcsk9-/-LDb* triple knockout mice were generated by crossing *Pcsk9-/-* with *LDb* mice, and confirmed genotype by PCR. The sequencing primers are:

Ldlr forward: 5′-ACC CCA AGA CGT GCT CCC AGG ATG A

Ldlr reverse: CGG AGT GCT CCT CAT CTG ACT TGT.

Apobec1 forward: 5′-TGA GTG AGT GGT GGT GGT AAA

Apobec1 reverse: CGA AAT TCC TCC AGC AGT AAC.

Pcsk9 forward: 5′-ATT GTT GGA GGG AGA AGT ACA GGG GT

Pcsk9 reverse: 5′-GGG CGA GCA TCA GCT CTT CAT AAT CT.

Neo forward: 5′-ATT GTT GGA GGG AGA AGT ACA GGG GT

Neo reverse: 5′-GAT TGGGAA GAC AAT AGC AGG CAT GC.

Mice were kept in a barrier facility with a 12:12 h dark–light cycle and maintained on a standard laboratory chow diet. All the animal experiments were conducted in accordance with the Guidelines of the Animal Protocol Review Committee of the University of Texas Health Science Center at Houston.

2. Cell lines used for this study

Stably expressing human apo-18,-48, and -100 McArdle RH-7777 (McA-RH7777) cell lines: These 3 stable cell lines were obtained from Dr. Zemin Yao's laboratory at University of Ottawa, Ottawa, Canada. These cells were maintained in Dulbecco's Modified Eagle's Medium (DMEM) supplemented with 10% fetal bovine serum, 100 Units/mL penicillin G sodium, 100 μg/mL streptomycin sulfate, and 200 μg/mL G418.

HepG2 cells (human hepatocellular carcinoma): The cells were cultured in MEM supplemented with 10% fetal bovine serum, 100 Units/mL penicillin G sodium, 100 µg/mL streptomycin sulfate, 1X non-essential amino acid, and 1X sodium pyruvate.

HepG2 cell line stably expressing Apobec1: This stable cell line expressing the rat Apobec1 was generated in Teng's laboratory. The cells were cultured in MEM supplemented with 10% fetal bovine serum, 100 Units/mL penicillin G sodium, 100 µg/mL streptomycin sulfate, 1X non-essential amino acid, 1X sodium pyruvate, and 200 µg/mL G418.

COS1 cells (African green monkey kidney fibroblast-like cell line): These cells were maintained in DMEM supplemented with 10% fetal bovine serum, 100 Units/mL penicillin G sodium, and 100 µg/mL streptomycin sulfates.

HEK293 cells (human embryonic kidney cell line): These cells were maintained in high glucose DMEM supplemented with 10% fetal bovine serum, 100 units/mL penicillin G sodium, and 100 µg/mL streptomycin sulfate.

E.C7 cells (HEK293 cell stably expressing adenoviral DNA polymerase, (94)) The cell line was obtained from Etubics Co. (Seattle, WA). These cells were maintained in DMEM supplemented with 10% fetal bovine serum, 100 units/mL penicillin G sodium, and 100 µ/mL streptomycin sulfate.

All cell lines were maintained at 37°C in a humidified incubator containing 5% CO_2.

3. Plasmid vectors constructed for this study:

pcDNA3-hPCSK9: Full-length human PCSK9 (NM_174936) with a FLAG tag in *Eco*RI and *Xho*I site of pcDNA3 vector were obtained from Dr. Jay D Horton at University of Texas Southwestern Medical Center.

pcDNA3-mPcsk9: Full-length mouse PCSK9 (NM_153565) with a FLAG tag were PCR amplified from pcDNA3-mPcsk9 (provided by Dr. Jan L Breslow from Rockefeller University) and cloned into *Eco*RI and *Xho*I site of pcDNA3 vector. The primer sequences are -Forward: 5′-CCA GTG TGC TGG AAT TCG CCA CCA TGG GCA CCC ACT GCT CTG CG, and Reverse: 5′-CCC CTC GAG

TCA CTC ACT TGT CAT CGT CGT CCT TGT AGT CCT GAA CCC AGG AGG CCT TTG CTG AAG G.

pcDNA3-LDLR-FLAG: Full-length mouse LDLR (NM_001252658) with a FLAG tag were amplified by PCR with primers − Forward: 5′-AGT GAA GCT TGA ATT CGC CAC CAT GGG GCC CTG GGG CTG GAA A and Reverse: 5′-CCC TCT AGA TCA CTC ACT TGT CAT CGT CGT CCT TGT AGT CCT GGA GCG CCA CGT CAT CCT CCA GAC TGA C−, and cloned into *Hind*III and *Xba*I site of pcDNA3 vector.

pVP-16-PCSK9: Full-length human PCSK9 cDNA was cloned into pVP-16 vector of *EcoR*I and *Xba*I sites, which generated a fusion protein of the VP-16 activation domain and PCSK9 as pVP16-PCSK9.

pM-apoB18: pCMV-apo18 was obtained from Dr. Zemin Yao's laboratory at University of Ottawa, Ottawa, Canada. We designed primers−forward: 5′-TAT GAA TCC ATG GAC CCG CCG AGG CCC and reverse: 5′-TAT GGA TCC CTA GAT CCC CTG CAG AGT−flanking the apoB-18 cDNA (NM_000384, nucleotides 129-2555) of pCMV-apoB-18 to amplify the apoB18 DNA. The amplified fragment was sequenced and cloned into *EcoR*I and *BamH*I sites of pM vector. This recombinant vector produced a fusion protein of GAL4-binding domain and apoB18 as pM-apoB-18.

pM-Apobec1: This vector was previously cloned by Teng's laboratory (95). The full-length rat Apobec1 (NM_001134391) was cloned into *EcoR*I and *BamH*I site of pM vector and generated a fusion protein of GAL4-binding domain and Apobec1.

pM-LDLR: Full length human LDLR (NM_001252658) were digested from pCMV-hLDLR (provided by Dr. Kazu Oka from Baylor College of Medicine) by *Ecl360*II (blunted) and *Xba*I sites, and subcloned into *Sma*I and *Xba*I site of pM vector and generated a fusion protein of GAL4-binding domain and LDLR.

All plasmid vectors were sequenced by commercial sequencing company from both directions and the sequences were confirmed with NCBI public sequences.

4. Cell transfection assay used in this study:

We used lipofectamine2000 (Invitrogen) to perform plasmid DNA transfection assay into cells. Briefly, cells were seeded onto a 12-well plate at 70–80% confluence in antibiotic-free media. The next day, 1 μg of each plasmid DNA was prepared in 200 ul serum free medium with 4 μg lipofectamine-2000. After 20 min incubation at room temperature, the mixture was added into each well, which had been changed with 1 mL fresh antibiotic-free medium. The cells were incubated with the plasmid DNA for 6 h at 37°C, 5% CO_2, followed by addition of 2 mL fresh complete media. At 48 h after transfection, the cells were lysed with 1X RIPA lysis buffer (Radioimmunoprecipitation assay buffer from Cell Signaling, Danvers, MA. It contains 20 mM Tris-HCl, pH 7.5, 150 mM NaCl, 1 mM Na_2EDTA, 1 mM EGTA, 1% NP-40, 1% Na-deoxycholate, 2.5 mM Na-pyrophosphate, 1 mM beta-glycerophosphate, 1 mM Na3VO4, 1 μg/mL leupeptin) and both cell lysates and media were collected for the analysis of protein expression.

5. Construction and Production of E1-, E2b-, E3-deleted second-generation adenovirus type 5 vector expressing hPCSK9

We chose to use the E1, E2b, and E3 genes deleted adenovirus vector to express PCSK9 for this study since this adenoviral vector has been shown to have low toxicity with long-term expression (94). The E1-, E2b-, E3-deleted adenovirus type 5-vector pAd-del-pol, adenoviral-CMV shuttle vector pD2007MCS, and E.C7 cell line were obtained from Etubics Corporation (Seattle, WA). The full-length hPCSK9 cDNA with a FLAG tag and a plasmid vector of pcDNA3-PCSK9-D374Y mutant were obtained from Dr. Jay D Horton, University of Texas Southwestern Medical Center (16).

Due to an original design defect that both the pD2007MCS shuttle vector and the pAd-del-pol adenoviral vector contain the same Amp resistance gene, which results in difficulties in the

cloning selection, we had to use the following modified strategy to construct the adenoviral vector. As shown in the flow chart of Figure M-1, we cloned the *PCSK9-FLAG* cDNA into *Hind*III/*Eco*RV sites of pAdEasy shuttle vector driven by CMV promoter (Invitrogen, CA). This pAd-Easy vector is Kanamycin resistant. This pAd-Easy-PCSK9-Kan shuttle vector was, then, co-transformed with pAd-del-pol-Amp vector into BJ5183 competent cells to generate the pAd-PCSK9-Kan (this is a 2nd generation adenoviral vector). However, the pAd-del-pol vector has an internal *Pac*I site, which prohibits us to use the *Pac*I site to linearize the pAd-PCSK9-Kan, so we had to do the second recombination to recombine the pAd-PCSK9-Kan with pD2007MCS-PCSK9 in BJ5183 competent cells to generate the pD2007MCS-PCSK9-Amp. This homologous recombination was selected by Amp. After 2 cloning (pD2007-CMV-PCSK9 and pAd-Easy-PCSK9) and 2 recombination procedures, we generated a pAd-D2007-CMV-PCSK9-Amp vector ready for the production of adenovirus.

We linearized the pAd-D2007-CMV-PCSK9-Amp vector with *Fse*I site and transfected this recombinant vector into E.C7 cells to produce the recombinant adenovirus (Ad-PCSK9). The crude virus was purified by using 2 rounds of $CsCl_2$ density gradient ultracentrifugation. Briefly, NVT65 centrifuging tubes were preloaded with 3 mL of 1.25 g/mL CsCl solution (top) and 3 mL 1.5 g/mL CsCl solution (bottom). The crude virus lysates (~5 mL) were loaded onto the top of 1.25 g/mL CsCl solution and subjected to ultracentrifuge at 35,000 rpm in NVT65 rotor for 3 h. We collected a high-density band by using a 21G needle between the layers of 1.25 g/mL CsCl solution and the 1.5 g/mL CsCl solution. The collected band was loaded onto 7 mL of 1.34 g/mL CsCl solution and ultracentrifuged again under the same conditions. Purified virus bands were dialyzed against 4 L of 0.01 M Tris pH 8.0 containing 1% glycerol overnight. We used qPCR to quantify the titer of Ad-PCSK9 virus (usually 10^{12}–10^{13} viral particles/mL). The primers and probe sequences targeting at CMV promoter for the qPCR are as follows:

Forward: 5′- ATA CGT CAT TAT TGA CGT CAA TG;

Reverse: 5′- CGT TAC ATA ACT TAC GGT AAA TG;

Probe: 5′- 6-FAM/CCT GGC TGA CCG CCC AAC GAC.

A control adenovirus, referred as Ad-Null, was constructed the same way without the cDNA insert. We also constructed and produced the adenoviral vector expressed mouse PCSK9, termed Ad-mPcsk9.

To confirm the expression of recombinant PCSK9 protein by Ad-mPcsk9 and Ad-hPCSK9, we infected the 293 cells with the adenoviral vectors (Ad-Null, Ad-mPcsk9, and Ad-hPCSK9). At 48 h after infection, cell lysates and cell media were collected, followed by SDS-7.5% PAGE gel electrophoresis. The proteins were transferred to PVDF membrane and hybridized with anti-Flag antibody (Sigma). We also transfected 293 cells with pcDNA3-PCSK9 vector, and the protein expressed by this transfection method was used as a PCSK9 marker. As shown in Figure M-2, both the pre (74kDa) and mature (63 kDa) forms of PCSK9 were expressed by Ad-mPcsk9 and Ad-PCSK9. Notice, most of the proteins expressed are mature PCSK9 in both cell lysates and cell media.

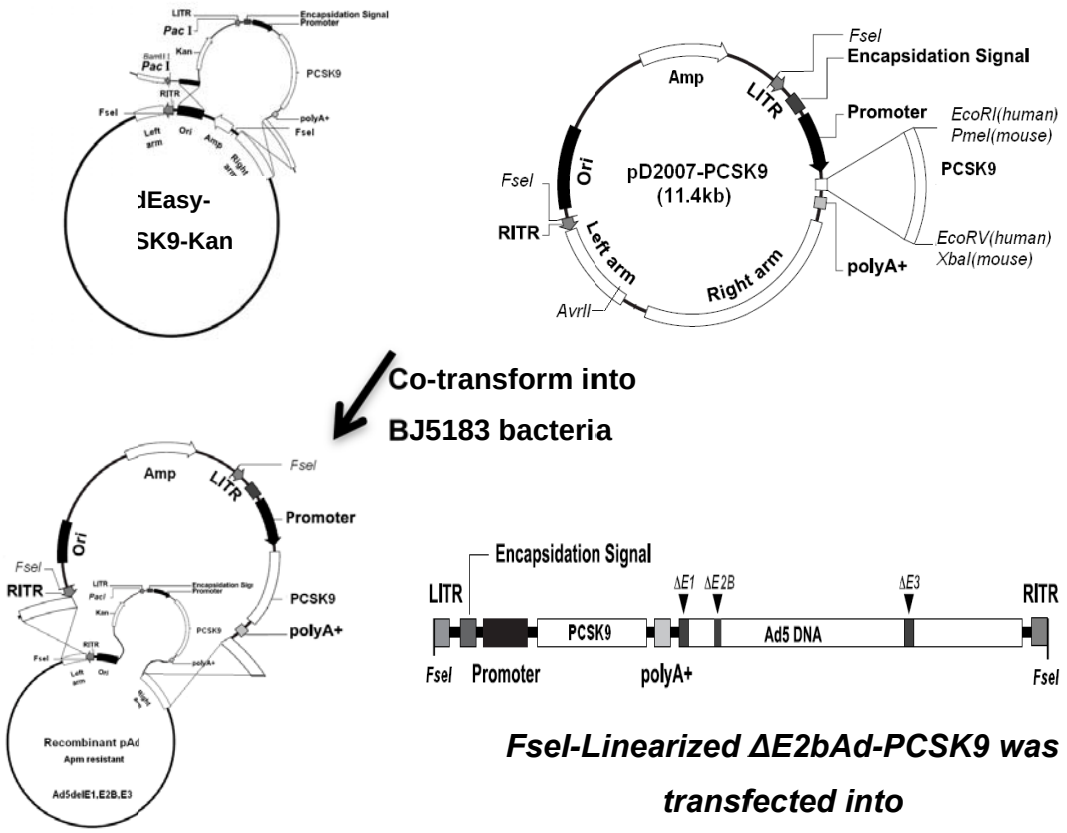

Figure M-1. Construction of E2b-Ad-PCSK9.

PCSK9-FLAG cDNA was cloned into *Hind*III/*Eco*RV sites of pAdEasy shuttle vector driven by CMV promoter. This pAd-Easy-PCSK9-Kan shuttle vector was then co-transformed with pAd-del-pol-Amp vector into BJ5183 competent cells to generate the pAd-PCSK9-Kan (this is a 2nd generation adenoviral vector). The second recombination was performed by recombining the pAd-PCSK9-Kan with pD2007MCS-PCSK9 in BJ5183 competent cells to generate the pD2007MCS-PCSK9-Amp. This homologous recombination was selected by Amp. After two recombination procedures, pAd-D2007-CMV-PCSK9-Amp vector was generated ready for the production of adenovirus. The vector was linearized with *Fse*I and transfected into E.C7 cells to produce the recombinant adenovirus (E2b-Ad-PCSK9).

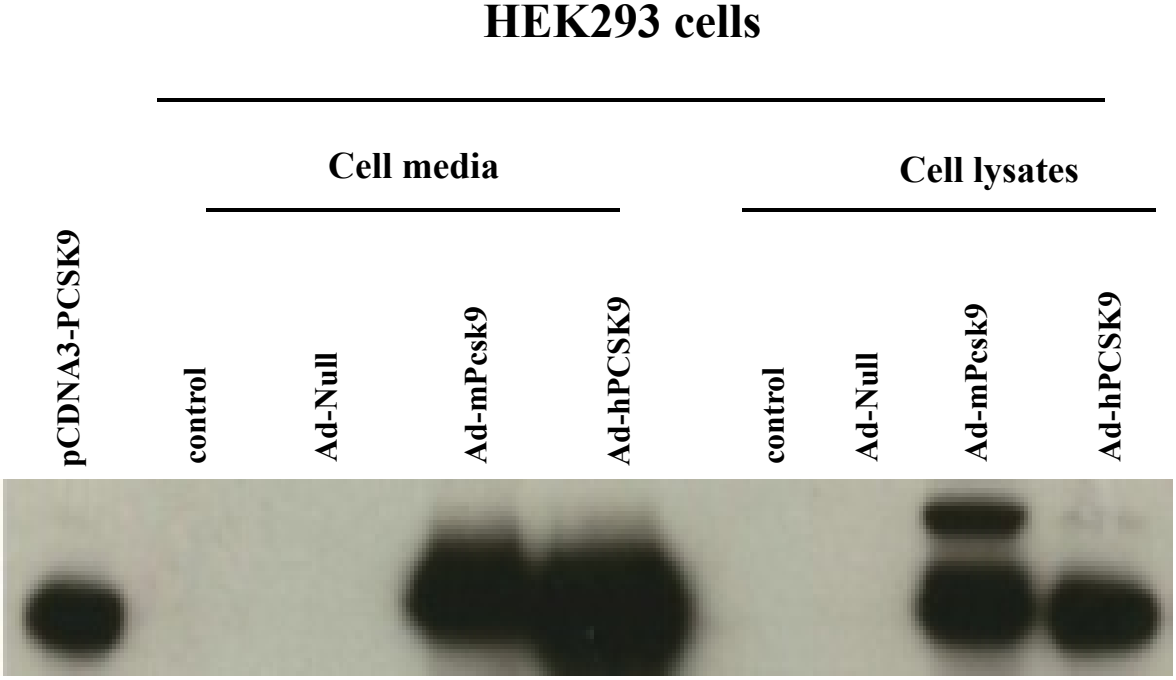

Figure M-2. Western blot analysis of PCSK9 in HEK-293 cells infected with Ad-PCSK9. The 293 cells were infected with Ad-PCSK9 or Ad-Null. Cell lysates and cell media were subjected to SDS/PAGE, followed by Western blot analysis using anti-FLAG antibody. The position of PCSK9 is marked. The upper bands are the pre-form of PCSK or Pcsk9, and the lower bands are the mature form of PCSK9 or Pcsk9.

6. Transduction of Ad-PCSK9 and Ad-Null into mice

Male *C57BL/6J, Ldlr-/-,* and *LDb* mice (n = 24 for each group) at 2 months of age were transduced with Ad-PCSK9 or Ad-Null virus (1×10^{10} viral particles/mouse) via tail vein injection. Fasting (~16 h) blood samples were collected prior to (day 0) and post adenovirus injection at days 7, 14, 21, and 30, respectively. We collected blood (250 μL) via retro-orbital plexus using heparin coated capillary tubes (Fisher Scientific) under general anesthesia with 1.25% Avertin. At the end of the indicated time, each animal was anesthetized, sacrificed, and perfused using 20 mL ice-cold PBS. The tissue samples were collected, snap frozen in liquid nitrogen, or embedded in OCT. The samples were stored at –80°C until analysis.

7. Separation of plasma lipoproteins by Fast Protein Liquid Chromatography

We used Fast Protein Liquid Chromatography (FPLC) with 2 continuous Superose 6 columns (GE, Piscataway, NJ) to separate lipoprotein particles from mouse plasma. In general, pooled mouse plasma (225 μ) was separated by FPLC into VLDL, LDL, and HDL particles. Fractions (0.5 mL each, total 40 fractions) were eluted using 150 mM NaCl, 1 mM EDTA, and 0.02% NaN_3 pH 8.2 (20, 42). Each fraction was analyzed for the levels of cholesterol, triglyceride, and apolipoproteins.

8. Measurement of lipids values in plasma and plasma lipoprotein fractions

Cholesterol and TAG concentrations in either plasma or each FPLC fraction were determined using the Cholesterol E and the L-Type Triglyceride M kits (Wako Chemicals, Richmond, VA), respectively.

9. Western blot analysis

Plasma and lipoprotein fractions from plasma:

Mouse plasma samples (3 μL from C57BL/6J, 1 μL from Ldlr-/- or LDb) or FPLC fractions (10 μL/fraction) were resolved by SDS-PAGE. We used 6% ProSieve-50 gel (FMC BioProducts, Rockland, ME) to separate apoB100 and apoB48 proteins. We used SDS-7.5%PAGE to separate PCSK9, and SDS-12.5%PAGE to separate apoE and apoA-I. The proteins were transferred onto PVDF membrane (Millipore). The antibodies used for the analysis of apolipoproteins are as follows:

Anti-mouse apoB (1:10,000 dilution, Abcam, Cambridge, MA) was used to detect mouse apoB-100 and apoB-48.

Monoclonal antibody 1D1 (Heart Institute, University of Ottawa, Ottawa, Canada) was used to detect human apoB.

Anti-mouse apoE (1:5,000 dilution) and ***anti-mouse apoA-I*** (1:10,000 dilution) were obtained from Dr. B Ishida, University of San Francisco to detect mouse apoE and mouse apoAI, respectively.

Anti-FLAG antibody (1:5,000 dilution, Sigma) was used to detect the expressed recombinant PCSK9 containing the FLAG tag.

10. Liver Proteins from Liver homogenates

The frozen liver samples (~100 mg) were homogenized in 1X RIPA lysis buffer containing complete protease inhibitor cocktail (Roche Mannheim, Germany). The homogenates were centrifuged at 13,000 rpm for 10 min and the supernatants were subjected to protein concentration determination by Bradford assay. To analyze the liver proteins, we used 50 μg of total protein to be separated by SDS-PAGE;

SDS-6% PAGE for FAS (fatty acid synthetase); SDS-7.5% PAGE for SREBP-1a, -1c, -2 (Sterol Regulatory Element-Binding Protein); SDS-7.5% PAGE for HMG-CR (3-hydroxy-3-methyl-glutaryl-CoA reductase); and SDS-10% PAGE for SCD1 (stearoyl-CoA desaturase-1). The antibodies used to detect these proteins are as follows:

Anti-Srebp1 (1:2,000, Abcam), anti-Srebp2 (1:2,000, Cayman Chemical, Ann Arbor, MI), anti-FAS (1:2,000, Abcam), anti-SCD1 (1:2,000, Abcam), and anti-HMGCR (1: 2,000, Santa Cruz).

In general, after the proteins were transferred to PVDF membrane, the membrane was incubated with the primary antibodies at 4°C overnight. On the next day, the membrane was washed and blotted with secondary antibodies such as Alexa-680 conjugated anti-rabbit secondary antibody (1:10,000) at RT for 1 h. The membrane was washed and scanned using Odyssey Infrared Imaging system (Li-COR, Lincoln, NE). The intensities of protein bands were semi-quantified using the software of the Li-COR system.

11. Real-time Quantitative PCR

Total RNA was extracted from mouse livers by using the Qiazol RNA extraction reagent (Qiagen, Valencia, CA). The concentrations of the RNAs were determined by using Nanodrop 2000 (Thermo Scientific). Two micrograms of total RNA were digested with DNase I (Ambion, Austin, TX) to remove any trace of genomic DNA. The DNAse I treated RNA was transcribed into cDNA using Achieve Reverse Transcription Kit (Applied Biosystems, Foster City, CA). Real-time quantitative PCR (qPCR) was performed on ABI Prism 7900-HT Sequence Detection System (Applied Biosystems).

We used both SYBR Green (SYBR Green PCR Master Mix, Bio-Rad) and TaqMan assays (Applied biosystem) to quantify gene expression levels. For SYBR Green assay, each primer set was optimized to eliminate primer-dimer formation. The following 10 genes were determined using SYBR Green standard curve qPCR assay: HMG-CoA synthetase, HMG-CoA reductase, acetyl-CoA carboxylase, fatty acid synthase, stearoyl-CoA desaturase-1, glycerol-3-phosphate acyltransferase, diacylglycerol acyltransferase-1, SREBP1-a, –c, and 2. The gene expression levels were normalized with mouse 16S RNA.

The mouse apoB RNA levels were quantified using the TaqMan primer/probe standard curve assay. The mouse apoB RNA levels were normalized with 18S RNA. Sequences of primers and probes used in this study are listed in Table 1.

Table 1. Primer sequences and optimized primer concentrations used for SYBR real-time quantitative PCR. All the primers and probes were designed by using Primer Express software (Applied Biosystems Inc.)

F = forward primer; R = reverse primer

Gene Symbol	Access number	Primer and probe sequence	Optimized concentrat-ion (μM)
Srebp-1a	NM_011480	F: 5' CGGCTCTGGAACAGACACTG	2
		R: 5' GAAGTCACTGTCTTGGTTGTTG	2
Srebp1-c	NM_011480	F: 5' ATCGGCGCGGAAGCTGTCGGGGTAGCG	2
		R: 5' GAAGTCACTGTCTTGGTTGTTG	2
Srebp2	NM_033218	F: 5' GTTCTGGAGACCATGGAG	5
		R: 5' AAACAAATCAGGGAACTCTC	5
HMGCoA reductase	NM_008255	F: 5' CTTTCAGAAACGAACTGTAGCTCAC	2
		R: 5' CTAGTGGAAGATGAATGGACATGAT	2
HMGCoA synthase	NM_145942	F: 5' CAGCCATTTGTTACAGCTTATTCTC	2
		R: 5' TCTTTTTAATTGCCACATATTATTTTAGAA	2
Fas	NM_007988	F: 5' AGCACTGCCTTCGGTTCAGTC	2
		R: 5' AAGAGCTGTGGAGGCCACTTG	2
Scd1	NM_009127	F: 5' CTGCAGGTTGTGCTAGATGGGATGG	2
		R: 5' GCCTGGGGTCTTTGGTAAGTAGGC	2
Acc	NM_133904	F: 5' TTATCTCTGGAGAACCTCTCTAATGG	2
		R: 5' AGACACTTAGCAAGAGCAAAAATGA	2
Gpat	NM_008149	F: 5' CCTCTCAGTGGTAGTGGATACTCTGT	1
		R: 5' GTGACCTTCGATTATGCGATCAT	1
Dgat1	NM_012079	F: 5' GGCATTCACAGCAATGATGGC	2
		R: 5' CCACACAGCTGCATTGCCATA	2
m16S	XM_003085753	F: 5' AGGAGCGATTTGCTGGTGTGG	0.5
		R: 5' GCTACCAGGGCCTTTGAGATG	0.5
mApoB	NM_009693	F: 5' ATGTACTAATTGCCATAGATAGTGCCA	0.25
		R: 5' TCGCGTATGTCTCAAGTTGAGAG	0.25
		Probe: 6FAM-ATCAACTTCAATGAAAAA-MGBNFQ	0.12
18S	X00686	F: 5' TAACGAACGAGACTCTGGCAT	0.17
		R: 5' CGGACATCTAAGGGCATCACAG	0.17
		Probe: 6FAM-TGGCTGAACGCCACTTGTCCCTCTAA-TAMRA	0.11

12. Pulse-chase experiment of apoB biosynthesis in mouse primary hepatocytes

Mouse primary hepatocytes were isolated using a modified procedure established by David Moore's laboratory (43) from Baylor College of Medicine, Houston, TX. Mice (*C57BL/6J, Ldlr-/-,* and *LDb*) were anesthetized, the livers were first perfused with 50 mL HBSS (Invitrogen) containing 0.5 mM EGTA at a rate of 3 mL/min via the portal vein, followed by 50 mL EBSS (Invitrogen) containing 0.3 mg/mL liberase blendzyme (Roche) and 0.04 mg/mL trypsin inhibitor (Invitrogen) at 37°C. After perfusion, the liver was removed, the hepatic capsule was peeled off, and hepatocytes were dispersed by shaking the digested liver in a pre-warmed William's E medium (Invitrogen) at 37°C. The hepatocytes were filtered through a 100-μm nylon cell strainer (BD Falcon, Franklin Lakes, NJ), the cells were washed twice with William's E medium, and re-suspended in 20 mL William's E medium. The hepatocytes were then loaded onto a 50 mL falcon tube containing a discontinuous Percoll gradient solution (Invitrogen) (from top to bottom: 5 mL 1.06 g/mL, 7 mL 1.08 g/mL, 5 mL 1.12 g/mL). After centrifugation at 700 *g* for 20 min, the cells were collected from the layer between 1.08 and 1.12 g/mL. The cells were washed twice with 20 mL William's E Medium, and re-suspended in hepatocyte culture medium (William's E Medium supplemented with 10% fetal bovine serum, 100 units/mL penicillin G sodium, 100 μg/mL streptomycin sulfate, and 1X insulin-transferrin-selenium solution (Invitrogen)). The viability of cells (90–95%) was determined using trypan blue dye exclusion.

The cells were plated (0.5×10^6 cells/well) onto a 6-well plate pre-coated with 1 mg/mL mouse type IV collagen, incubated for 6 h, followed by infection overnight with Ad-Null or Ad-PCSK9 (multiplicity of infection, MOI = 50:1). On the next day, the media were changed to Met/Cys-free DMEM for 30 min prior to pulse labeling. The cells were pulsed with 100 μCi/mL [^{35}S] Methionine/Cysteine (Perkin Elmer, Waltham, MA) in Met/Cys-free DMEM for 15 min, followed by chasing with serum-free DMEM containing 2 mM Met for 30, 60, 120, 180, and 240 min. At the indicated time point, media were collected, and cells were lysed with 100 μL RIPA buffer (Cell Signaling) containing a protease inhibitor cocktail (Roche).

The media (400 μL) and cell lysates (50 μL) were incubated with 10 μL anti-mouse apoB (Abcam) or anti-albumin (GenWay Biotech, San Diego, CA) antibodies in 500 μL 1X RIPA buffer containing protein-A-agarose beads (Roche) at 4°C for 1 h with rotation to immunoprecipitate the apoB or albumin. The immunoprecipitates were washed with 500 μL 1X RIPA buffer for 5 times and then eluted with SDS sample loading buffer and subjected to gel electrophoresis (6% Prosieve gel for apoB and SDS-10% PAGE for albumin). The gels were fixed and amplified in 1 M sodium salicylate (Sigma-Aldrich) for 15 min, dried, and scanned by a PhosphoImage system (Bio-Rad). The bands were quantified using QuantityOne software (Bio-Rad). The results are expressed as total radioactivity of each band.

13. ELISA to measure mouse and human PCSK9

Mouse PCSK9:

We used Mouse/Rat PCSK9 ELISA kit (Circulex Bio, Ltd.) to determine the PCSK9 levels in mouse plasma and FPLC fractions separated from mouse plasma. Briefly, diluted samples (1:100 *C57BL/6* serum, 1:1000 for *Ldlr-/-* and *LDb*, 1:20 for FPLC fractions) and PCSK9 standards (provided by the kit) were incubated in the 96-well plate at room temperature for 1 h with horizontal shaking. After washing 4 times with washing buffer, 100 μL HRP conjugated detection antibody were added to each well and incubated at RT for 1 h with horizontal shaking. Each well was then washed 4 times with washing buffer, followed by addition of 100 μL substrate reagents onto each well and incubated at RT for 10 min. The color reactions were stopped by adding 100 μL stopping solutions. The absorbance was measured at 450 nm wavelength and the results were analyzed by 4-parameter evaluation method on Tecan infinite m200 microplate reader (TECAN, San Jose, CA).

Human PCSK9:

We used human PCSK9 ELISA kit (R&D, Ltd.) to determine the recombinant human PCSK9 expressed by Ad-PCSK9 in mouse plasma and FPLC fractionations separated from mouse plasma. Briefly, diluted samples such as Ad-PCSK9 transduced mouse plasma (1:100,000), FPLC

fractions (1:1,000), and PCSK9 standards (provided in the kit) were incubated in the ELISA wells at room temperature for 2 h. After washing 4 times with washing buffer, 100 μL HRP conjugated detection antibody were added to each well and incubated at RT for 2 h. Each well was then washed 4 times with washing buffer, followed by addition of 100 μL substrate reagents onto each well and incubated at RT for 30 min. The color reactions were stopped by adding 50 μL stopping solutions. The absorbance was measured at 450 nm wavelength and the readings were analyzed by 4-parameter evaluation method on Tecan infinite m200 microplate reader (TECAN).

14. Co-immunoprecipitation of PCSK9 and apoB

McA-RH7777 cells stably expressing human apoB-18 or apoB-48 were maintained as described. The cells were plated onto a 6-well plate at density of 10^6 cells/well, and cultured for 18 h in DMEM containing 10% FBS and 200 μg/mL G418. The cells were infected with Ad-PCSK9-FLAG or Ad-Null (MOI = 50:1). At 24 h after infection, the cells were washed with PBS twice and lysed with 100 μL 1X RIPA buffer. The cell lysates were centrifuged at 10,000 rpm for 10 min, the supernatants were collected and incubated with 50 μL anti-FLAG M2 agarose (Sigma-Aldrich) for 3 h at 4°C to precipitate FLAG-tagged PCSK9. The immunocomplexes were washed 3 times with 500 μL RIPA buffer, eluted with SDS sample-loading buffer by boiling them for 5 min. The mixtures were subjected to SDS-PAGE (6% Prosieve gel for apoB and 7.5% gel for PCSK9). After gel electrophoresis, the proteins were transferred to the PVDF membrane, the membrane was incubated with mAb 1D1 (1:5,000) to detect human apoB-18 and apoB-48, and anti-FLAG to detect PCSK9.

15. Protein-Protein interaction: Mammalian matchmaker Two-hybrid System

We used a mammalian matchmaker two-hybrid system (Clontech, Mountain View, CA) to examine the protein–protein interaction. The plasmid vectors used for this assay were described above.

Three plasmid vectors: pM-apoB-18 (0.5 μg), pVP-16-PCSK9 (0.5 μg), and pG5-SEAP (0.5 μg) were co-transfected into either 293 cells or COS-1 cells using lipofectamine 2000 (Invitrogen). At the end of the experiment (48 h after transfection), the interaction between these 2 proteins was detected by measuring SEAP activities in the cell media using Great EscAPe SEAP Chemiluminescence Detection Kit (Clontech). The Light Unit was determined using Tecan infinite m200 chemiluminescent reader (TECAN, San Jose, CA). The negative controls of pM and pVP16 or pM-Apobec1 and pVP16-PCSK9 with the pG5-SEAP; and the positive controls of pM-LDLR, pVP-16-PCSK9, and pG5-SEAP were performed simultaneously. The results were expressed as light units.

16. Duolink *in situ* proximity ligation assays (PLA) and Immunofluorescence analysis

Duolink *in situ* proximity ligation assays (PLA):

We used *in situ* PLA assay kit obtained from OLINK Bioscience (Uppsala, Sweden) to study the endogenous protein–protein interaction. The primary antibodies used for this assay were monoclonal antibody PCSK9 (mC33-Mab1), anti-ApoB (Abcam), anti-Apobec1 (provided by Dr. Lawrence Chan's laboratory from Baylor College of Medicine), and anti-LDLR (Cayman). HepG2 cells or HepG2 cell line stably expressing Apobec1 were seeded onto a chamber slide (NUNC, Naperville, IL) at 10^4 cells/well and cultured overnight at 37°C, 5% CO_2. On the next day, the cells were washed with ice-cold PBS, fixed in 4% paraformaldehyde at RT for 10 min, followed by permeabilization with PBS containing 0.25% Triton X-100 for 10 min. The cells were blocked with blocking buffer (PBS containing 1% BSA) for 1 h at RT, followed by incubation with primary antibody (1:100 dilution in blocking buffer) at 4°C overnight. Note, to study the interaction between LDL receptor and PCSK9, we did not permeabilize the cells since permeabilization would poke holes in the cell membrane and change the confirmation of the protein.

We followed the instruction of *in situ* PLA commercial kit to detect protein–protein interaction. Briefly, after primary antibodies incubation the cells were washed with PBS, followed by

incubation with PLA secondary probes (1:5 dilution in blocking solution; anti-rabbit/PLUS and anti-mouse/MINUS PLA probes) for 1 h at 37°C. The slide was washed 2 times with Wash Buffer-A, 5 min each time. The cells were then incubated with 1:40 diluted Ligase for 30 min at 37°C in a pre-heated humidity chamber for ligation. After the ligation step, the slides were washed 2 times with Wash Buffer-A, 2 min each. The slides were then incubated with 40 μL diluted polymerase (5 units, 1:80 dilution) for 100 min at 37°C in a pre-heated humidity chamber to amplify the signal. At the end of the reaction, the slides were washed quickly with Wash Buffer-B to remove all the ingredients, followed by 10 min wash with Wash Buffer-B again 2 times, and finally rinsed with 1:100 diluted Wash Buffer-B for 1 min. The slides were dried at room temperature in the dark, and then mounted with Duolink II mounting medium containing DAPI. We examined the slides by using a Zeiss Axio Observer.D1m fluorescence microscopy with DAPI, FITC, and Texas Red filters. Control slides without primary or secondary antibodies were performed at the same time.

Immunofluorescence analysis:

Before the *in situ* PLA assay, we performed immunofluorescence analysis by using each antibody to confirm the specificities of the antibodies. Briefly, after the cells were incubated with a single antibody overnight, followed by fixing and permeabilization, the cells were washed with PBS and incubated with fluorescence dye conjugated-secondary antibodies at 1:300 for 1 h at room temperature. After washing off the secondary antibody, the slides were incubated with DRAQ5 nuclear staining reagent (Abcam) at 1:1,000 in PBS for 2 h at room temperature. The slides were mounted and examined using a Leica DM 600B confocal microscope with 488 nm, 594 nm, and 633 nm filters.

17. Autophagosome isolation

We isolated autophagosomes from cells or mouse liver using the method described by Stromhaug et al. (46). Briefly, we used glass tissue grinder type B (Kimble Chase) to homogenize the McA-RH7777 cells or mouse livers from *C57BL/6 or Ldlr-/- or LDb, or Pcsk9-/- or LDb/Pcsk9-*

/- in a homogenization buffer (HB, 0.25 M sucrose, 10 mM Hepes, 1 mM EDTA, 0.5 mM glycyl-l-phenylalanine 2-naphthylamide (GPN), 1% DMSO, pH 7.3, ρ = 1.030 g/mL). After 6 min incubation at 37°C, the homogenate was centrifuged at 2,000 *g* for 2 min to separate nuclear pellet from supernatant. The supernatants were layered on the top of a discontinuous Nycodenz gradient solution (4 mL -1.072 g/mL and 4 mL-1.127 g/mL). The Nycodenz gradient was centrifuged at 4°C for 1 h at 141,000 *g* using NVT65 rotor (Bechman Coulter). The interface band (~1 mL), which contains the autophagosomes, was collected using a 21G needle. This band was diluted with 5 mL of HB and layered on top of the 2nd discontinuous gradient (4 mL 33% Percoll in HB and 5 mL 22.5% Nycodenz [1.127 g/mL] in HB). The gradients were centrifuged for 30 min at 72,000 *g* using NVT65 rotor (Bechman Coulter). We collected the purified autophagosome band at the interface between Percoll and Nycodenz solution using a 21G needle. The autophagosomes were lysed in 1X RIPA buffer, and we then used 30 μg of the lysed autophagosomes for SDS-PAGE analysis (6% Prosieve gel for apoB; 12.5% gel for PCSK9 and LC3). The proteins were then transferred to Immbolion-FL membrane, and probed with antibodies of anti-mouse apoB (1:5,000 dilution), anti-PCSK9 (Cayman Chemical, 1:2,000 dilution), and anti-LC3 (Cell Signaling, at 1:3,000 dilution), followed by anti-rabbit secondary antibody (1:10,000). The intensities of the protein bands were quantified using an Odyssey Infrared Imaging system (Li-COR).

18. Statistics

All the results were expressed as mean ± SD. All comparisons were performed using GraphPad Prism software (ver 5) unpaired student *t*-test with two-tailed *p* value, except the long term cholesterol, TAG, and liver gene expression levels in which one-way and 2-way ANOVA were used. A *p* value of <0.05 was considered to be statistically significant.

RESULTS

1. The rationale of using the 3 animal models for this study.

The mechanism of how PCSK9 negatively regulates LDLR to increase LDL cholesterol levels has been intensively studied; however, the impact of PCSK9 on apoB production remains controversial and poorly understood. Here, I am re-emphasizing the rationale for our hypothesis, and I will provide the rationale for using the animal models for this study.

ApoB is the structural protein for LDL, which is removed from circulation via LDLR. Thus, the regulation of LDLR by PCSK9 might alter apoB levels. Clinically, increased apoB concentration is associated with coronary artery disease (96). Therefore, we proposed to investigate the relationship of PCSK9 and apoB.

The publication by Sun et al. showed that McA RH-7777 cells stably expressing PCSK9 D374Y mutant increased secretion of apoB containing lipoproteins in this stable cell line (27). Similarly, the increase of apoB containing lipoproteins secretion is also observed in humans with D374Y or S127R variant of PCSK9 (27, 97). In mice, the effects of PCSK9 on apoB secretion were not consistent. In wild-type *C57BL/6* or *Ldlr-/-* mice, over-expression of wild-type PCSK9 or the S127R mutant for 3 days has no significant increase in apoB synthesis or production (20, 98, 99). Unchanged plasma apoB levels were also observed in both *C57BL/6* and *Ldlr-/-* mice overexpressing PCSK9 for 5–6 days (98, 99). On the other hand, overexpression of PCSK9 in *Ldlr-/-* mice for 7 days resulted in an approximately 2-fold increase in LDL-cholesterol and apoB levels (20). Thus, the apparent discrepancy among these experiments does not provide conclusive evidence on whether PCSK9 plays a role in apoB production.

Interestingly, Pcsk9 deficient mice (*Pcsk9-/-*) had decreased production of apoB-containing lipoproteins (19, 93). These studies suggested that PCSK9 plays a role in apoB production, probably

via LDLR protein expression. Taken together, we proposed to test the hypothesis that PCSK9 regulates apoB production, and to investigate whether LDLR is a necessary component.

We proposed to test our hypothesis in the following 3 mouse models: *C57BL/6J, Ldlr-/-,* and *LDb (Ldlr-/-Apobec1-/-). C57BL/6J* mice, which express both LDLR and PCSK9 proteins are wild-type and used as control. *Ldlr-/-* mice, which lack Ldlr gene were purchased from the Jackson laboratory. The third mouse model is *LDb* mice. Our laboratory crossbred *Ldlr-/-* mice with Apobec1-/- mice to produce a double knockout mouse model (*Ldlr-/-Apobec1-/-)* (62). In contrast to wild-type mice or *Ldlr-/-* mice, the phenotype of the *LDb* mice closely mimics humans with hyperlipidemia characterized by the secretion of apoB-100-containing lipoproteins only, with increased plasma levels of VLDL and LDL cholesterol and decreased levels of HDL cholesterol. In addition, these *LDb* mice spontaneously develop severe atherosclerotic lesions, when fed on a normal chow diet. Thus, LDb mice are distinctly different from *Ldlr-/-* mice, despite both lacking the LDLR. The lipoprotein phenotypes of these 3 mouse models are shown in Figure 1. Wild-type *C57BL/6* mice have minute amounts of VLDL and LDL particles, and they carry most of their cholesterol in HDL particles. In contrast, mice deficient of LDLR *(Ldlr-/-)* have slightly elevated LDL, but most of the cholesterol is still carried by HDL. Mice deficient of both LDLR and Apobec1 genes (*LDb; Ldlr-/-Apobec1-/-),* have elevated VLDL and LDL levels with decreased HDL particles. This lipoprotein phenotype mimics humans with hyperlipidemia. Thus, *LDb* mice are a humanized hyperlipidemia mouse model.

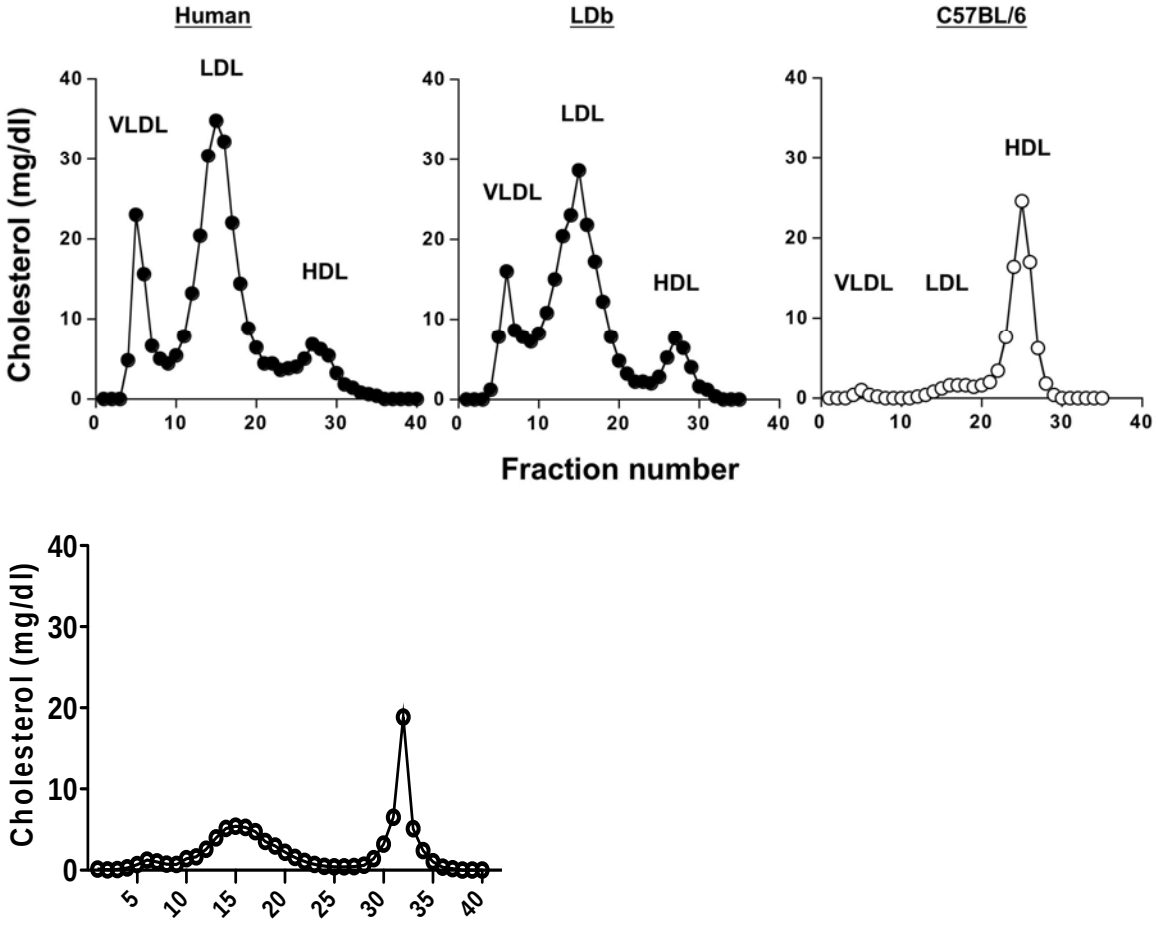

Figure 1. The cholesterol levels of lipoprotein fractions in patients with hyperlipidemia, *LDb* mice, wild-type *C57BL/6* mice, and *Ldlr-/-* mice.

Plasma from patient, *LDb, C57BL/6,* and *Ldlr-/-* mice was subjected to FPLC fractionation. Cholesterol levels in each fraction were measured using a commercial kit.

2. Recombinant PCSK9 with or without a FLAG tag have the same effect on apoB production

Here, we examined whether recombinant PCSK9 with or without a FLAG tag have the same effect on apoB production in cells. We transfected HepG2 and McA-RH7777 cells with either pcDNA3-PCSK9 or pcDNA3-PCSK9–FLAG, and, 48 h after transfection, we collected the cell media, subjected them (50 μL) to SDS-7.5%PAGE, followed by Western blot analysis. We included pcDNA3 vector as the control and pcDNA3-PCSK9–D374Y-FLAG as the positive control. As shown in Figure 2, cells overexpressed PCSK9, or PCSK9-Flag, or PCSK9-D374Y mutant had significantly increased apoB levels secreted into the media, when compared with cells transfected with pcDNA3 vector only. Importantly, there were no differences on apoB levels in the cell media between cells expressing recombinant PCSK9 with or without a FLAG tag. Transfection of McA-RH7777 cells with pcDNA3-PCSK9–D374Y-Flag results in more than 2-fold increase of apoB protein. This result was demonstrated by others as the consequence of a strong interaction of PCSK9 D374Y mutant with LDLR (27). Taken together, our results show that the expression of PCSK9 with or without a FLAG tag yielded similar effects on apoB production in cells.

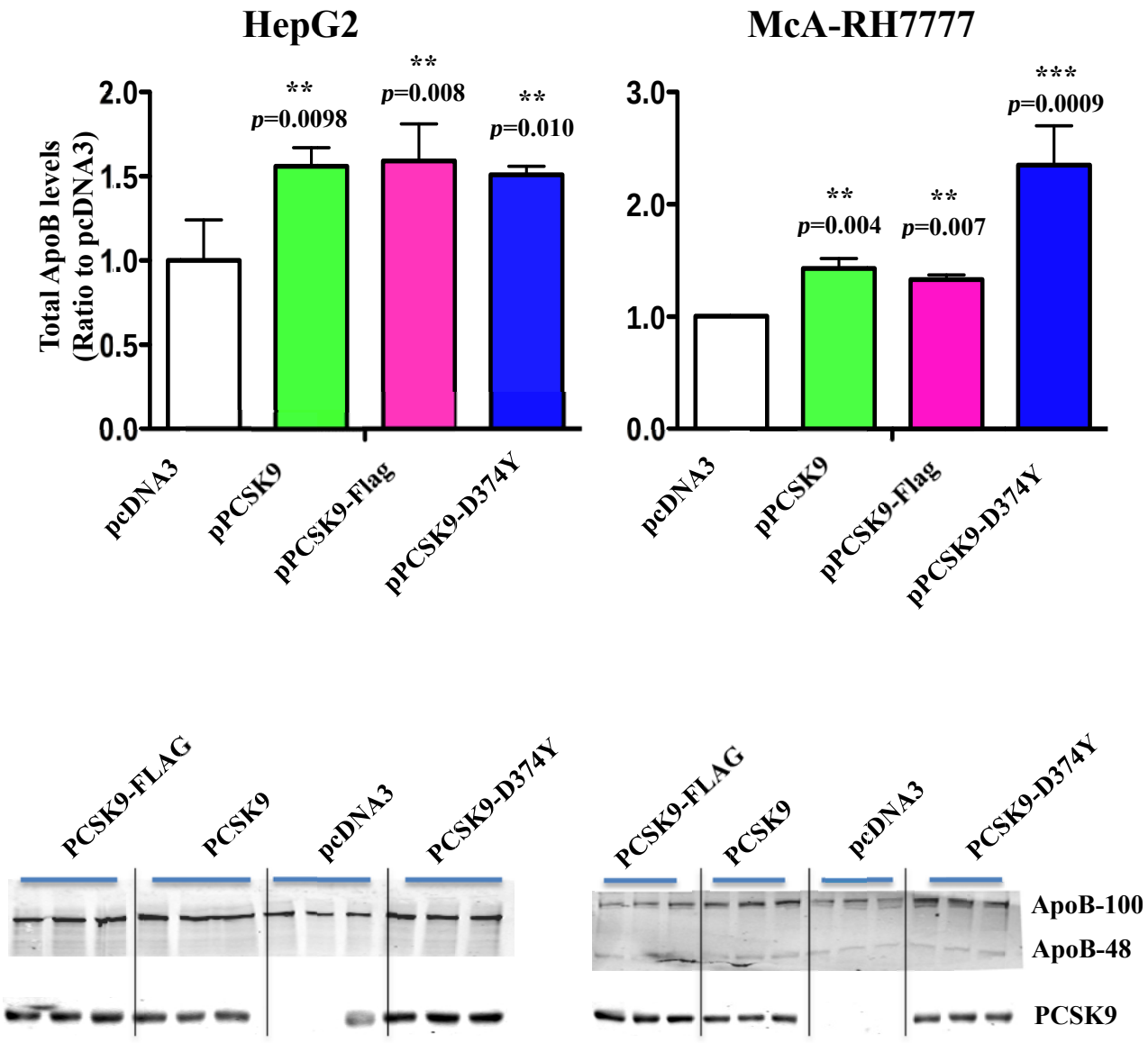

Figure 2. The effects of PCSK9, PCSK9-FLAG, and PCSK9-D374Y on apoB secretion in cells. Plasmid vectors of pcDNA3-PCSK9, PCSK9-FLAG and PCSK9-D374Y were constructed as described in the Methods. The vectors were transfected into HepG2 cells or McARH-7777 cells. After 48 h, the cells media were collected to detect apoB and PCSK9 secretion by Western blot using anti-apoB antibody and anti-PCSK9 respectively. The bands were scanned and the densities of the bands were quantified. The data were presented as the ratio of densities of experimental groups to control group (pcDNA3 empty vector). * $p < 0.05$ was considered as significant difference.

3. Recombinant PCSK9 mediated by Ad-PCSK9 is expressed vividly in *C57BL/6J, Ldlr-/-* and *LDb* mice. The recombinant PCSK9-FLAG protein is biologically active

Since the FLAG tag has no obvious adverse effect on apoB secretion, we chose to express FLAG-tagged human PCSK9 protein (Ad-PCSK9) using an Adenovirus E2b-region (pol gene) deleted second-generation adenoviral vector that exhibits a long-term gene expression and lower toxicity (94, 100). Because of the designing defect of antibiotic selection in the original E2b-deleted adenovirus system, we had to perform one extra step of recombination to replace the antibiotic resistant gene as described in detail in the Methods. The same adenovirus vector without the insert was constructed and used as control (Ad-Null).

We transduced *C57BL/6J, Ldlr-/-,* and *LDb* male mice at 2-months of age (n = 24/group) with Ad-PCSK9 and Ad-Null for this study. The plasma samples were collected at day 0 before treatment and days 7, 14, 21, and 30 after the adenovirus administration. As shown in Figure 3, the levels of human PCSK9 proteins were expressed vividly up to 30 days in the mouse liver of the 3-mouse model studied. The levels of recombinant PCSK9 were ~400-fold above the baseline as determined by ELISA (Figure 4); *C57BL/6* = 646±48 μg/mL, *Ldlr-/-* = 967±44 μg/mL, and *LDb* = 944±66 μg/mL.

To confirm the biological function of the recombinant PCSK9 expressed by adenovirus, we used Western blot analysis to determine the LDL receptor levels in *C57BL/6* mice. As expected, the expression of PCSK9 in *C57BL/6* mice markedly decreased the LDLR protein in the liver (Figure 3). This effect demonstrates that the recombinant PCSK9-FLAG protein expressed by Ad-PCSK9 is biologically active.

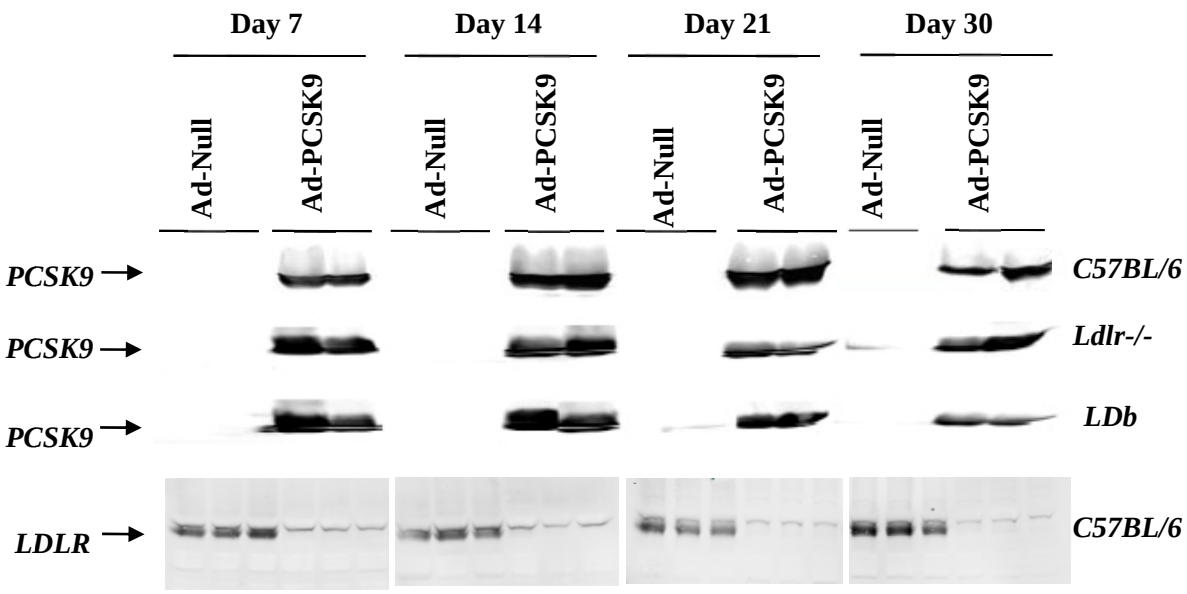

Figure 3. The levels of overexpression human PCSK9 in mouse models transduced with Ad-PCSK9 and the levels of mouse LDL receptor after Ad-PCSK9 treatment.

C57BL/6, Ldlr-/-, and *LDb (Ldlr-/-Apobec1-/-)* mice were transduced with either Ad-Null or Ad-PCSK9. The hepatic protein samples (50 μg) were separated by SDS-PAGE and immunoblotted with their respective antibodies (FLAG and LDLR) as indicated. Western blot analysis showed PCSK9 was expressed vividly in the liver lysates of C57BL/6, Ldlr-/-, and LDb mice after transduction, and the levels of LDLR in C57BL/7 mice were decreased markedly after Ad-PCSK9 transduction (bottom panel).

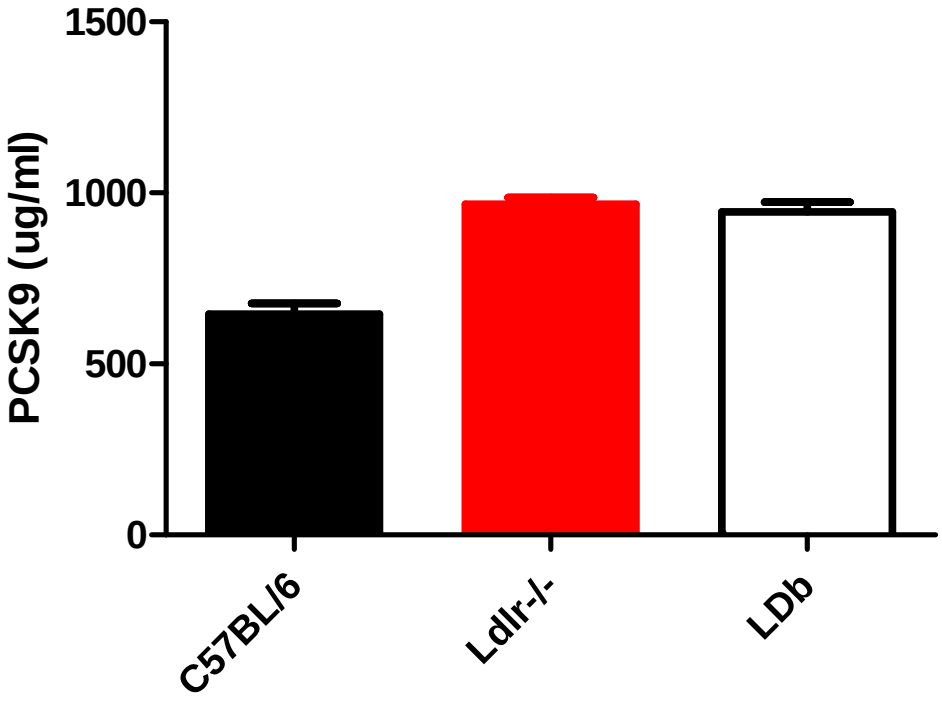

Figure 4. The levels of over-expressed human PCSK9 in mice treated with AdPCSK9. We used commercial ELISA method to measure the human PCSK9 levels in each mouse after treated with AdPCSK9. Mouse plasma was diluted to 1:100. The diluted plasma was incubated in a pre-coated well with PCSK9 antibody. Standard ELISA procedure was performed according to the commercial manual. The plasma PCSK levels are represented as mean ± SD (n = 5).

4. Recombinant PCSK9 expressed via Ad-PCSK9 is detected mostly in the liver.

The next question we asked was the distribution of recombinant PCSK9 after Ad-PCSK9 transduction. We used real-time quantitative PCR and ELISA to examine the tissue distributions of endogenous mouse PCSK9 and recombinant human PCSK9 via Ad-PCSK9. Tissues such as liver, spleen, kidney, small intestine, and heart from *C57BL/6* mice at day 7 after transduction with either Ad-Null or Ad-PCSK9 were analyzed. As shown in Figure 5, most of the endogenous Pcsk9 mRNAs were expressed in the liver and a lesser amount was expressed in the kidney, small intestine, heart, and spleen. Endogenous mouse PCSK9 protein was also expressed mostly in the liver with some amount detected in the small intestine. These results were similar to the reports by others (101).

Most of the recombinant human PCSK9 mediated by Ad-PCSK9 (>95%) was also detected in the liver with minute amounts detected in the spleen, small intestine, and heart as shown in the gene expression of PCSK9 by real-time quantitative PCR and protein expression determined by ELISA method specific for Human PCSK9. Thus, liver is the predominant site for Ad-PCSK9 mediated gene expression. Our results agreed with others that adenoviral vector preferably targeted the liver, since adenoviral "CAR" receptor is expressed mainly in the liver (102).

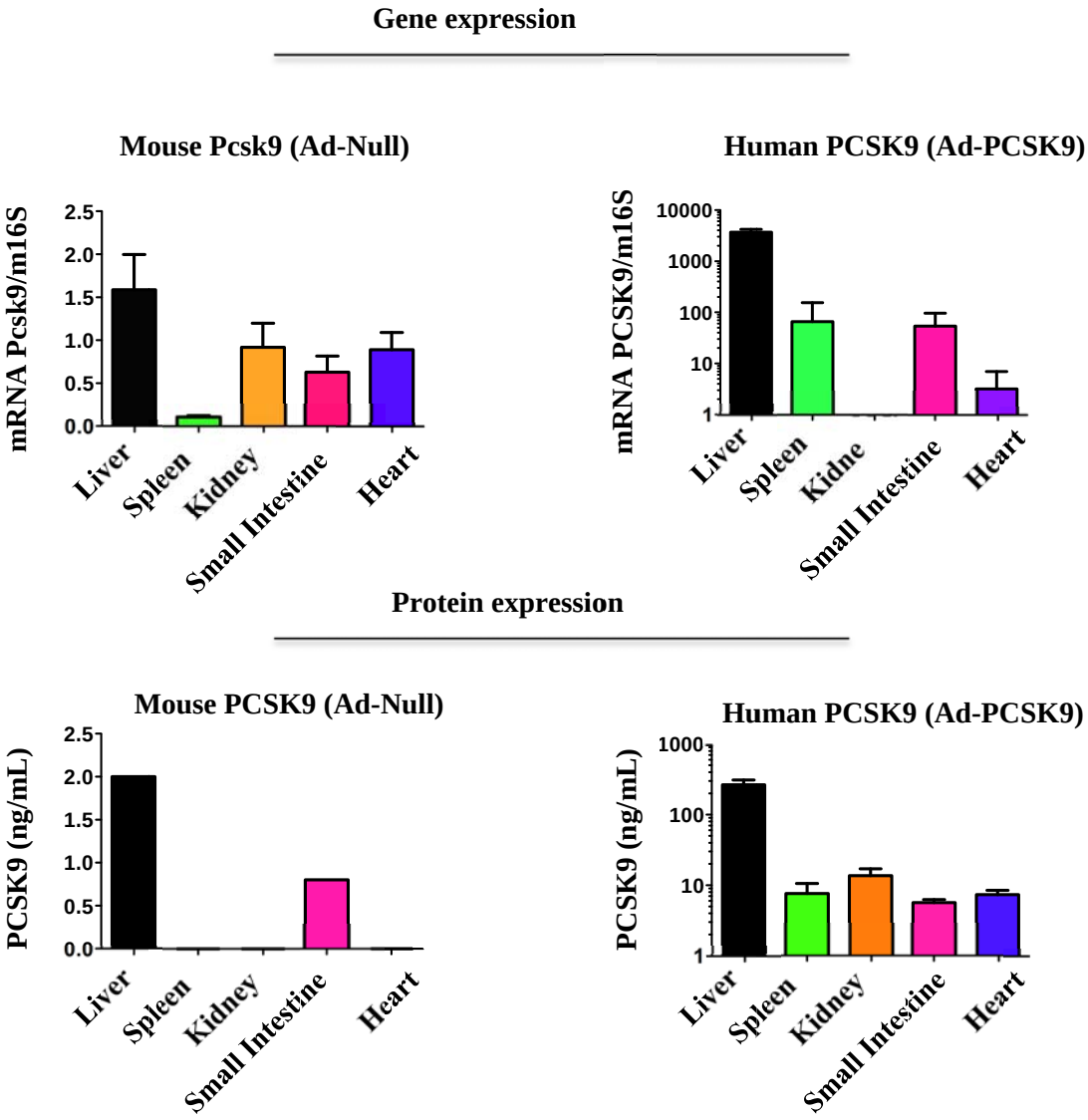

Figure 5. The biodistribution of endogenous mouse PCSK9 and the overexpression of human PCSK9 in *C57BL/6* mice.

Liver, spleen, kidney, small intestine, and heart were collected 7 days after adenovirus transduction. The total RNA and proteins were prepared as described in the Methods. The mRNA levels of PCSK9 in tissues (top panel) were measured by relative quantitative PCR and normalized with mS16 (Ad-Null) or GADPH (Ad-PCSK9). The protein levels of PCSK9 in tissues (bottom panel) were measured by commercial ELISA kits (mouse or human PCSK9) (n = 3 for each group).

5. Overexpression of PCSK9 increases plasma cholesterol and triacylglycerol levels in an LDLR-independent fashion.

Overexpression of PCSK9 via Ad-PCSK9 resulted in highly significant increased levels of plasma cholesterol and TAG in all 3-mouse models (Figure 6). The effect of PCSK9 expression on plasma cholesterol and TAG was much greater in *C57BL/6* mice than that in the LDLR-null mice (*Ldlr-/- and LDb*). In C57BL/6 mice, the levels of plasma cholesterol and TAG were increased to an average of 3.7-fold and 8.5-fold, respectively, upon PCSK9 expression as compared to Ad-Null. The increase in the levels of plasma cholesterol and TAG in *Ldlr-/-* mice were 1.7-fold and 3.4-fold, respectively, and 1.5-fold and 1.5-fold, respectively, in *LDb* mice upon PCSK9 expression. The smaller increase in plasma cholesterol and TAG levels upon PCSK9 expression in LDLR-null mice (i.e., *Ldlr-/- and LDb*) was due to elevated baseline levels of the lipids in these animals. It was also noted that the increase in plasma TAG was much greater than that observed in case of plasma cholesterol upon PCSK9 expression, suggesting the increased VLDL secretion. The present results showing the effects of PCSK9 expression on plasma lipid levels in *C57BL/6* mice are in accord with previous observations. (98, 103-106) The effect of PCSK9 expression on plasma lipids in the LDLR-null mouse models is in agreement with results reported by Benjannet et al. (103) showing increased plasma lipid levels in *Ldlr-/-* mice.

We used both one-way and 2-way ANOVA to analyze the effects of overexpression PCSK9 on plasma cholesterol and triglyceride levels in mice. The STAT software is used to conduct one-way and 2-way analyses of variance ANOVA (http://www.stata.com/capabilities/anova-manova/). For each time point, one-way ANOVA was used to test for significant difference between the mean values of phenotypes (cholesterol and triacylglycerol) of the Ad-PCSK9 group and the control virus Ad-Null group. As shown in Figure 7 and Table 2, one-way ANOVA shows that there were no differences at day 0 before treatment among the animals grouped to Ad-PCSK9 or Ad-Null. There were significant differences at each time point after the treatment in cholesterol and triglyceride

levels between Ad-Null and Ad-PCSK9 groups. Furthermore, the treatment resulted in significant increase of cholesterol (TC) and triacylglycerol levels (TAG).

Two-way ANOVA was used to analyze the main and interaction effects of treatment and time on the phenotype. The 2 factors were treatment (Ad-PCSK9 or control virus Ad-Null) and time. Two-way ANOVA for significant differences was performed between the mean values of the phenotypes of Ad-PCSK9 and Ad-Null, and for the relationship between treatment and time. The results are shown in Table 3. The analyses demonstrated that overexpression of PCSK9 significantly increased cholesterol and TAG levels in all the mice studied. The interaction effects of treatment and time on the phenotype were significantly different.

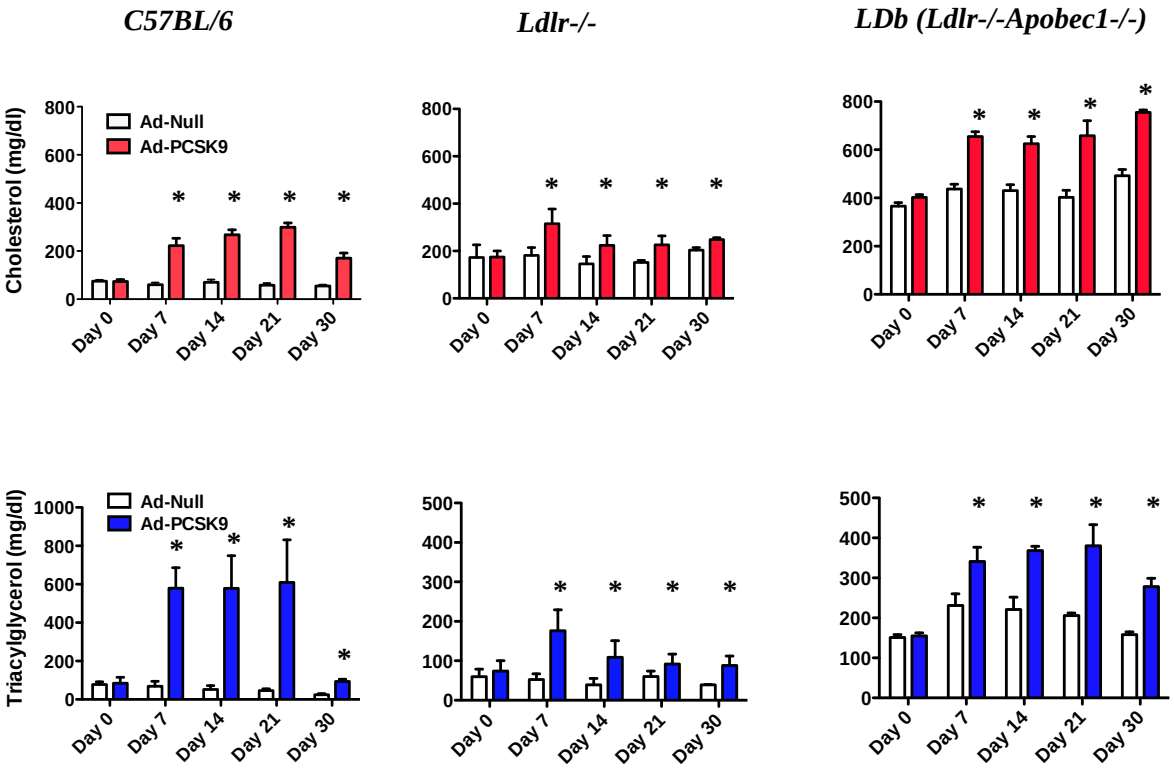

Figure 6. The levels of plasma cholesterol and triacylglycerol in *C57BL/6, Ldlr-/-,* and *LDb* mice after transduction with Ad-PCSK9 or Ad-Null.

C57BL/7, Ldlr-/-, and *LDb* mice were transduced with either 10^{10} viral particles (VP) Ad-Null or Ad-PCSK9. The open bars represent the value of plasma cholesterol and TAG, respectively, from Ad-Null treated mice. The closed bars represent the levels of plasma cholesterol and TAG, respectively, from the Ad-PCSK9 treated mice. * Statistical analysis was performed using 2-way ANOVA, and the difference between the Ad-PCSK9 and Ad-Null groups was highly significant.

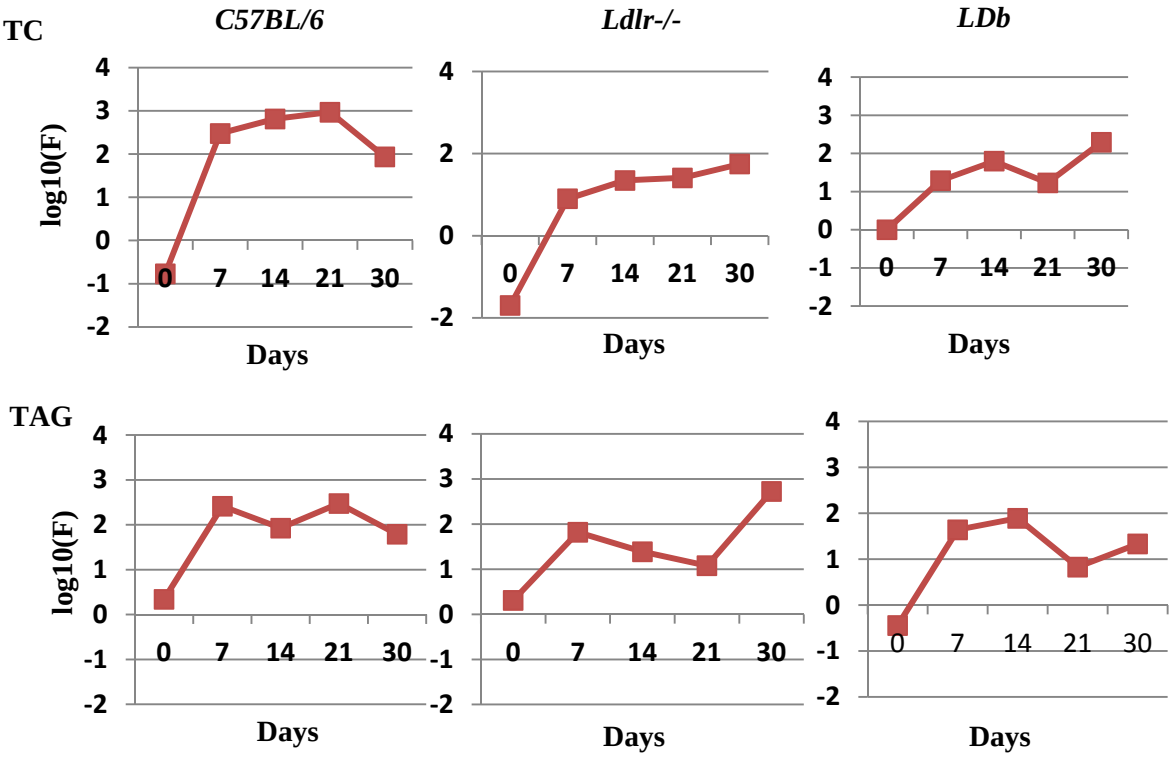

Figure 7. The one-way ANOVA analysis of plasma cholesterol and TAG levels after Ad-PCSK9 transduction.

The one-way ANOVA shows significant difference in the levels of plasma cholesterol (top panel) and triacylglycerol (bottom panel) between Ad-PCSK9 treated and Ad-Null treated *C57BL/6*, *Ldlr-/-*, and *LDb* mice. The one-way ANOVA was performed using STATASE software.

Table 2. One-way ANOVA (Treatment comparison of Ad-Null versus Ad-PCSK9) on plasma cholesterol and triacylglycerol levels in wild-type C57BL/6J, Ldlr-/-, and LDb mice. P values are shown. P < 0.05 is significant.

	Treatment p Values (Ad-PCSK9 versus Ad-Null)				
	Day-0	**Day-7**	**Day-14**	**Day-21**	**Day-30**
Cholesterol					
C57BL/6	0.6874	0.0000	0.0000	0.0000	0.0008
Ldlr-/-	0.8958	0.0100	0.0002	0.0005	0.0017
LDb	0.5244	0.0001	0.0066	0.0175	0.0021
Triacylglycerol					
C57BL/6	0.1519	0.0000	0.0000	0.0000	0.0014
Ldlr-/-	0.1668	0.0000	0.0001	0.0061	0.0000
LDb	0.5582	0.0000	0.0000	0.0357	0.0098

Cholesterol and triacylglycerol levels in wild-type C57BL/6J, Ldlr-/-, and LDb mice. P values are shown. P < 0.05 is significant.

Table 3. Two factors (Treatment and Time) ANOVA on plasma cholesterol and triacylglycerol levels in *wild-type C57BL/6, Ldlr-/- and LDb* mice treated with Ad-Null and Ad-PCSK9. *P* values are shown.

	Main Factor		**Interaction**
	Treatment	***Time***	***Treatment x Time***
Cholesterol			
C57BL/6	0.0000	0.0000	0.0000
Ldlr-/-	0.0000	0.0081	0.0360
LDb	0.0000	0.0000	0.0000
Triacylglycerol			
C57BL/6	0.0000	0.0000	0.0000
Ldlr-/-	0.0000	0.0000	0.0000
LDb	0.0000	0.0000	0.0000

6. Overexpression of PCSK9 increases the levels of VLDL, LDL, but not HDL

We used Fast Protein Liquid Chromatography (FPLC) technique to separate mouse plasma into VLDL, LDL, and HDL fractions. We measured the cholesterol and TAG levels of each fraction. In agreement with the total plasma lipid data on Figure 6, VLDL and LDL, but not HDL fractions had increased cholesterol and TAG levels in all the 3 mouse models that overexpressed PCSK9 (Figures 8A and 8B, respectively). Overexpression of PCSK9 had the most significant effect on the levels of cholesterol and TAG in VLDL and LDL fractions of wild-type *C57BL/6* mice. These may be the result of decreasing LDLR in *C57BL/6* mice. The most interesting finding was that the increase of TAG levels in VLDL fractions in all 3 mouse models, suggesting that PCSK9 expression promoted VLDL production, irrespective of the LDLR.

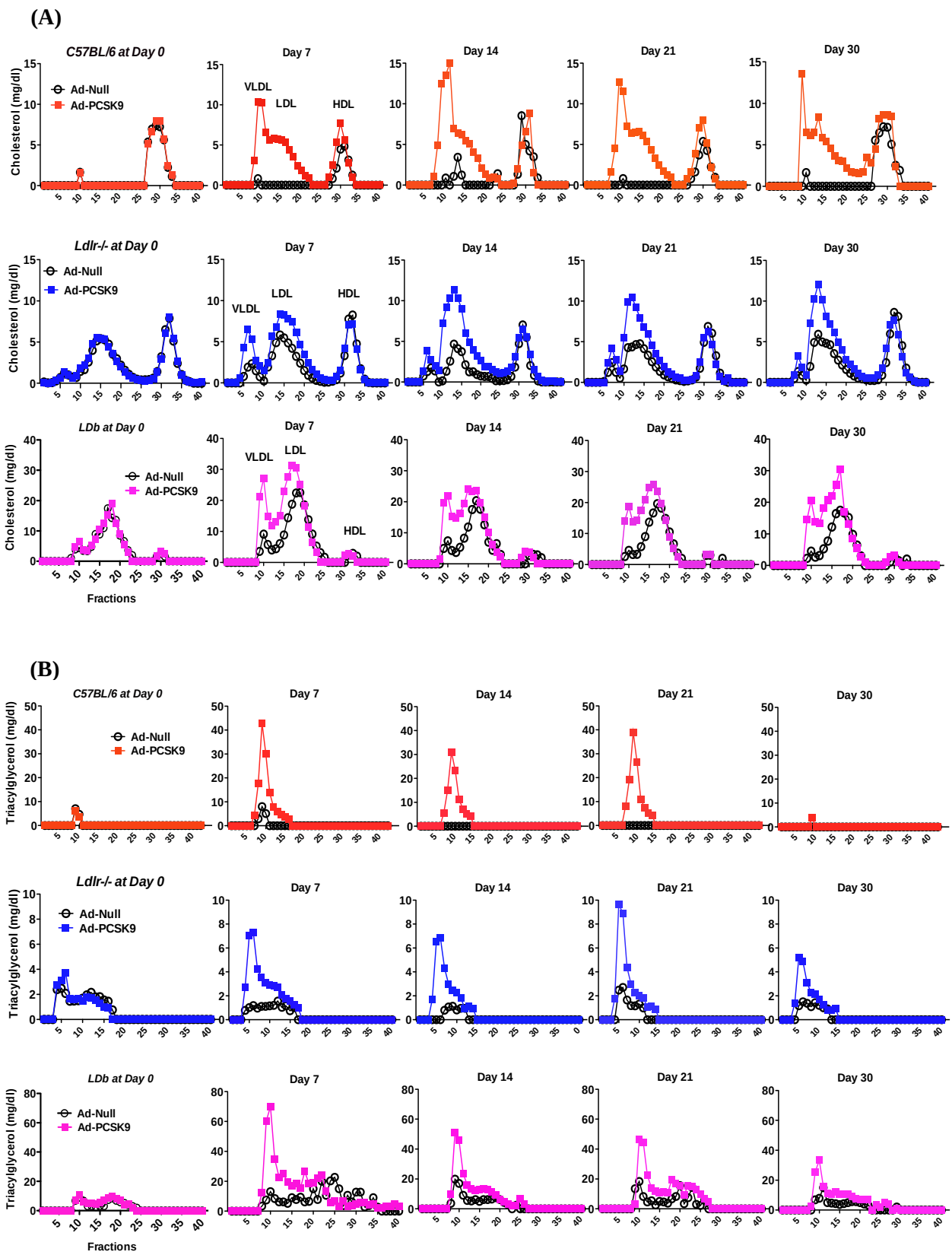
(A)
C57BL/6 at Day 0
Day 7
Day 14
Day 21
Day 30
Ldlr-/- at Day 0
LDb at Day 0
Ad-Null
Ad-PCSK9
VLDL
LDL
HDL
Cholesterol (mg/dl)
Fractions
(B)
Triacylglycerol (mg/dl)

Figure 8. The levels of cholesterol and TAG in VLDL and LDL in *C57BL/6, Ldlr-/-*, and *LDb* mice transduced with Ad-Null or Ad-PCSK9. (A) *C57BL/6* (orange), *Ldlr-/-* (blue), and *LDb* (Pink) mice were transduced with either Ad-PCSK9 (closed circle) or Ad-Null (open circle). Pooled plasma samples from each group at indicated time were fractionated by FPLC. The fractionated plasma was subjected to cholesterol measurement using a commercial kit. Total cholesterol from each fraction was expressed as mg/dL. Positions of VLDL, LDL, and HDL are marked. (B) *C57BL/6* (orange), *Ldlr-/-* (blue), and *LDb* (Pink) mice were transduced with either Ad-PCSK9 (closed circle) or Ad-Null (open circle). Pooled plasma samples from each group at indicated time were fractionated by FPLC. The fractionated plasma was subjected to TAG measurement using commercial kit. TAG from each fraction was expressed as mg/dL. Positions of VLDL, LDL, and HDL are marked.

7. Overexpression of PCSK9 increases plasma apoB levels in an LDLR-independent fashion.

The increased VLDL and LDL levels in mice overexpression PCSK9 can be attributed to the elevated apoB production, which enhances the lipids export from the liver. Here we used Western blot analysis to determine the changes of apoB levels upon overexpression of PCSK9 in the 3 animal models. As shown in Figure 9, at day 7 after Ad-PCSK9 transduction, both plasma apoB-100 and apoB-48 levels rose markedly and remained elevated throughout the 30-day study. In *C57BL/6* mice, upon overexpression of PCSK9 apoB-100 levels increased 1.93-, 3.79-, 2.22-, and 1.68-fold on days 7, 14, 21, and 30, respectively, compared to day 0 before treatment. Likewise, apoB-48 levels were increased 3.53-, 4.73-, 4.34-, and 2.0-fold on days 7, 14, 21, and 30, respectively. Similar increases in apoB-100 levels were also observed in *LDb* mice from day 7 to day 30 upon PCSK9 expression. In *Ldlr-/-* mice, the increase in apoB-100 and apoB-48 levels only became prominent at day 14 and remained elevated to day 30.

We measured the plasma apoAI and apoE levels in these 3 mouse models upon overexpression of PCSK9. As shown in Figure 10, there was no obvious difference in plasma apoAI and apoE levels upon overexpression of PCSK9 in *Ldlr-/-* and *LDb* mice. However, plasma apoE levels were increased in *C57BL/6* mice after treatment. There was no difference in apoAI levels in *C57BL/6* mice after treatment.

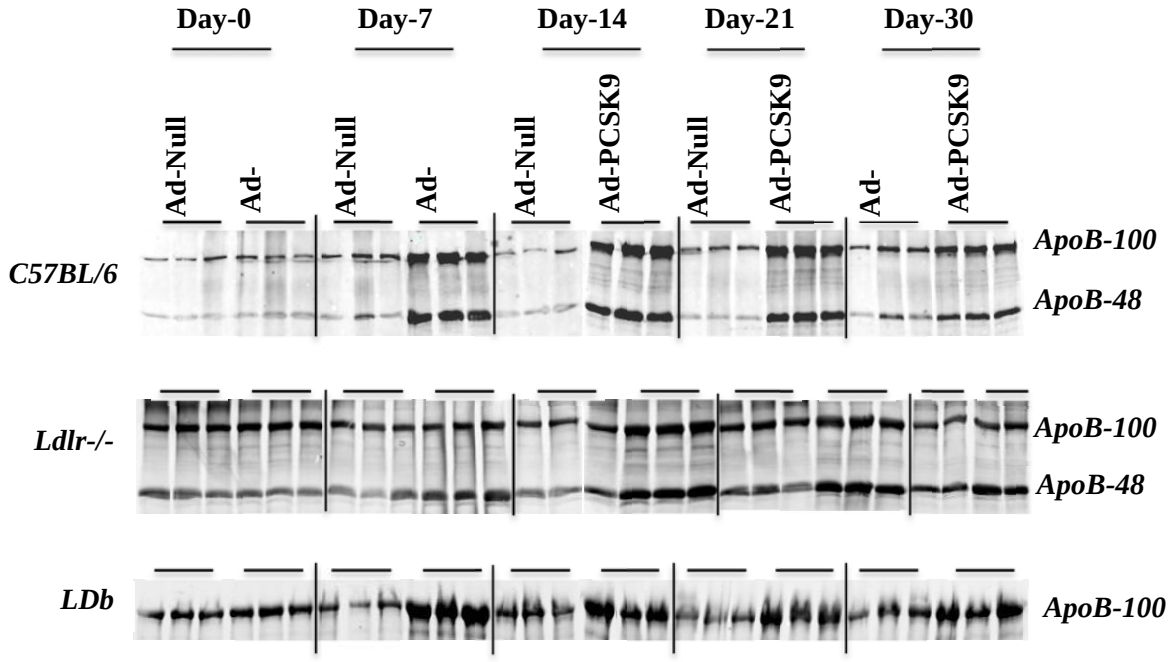

Figure 9. Western blot analysis of plasma apolipoprotein B.

C57BL/6, Ldlr-/-, and *LDb* mice were transduced with either Ad-PCSK9 or Ad-Null. One microliter of the plasma from each mouse was subjected to SDS-PAGE, followed by Western blotting with anti-mouse apoB. The positions of apoB-100 and apoB-48 are marked. The levels of plasma apoB are markedly elevated in mice transduced with Ad-PCSK9.

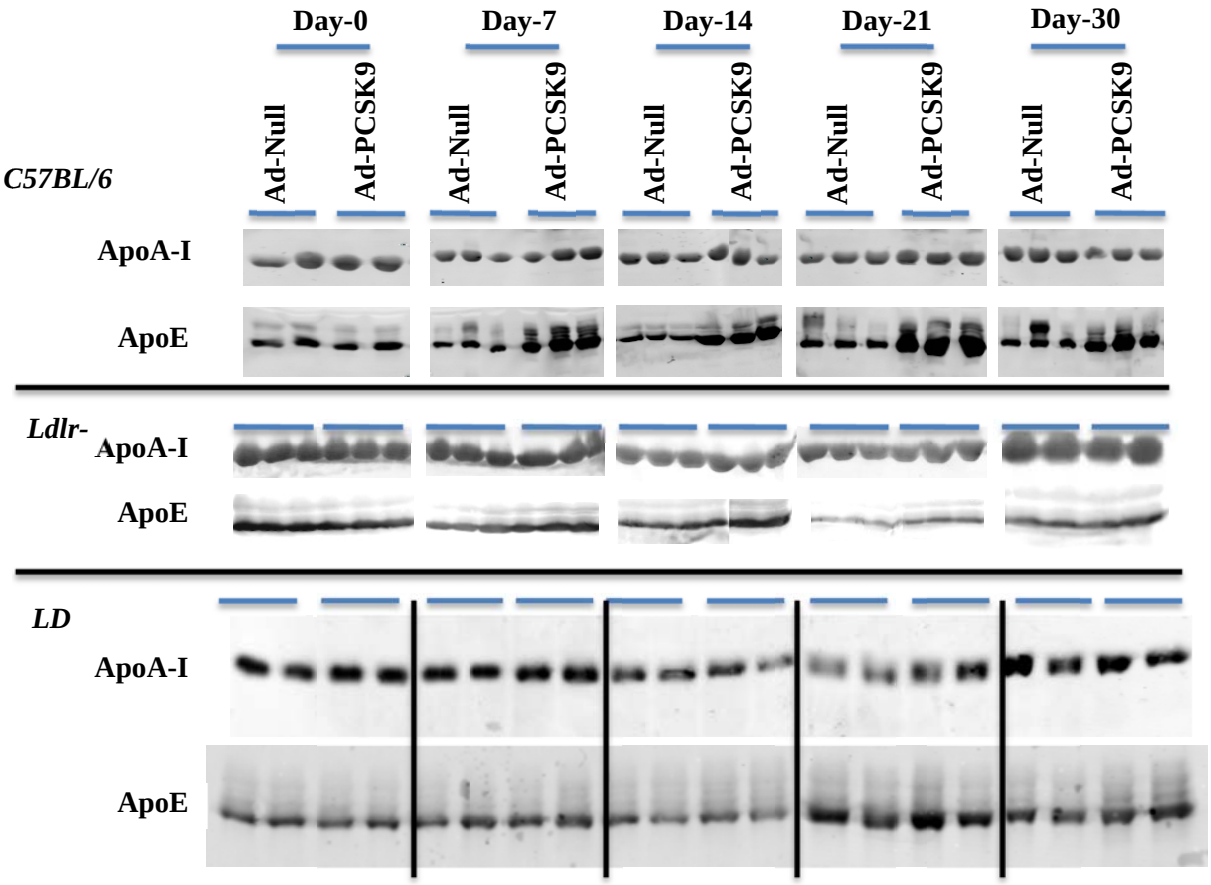

Figure 10. Western blot analysis of plasma apoA-1 and apoE.

C57BL/6, Ldlr-/-, and *LDb* mice were transduced with either Ad-PCSK9 or Ad-Null. One microliter of the plasma from each mouse was subjected to SDS-PAGE, followed by Western blotting with anti-mouse apoA-I or apoE. The positions of apoA-I and apoE are marked. There was no obvious difference in plasma apoAI and apoE levels upon overexpression of PCSK9 in *Ldlr-/-* and *LDb* mice. However, plasma apoE levels were increased in *C57BL/6* mice after treatment. There was no difference in apoAI levels in C57BL/6 mice after treatment.

8. Overexpression of PCSK9 increases apoB levels in VLDL and LDL

We then investigated the apoB, apoE, and apoAI levels by Western blot analysis in VLDL, LDL, and HDL fractions. We analyzed samples from *LDb* mice only. Upon overexpression of PCSK9 in *LDb* mice, the apoB-100 levels were increased in VLDL and LDL fractions as shown in Figure 11A. Unlike plasma apoE levels, the apoE levels in VLDL and LDL fractions were elevated in *LDb* mice treated with Ad-PCSK9, whereas there were no obvious changes in ApoAI levels in HDL fractions (Figure 11B).

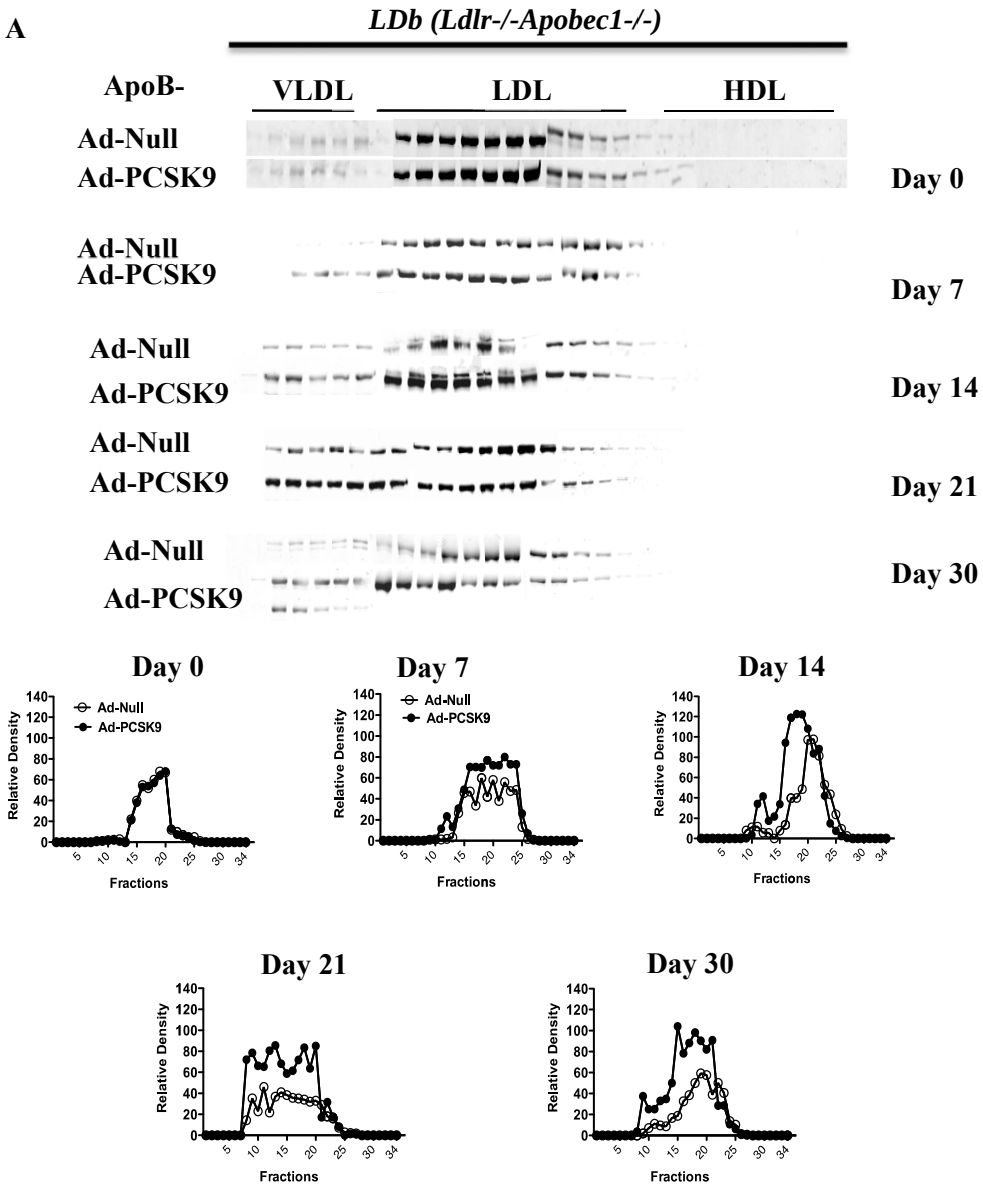
A
LDb (Ldlr-/-Apobec1-/-)
ApoB-
VLDL
LDL
HDL
Ad-Null
Ad-PCSK9
Day 0
Day 7
Day 14
Day 21
Day 30
Relative Density
Fractions
Ad-Null
Ad-PCSK9

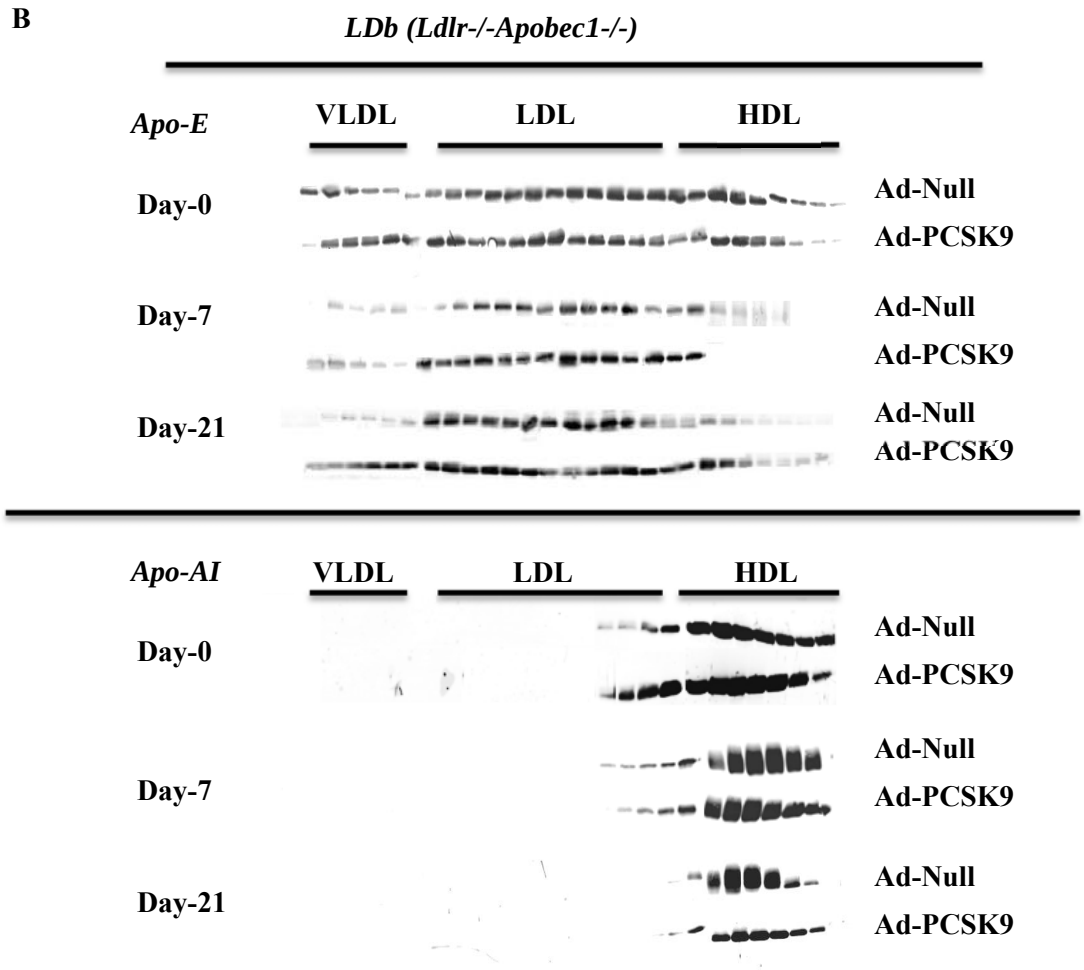

Figure 11. Western blot analysis of apoB, apoE, and apoAI in lipoprotein fractions.

(A) Western blot analysis of apoB levels in lipoprotein fractions. Pooled plasma samples from LDb mice at days 0, 7, 14, 21, and 30 were fractionated by FPLC. Fractions (10 μL) of VLDL, LDL, and HDL were analyzed by SDS-PAGE, followed by Western blotting with anti-mouse apoB. The intensity of each band was determined using an Odyssey Infrared Imaging system (Li-COR, Lincoln, NE). Western blot analysis shows the levels of apoB in VLDL and LDL fractions are markedly elevated in *LDb* mice transduced with Ad-PCSK9. Open circles represent Ad-Null group and closed squares represent Ad-PCSK9 group.

(B) Western blot analysis of apoA-I levels in lipoprotein fractions. Pooled plasma samples from *LDb* mice at days 0, 7, 21 were fractionated by FPLC. Fractions (10 μL) of VLDL, LDL, and HDL were analyzed by SDS-PAGE, followed by Western blotting with anti-mouse apoA-I or apoE. The intensity of each band was determined using an Odyssey Infrared Imaging system (Li-COR, Lincoln, NE). The apoE levels in VLDL and LDL fractions were elevated in *LDb* mice treated with Ad-PCSK9, whereas there were no obvious changes in ApoA-I levels in HDL fractions.

9. The influences of overexpression of PCSK9 on cholesterol and triacylglycerol synthesis pathway are not obvious

To investigate whether overexpression of PCSK9 alters the cholesterol or lipid synthesis pathway, we measured the genes and proteins expression levels on the key enzymes and transcriptional factors that play regulatory roles. The sequences of primers and probes specific for each gene are listed in Table 1. We performed real-time quantitative PCR to measure the mRNA levels of each gene, and we did Western blot analysis to detect the protein levels. The results were analyzed by one-way and 2-way ANOVA.

HMG-CoA synthetase and HMG-CoA reductase are the 2 key enzymes in cholesterol biosynthesis pathway. Acetyl-CoA carboxylase, fatty acid synthase, stearoyl-CoA desaturase-1, and glycerol-3-phosphate acyltransferase are the key enzymes in triacylglycerol biosynthesis pathway. SREBP1-a, and -1c are 2 very important transcriptional factors controlling fatty acid synthesis. SREBP-2 is the most important transcriptional factor that regulates intracellular cholesterol biosynthesis. Recent studies confirmed that it also regulates PCSK9 transcription. In this study, there were no obvious and consistent influences on gene expression levels by overexpression of PCSK9 (Figures 12A, 12B, 12C, and Tables 4 and 5). Moreover, no significant differences were noted in the protein levels of these gene products, as determined by Western blot analysis (Figures 13A, 13B, and 13C). Our results, in agreement with previous studies (16, 106), indicate that PCSK9 expression has no obvious effects on the genes governing cholesterol and TAG biosynthesis.

A

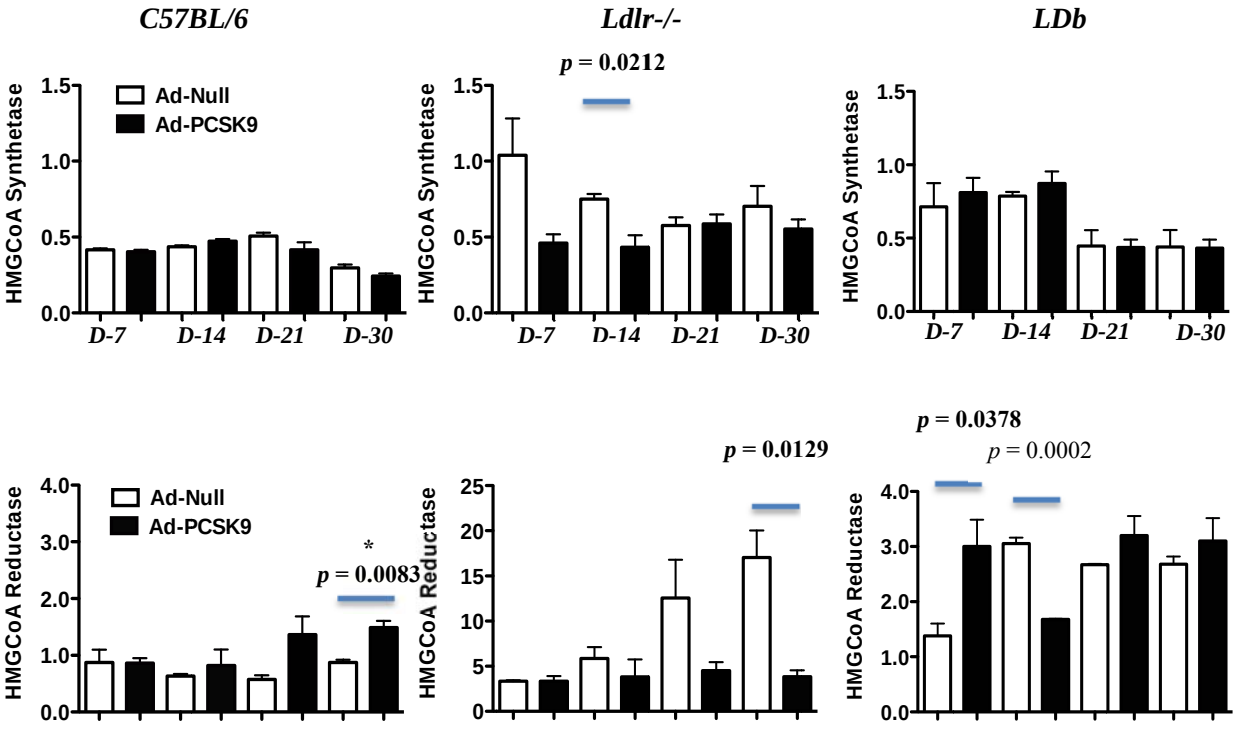
C57BL/6
Ldlr-/-
LDb
Ad-Null
Ad-PCSK9
HMGCoA Synthetase
HMGCoA Reductase
D-7
D-14
D-21
D-30
p = 0.0212
p = 0.0083
p = 0.0129
p = 0.0378
p = 0.0002
*

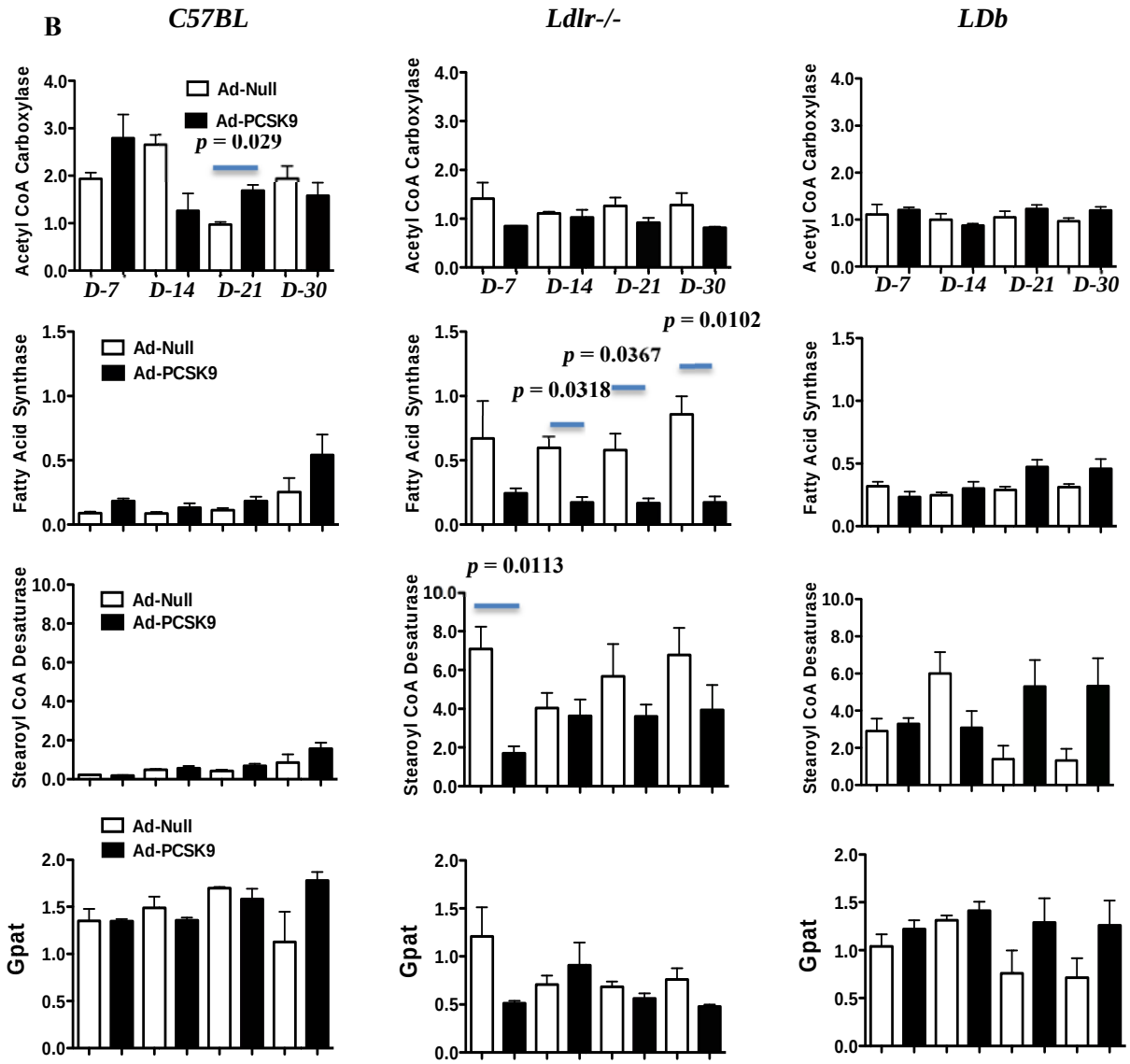
B
C57BL
Ldlr-/-
LDb
Acetyl CoA Carboxylase
Ad-Null
Ad-PCSK9
p = 0.029
D-7
D-14
D-21
D-30
Fatty Acid Synthase
p = 0.0102
p = 0.0367
p = 0.0318
Stearoyl CoA Desaturase
p = 0.0113
Gpat

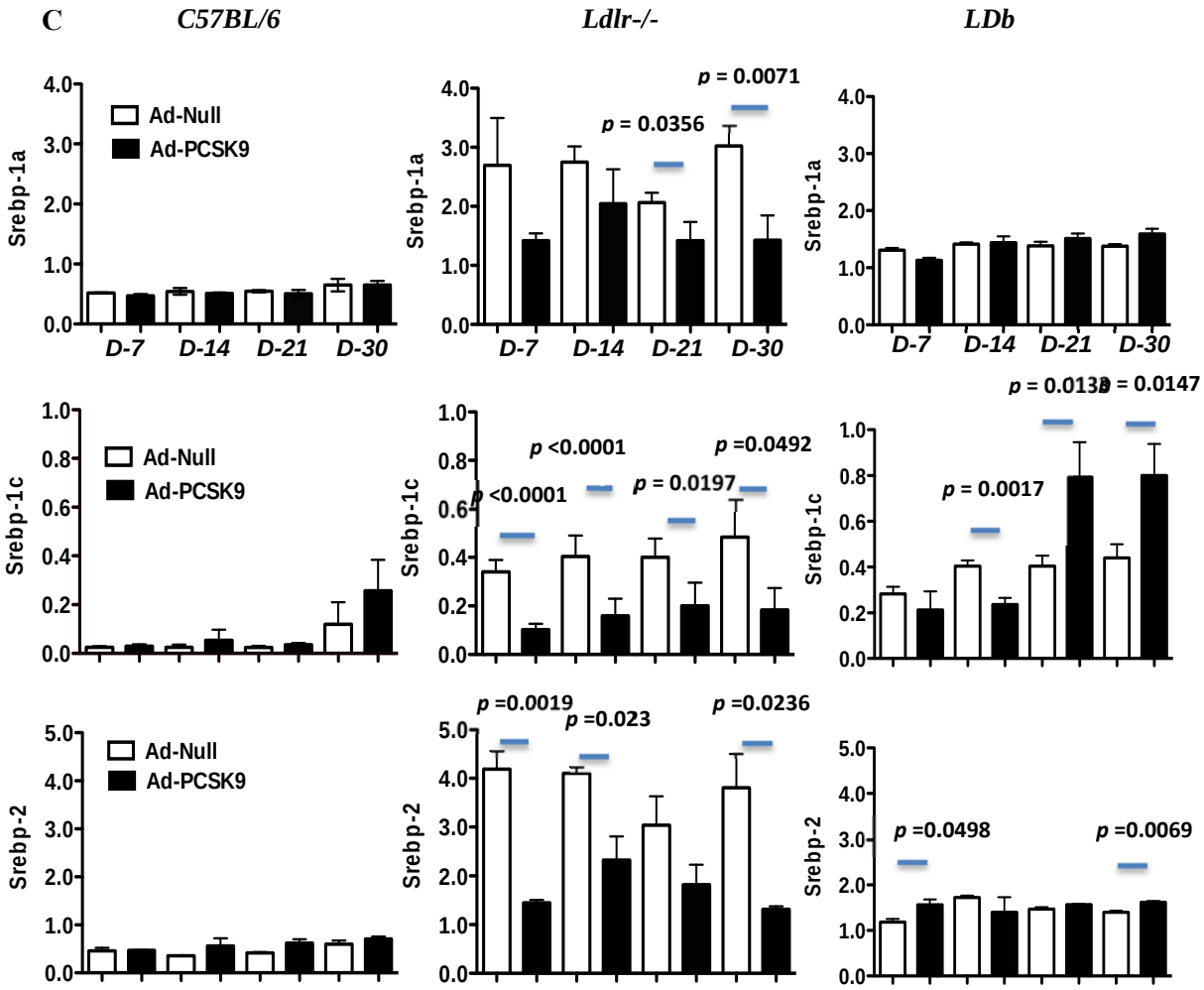

Figure 12. Quantitative RT-PCR hepatic gene expression analysis from *C57BL/6, Ldlr-/-*, and *LDb* mice after transduction with Ad-Null or Ad-PCSK9.

C57BL/6, Ldlr-/-, and *LDb* mice (n = 24 for each group; each time point n = 3) were transduced with either Ad-Null or Ad-PCSK9. The hepatic gene expression levels were determined using SYBR quantitative RT-PCR method. The results were normalized with 16S RNA and presented as mean ± SD. The black bars represent Ad-PCSK9 group and the open bars represent Ad-Null group.

(A) The hepatic cholesterol synthesis gene expression levels show no obvious changes upon Ad-PCSK9 transducing.

(B) The hepatic triglyceride synthesis gene expression levels show no obvious changes upon Ad-PCSK9 transducing.

(C) The hepatic transcriptional factor gene expressions show no obvious changes upon Ad-PCSK9 transducing.

Table 4. One-way ANOVA (Treatment comparison of Ad-Null versus Ad-PCSK9) on gene expression levels of HMG-CoA Synthetase, HMG-CoA Reductase, Acetyl CoA Carboxylase, Fatty Acid Synthase, Stearoyl CoA Desaturase 1, Gpat, Srebp-1a, Srebp-1c, and Srebp-2 in wild-type *C57BL/6J, Ldlr-/-, and LDb* mice. P values are shown. $P < 0.05$ is significant, and it is highlighted in yellow.

	Treatment p Values (Ad-PCSK9 versus Ad-Null)				
	Day-0	**Day-7**	**Day-14**	**Day-21**	**Day-30**
Cholesterol Biosynthesis Pathway					
HMG-CoA Synthetase					
C57BL/6	ND	0.4216	0.0835	0.1732	0.1432
Ldlr-/-	ND	0.0801	0.0212	0.0981	0.3680
LDb	ND	0.6386	0.3694	0.9376	0.9614
HMG-CoA Reductase					
C57BL/6	ND	0.9586	0.5448	0.0715	0.0083
Ldlr-/-	ND	0.3779	0.4255	0.1378	0.0129
LDb	ND	0.0378	0.0002	0.2104	0.3894
Triacyglycerol Biosynthesis Pathway					
Acetyl CoA Carboxylase					
C57BL/6	ND	0.1695	0.0290	0.0059	0.3819
Ldlr-/-	ND	0.1601	0.6349	0.1494	0.1316
LDb	ND	0.6952	0.4266	0.3352	0.0920
Fatty Acid Synthase					
C57BL/6	ND	0.0161	0.2417	0.1472	0.2146
Ldlr-/-	ND	0.2185	0.0138	0.0367	0.0102
LDb	ND	0.1835	0.4190	0.0438	0.1348
Stearoyl CoA Desaturase 1					
C57BL/6	ND	0.3099	0.4990	0.0770	0.2520
Ldlr-/-	ND	0.0113	0.7413	0.3064	0.2099
LDb	ND	0.6254	0.1146	0.0701	0.0692
GPAT					
C57BL/6	ND	0.9806	0.3524	0.3543	0.1209
Ldlr-/-	ND	0.0853	0.4760	0.1848	0.0752
LDb	ND	0.3113	0.3922	0.2017	0.1738
Transcription Factors					
Srebp-1a					
C57BL/6	ND	0.1242	0.6302	0.5772	0.9797
Ldlr-/-	ND	0.0538	0.1313	0.0356	0.0071
LDb	ND	0.0389	0.8713	0.3094	0.0967
Srebp-1c					
C57BL/6	ND	0.4391	0.3391	0.1430	0.1980
Ldlr-/-	ND	0.0000	0.0000	0.0197	0.0492
LDb	ND	0.2306	0.0017	0.0133	0.0147
Srebp-2					
C57BL/6	ND	0.8810	0.2403	0.0591	0.2943
Ldlr-/-	ND	0.0019	0.0230	0.4549	0.0236
LDb	ND	0.0498	0.3857	0.0831	0.0069

Table 5. **Two factors ANOVA (Treatment and Time) on gene expression levels of HMG-CoA Synthetase, HMG-CoA Reductase, Acetyl CoA Carboxylase, Fatty Acid Synthase, Stearoyl CoA Desaturase 1, Gpat, Srebp-1a, Srebp-1c, and Srebp-2 in wild-type *C57BL/6, Ldlr-/-* and *LDb* mice treated with Ad-Null and Ad-PCSK9**. P values are shown. $P < 0.05$ is significant and highlighted in yellow.

	Main Factor *Treatment*	*Time*	Interaction *Treatment x Time*
Cholesterol Biosynthesis Pathway			
HMG-CoA Synthetase			
C57BL/6	0.0856	0.0000	0.0764
Ldlr-/-	0.0044	0.4271	0.0882
LDb	0.5509	0.0009	0.9090
HMG-CoA Reductase			
C57BL/6	0.0074	0.1229	0.1426
Ldlr-/-	0.0012	0.0961	0.1366
LDb	0.1438	0.0367	0.0006
Triacyglycerol Biosynthesis Pathway			
Acetyl CoA Carboxylase			
C57BL/6	0.8001	0.0130	0.0026
Ldlr-/-	0.0079	0.9692	0.5416
LDb	0.2554	0.2355	0.4541
Fatty Acid Synthase			
C57BL/6	0.0261	0.0033	0.3490
Ldlr-/-	0.0001	0.6776	0.6835
LDb	0.0344	0.0333	0.0406
Stearoyl CoA Desaturase 1			
C57BL/6	0.0819	0.0008	0.2912
Ldlr-/-	0.0032	0.5816	0.1883
LDb	0.0723	0.4741	0.0081
GPAT			
C57BL/6	0.3159	0.2290	0.0372
Ldlr-/-	0.0497	0.2812	0.0555
LDb	0.0180	0.2013	0.5043
Transcription Factors			
Srebp-1a			
C57BL/6	0.4698	0.0504	0.9677
Ldlr-/-	0.0000	0.0956	0.2112
LDb	0.3748	0.0068	0.0649
Srebp-1c			
C57BL/6	0.0710	0.0003	0.1889
Ldlr-/-	0.0000	0.2144	0.8080
LDb	0.0019	0.0000	0.0000
Srebp-2			
C57BL/6	0.0183	0.0598	0.4803
Ldlr-/-	0.0000	0.2887	0.2896
LDb	0.3211	0.5116	0.0796

A

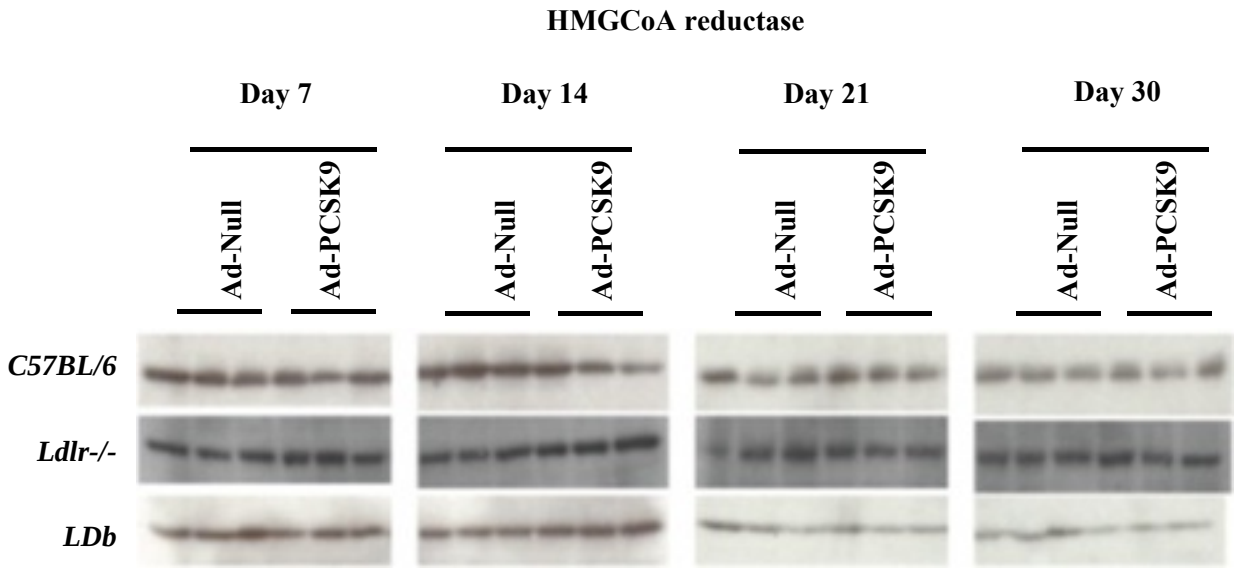
HMGCoA reductase
Day 7
Day 14
Day 21
Day 30
Ad-Null
Ad-PCSK9
Ad-Null
Ad-PCSK9
Ad-Null
Ad-PCSK9
Ad-Null
Ad-PCSK9
C57BL/6
Ldlr-/-
LDb

B

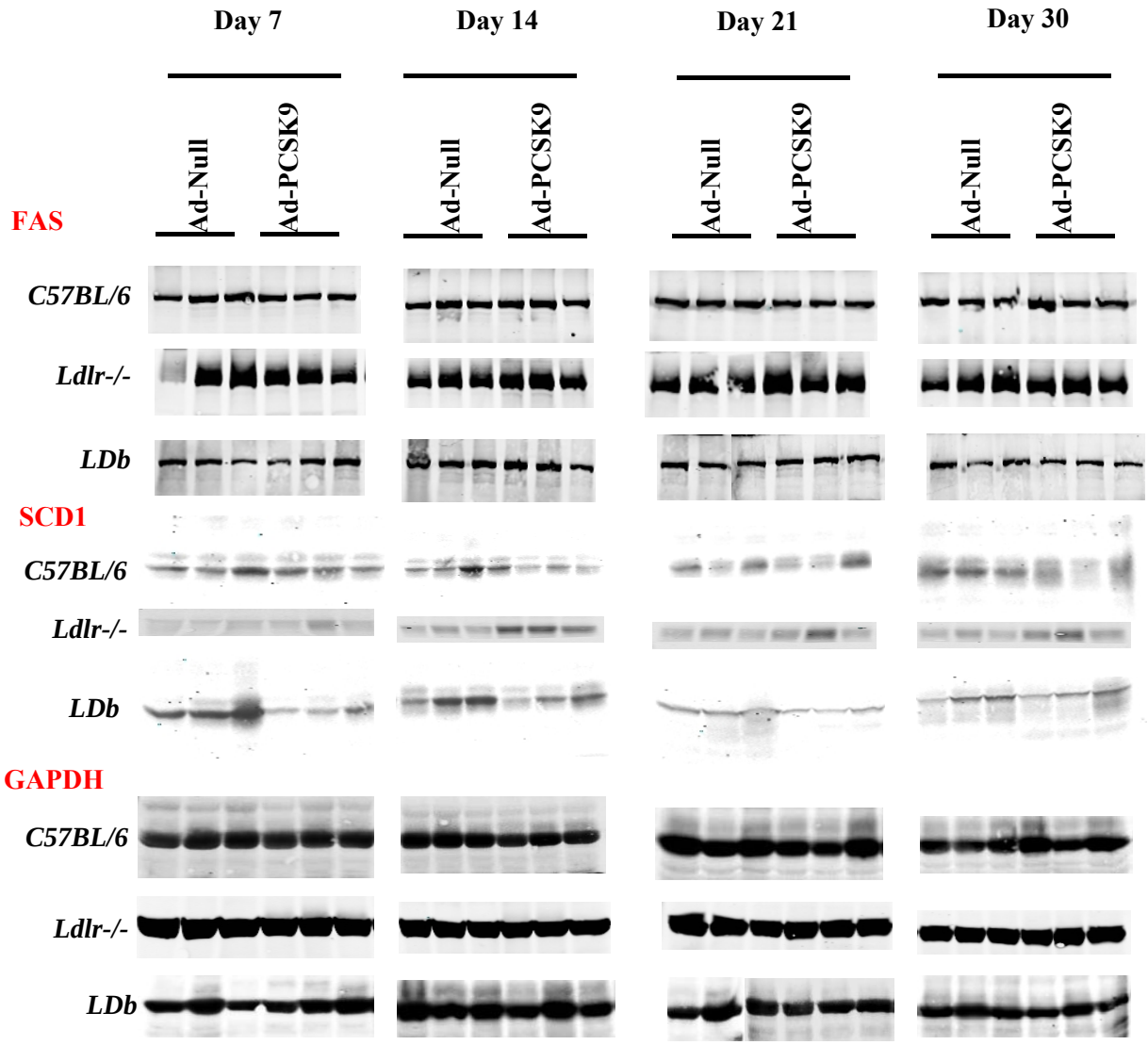
Day 7
Day 14
Day 21
Day 30
Ad-Null
Ad-PCSK9
FAS
C57BL/6
Ldlr-/-
LDb
SCD1
C57BL/6
Ldlr-/-
LDb
GAPDH
C57BL/6
Ldlr-/-
LDb

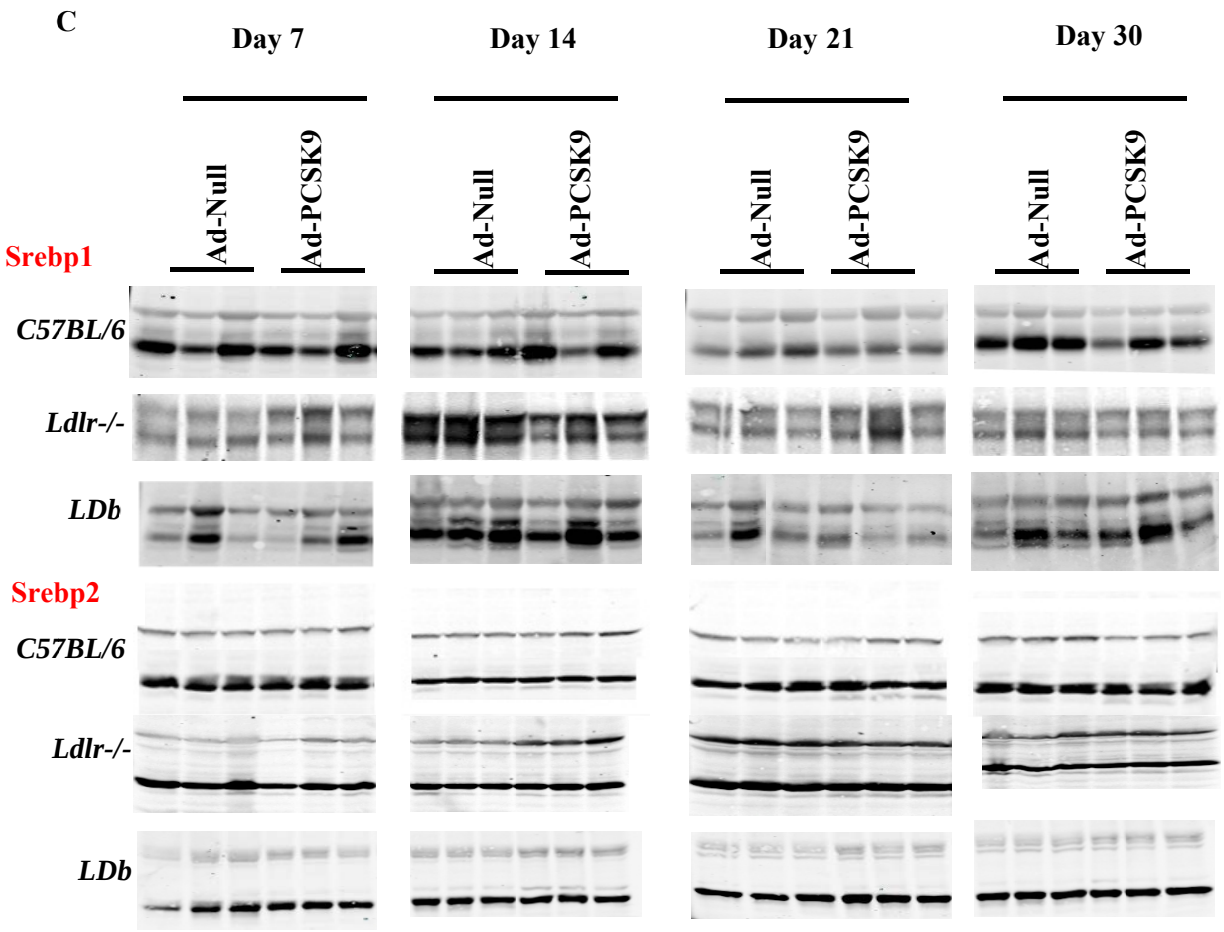

Figure 13. Western blot analysis of hepatic proteins from *C57BL/6, Ldlr-/-,* and *LDb* mice after Ad-Null or Ad-PCSK9 transduction.

C57BL/6, Ldlr-/-, and *LDb* mice (n = 24 for each group; each time point n = 3) were transduced with either Ad-Null or Ad-PCSK9. Fifty micrograms of total liver protein lysates were subjected to Western blotting using corresponding antibodies against the enzymes or transcriptional factors. The membranes were scanned by Li-cor Odyssey Infrared scanner. Gadph was used as loading control.

(A) The hepatic cholesterol synthesis enzyme levels show no obvious changes upon Ad-PCSK9 transduction.

(B) The hepatic triglyceride synthesis enzyme levels show no obvious changes upon Ad-PCSK9 transduction.

(C) The hepatic transcription factor levels show no obvious changes upon Ad-PCSK9 transduction.

10. Overexpression of PCSK9 has no effect on apoB mRNA levels in mice.

To investigate the effect of PCSK9 on apoB mRNA levels, we used real-time quantitative PCR to determine the apoB mRNA levels. As shown in Figure 14, upon over-expression of PCSK9, there was no difference on apoB mRNA levels when comparing the Ad-PCSK9 group with Ad-Null group. These results suggested that the increased apoB levels upon overexpression of PCSK9 might be regulated posttranscriptionally.

It is worth noting that the apoB mRNA levels in *Ldlr-/-* mice were 2-fold higher than that of *C57BL/6* mice. The apoB mRNA levels in *LDb* mice were 4-fold higher than that of *C57BL/6* mice. The reason that deficiency of LDLR resulted in increased apoB mRNA levels was not clear, but the increased apoB mRNA levels in *Ldlr-/-* and *LDb* mice are correlated with increased apoB production at baseline when compared with wild-type *C57BL/6* mice (Figure 9). In *Ldlr-/-* mice, apoB-100 and apoB-48 levels were 1.98- and 2.69 fold higher than that of *C57BL/6* mice, whereas *LDb* mice had 1.28 fold higher apoB-100 levels than that of *C57BL/6* mice.

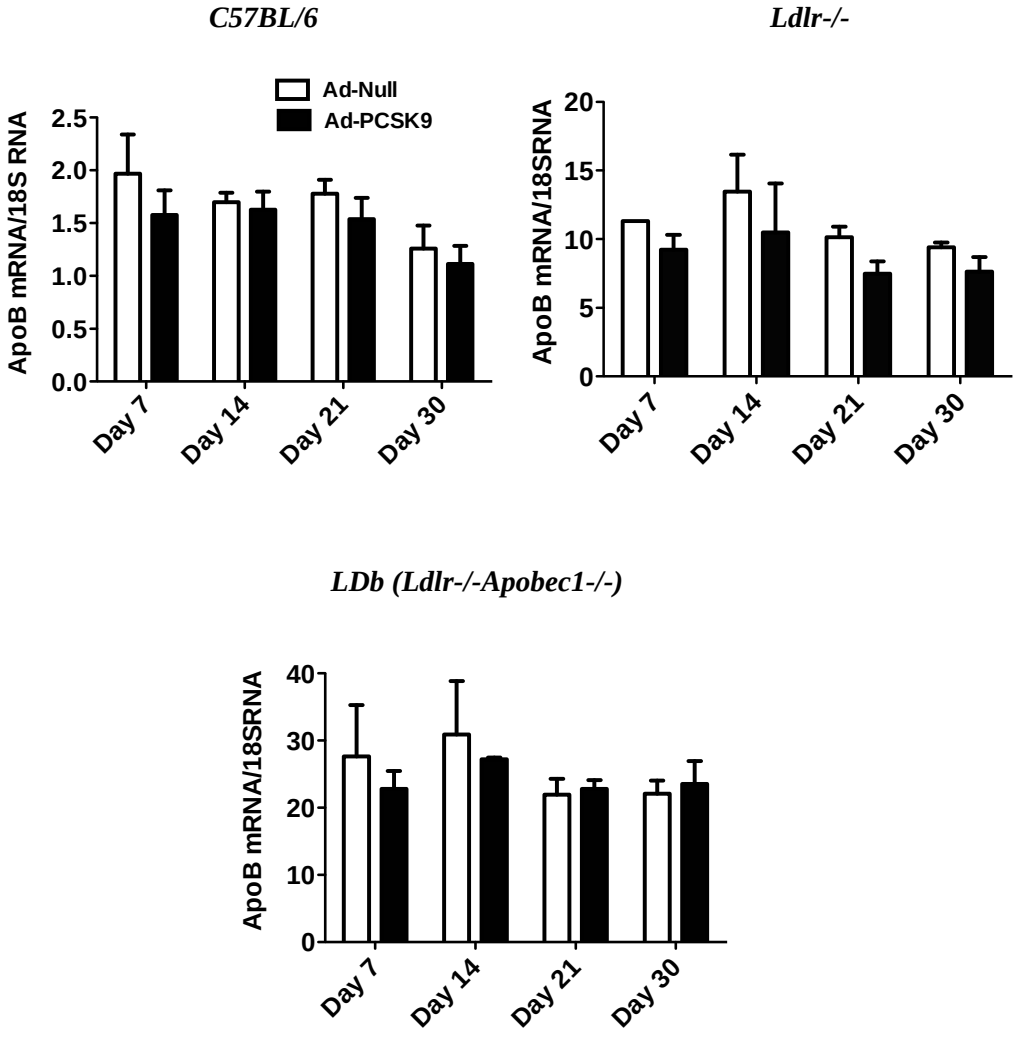

Figure 14. Quantitative RT-PCR apoB gene expression analysis from *C57BL/6, Ldlr-/-*, and *LDb* mice after transduction with Ad-Null or Ad-PCSK9.

Total RNAs were extracted from the livers of the mice transduced with Ad-Null or Ad-PCSK9. RNAs were subjected to reverse transcription into cDNA and the gene expression levels were detected by Taqman primers and probe real-time PCR. The results were normalized with 18S RNA and presented as mean ± SD. The black bars represent Ad-PCSK9 group and the open bars represent Ad-Null group.

11. PCSK9 is associated with VLDL and LDL, but mostly with LDL

Next, we determined whether PCSK9 is associated with apoB-containing lipoprotein particles. We measured endogenous mouse plasma PCSK9 levels in non-treated *C57BL/6, Ldlr-/-,* and *LDb* mice by using ELISA (92 ± 7.8, 2015 ± 140, and 1646 ± 380 ng/mL, respectively); mice lacking LDLR had ~20-fold more PCSK9 than wild-type C57BL/6 mice. Interestingly, the apoB levels of *Ldlr-/-* and *LDb* mice were ~ 2- and 1.2-fold, respectively higher than that of wild-type *C57BL/6* as determined by Western blot analysis. These results suggest that the regulation of PCSK9 and apoB are probably tightly associated intracellularly.

We also used ELISA to measure the endogenous mouse PCSK9 levels in the lipoprotein fractions. It shows that 30% and 41% of the plasma PCSK9 was associated with LDL in Ldlr-/- and LDb mice, respectively (Figure 15). The PCSK9 level in the fractions of C57BL/6 mice was too low to calculate the distribution percentage. Taken together, our results demonstrate that a substantial amount of endogenous PCSK9 is associated mostly with LDL in the circulation.

Next, we used ELISA to determine the distribution of overexpressed human PCSK9 in plasma lipoproteins. Unlike endogenous mouse PCSK9 distribution, a small percentage of recombinant human PCSK9 was in LDL fractions of *C57BL/6, Ldlr-/-,* and *LDb* mice; 11%, 16%, and 17%, respectively. Western blot analysis shows that PCSK9 was predominantly present in the LDL fractions from day 7 to day 30 in LDb mice (Figure 16A). When we concentrated the plasma fractions of VLDL, LDL, and HDL of *C57BL/6, LDb,* and *Ldlr-/-* mice, PCSK9 was detected in both VLDL and LDL, but not in HDL fractions, as shown on day 7 after Ad-PCSK9 transduction (Figure 16B). These results indicate that PCSK9 is associated with both VLDL and LDL, but mostly with LDL particles.

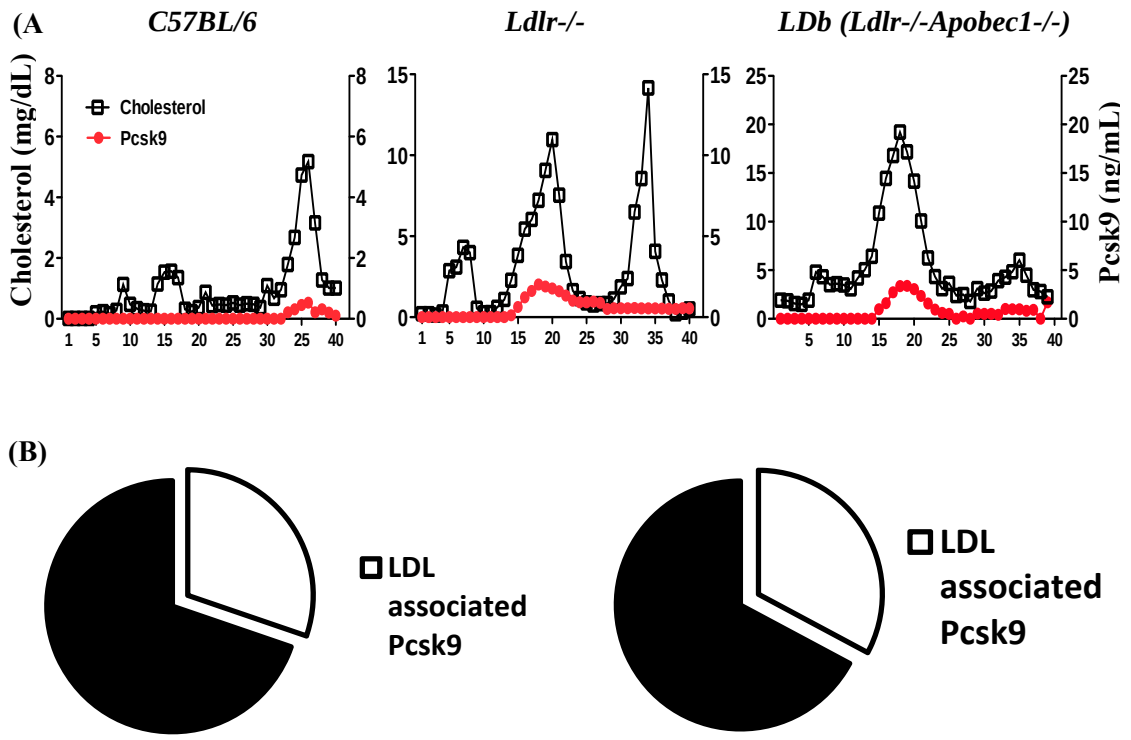

PCSK9 LDL association in *Ldlr-/-* mice

PCSK9 LDL association in *LDb*

Figure 15. PCSK9 is associated with VLDL and LDL, but mostly with LDL.

(A) **Association of endogenous mouse PCSK9 with lipoproteins**. Plasma samples of *C57BL/6, Ldlr −/−,* and *LDb* mice were fractionated by fast protein liquid chromatography (FPLC). The levels of total cholesterol (mg/dL) and mouse PCSK9 (ng/mL) were determined. The total cholesterol levels are shown as open squares, and the mouse PCSK9levels are shown as closed circles.

(B) **The proportions of PCSK9 levels associated with LDL fractions**. PCSK9 levels in the fractionated mouse plasma were measured with standard ELISA procedure according to the company manual. The total amount of PCSK9 levels in the LDL fractions was calculated according to the volume of the plasma loaded into the FPLC system. The data were presented as percentages of LDL associated PCSK9 in total loaded plasma PCSK9.

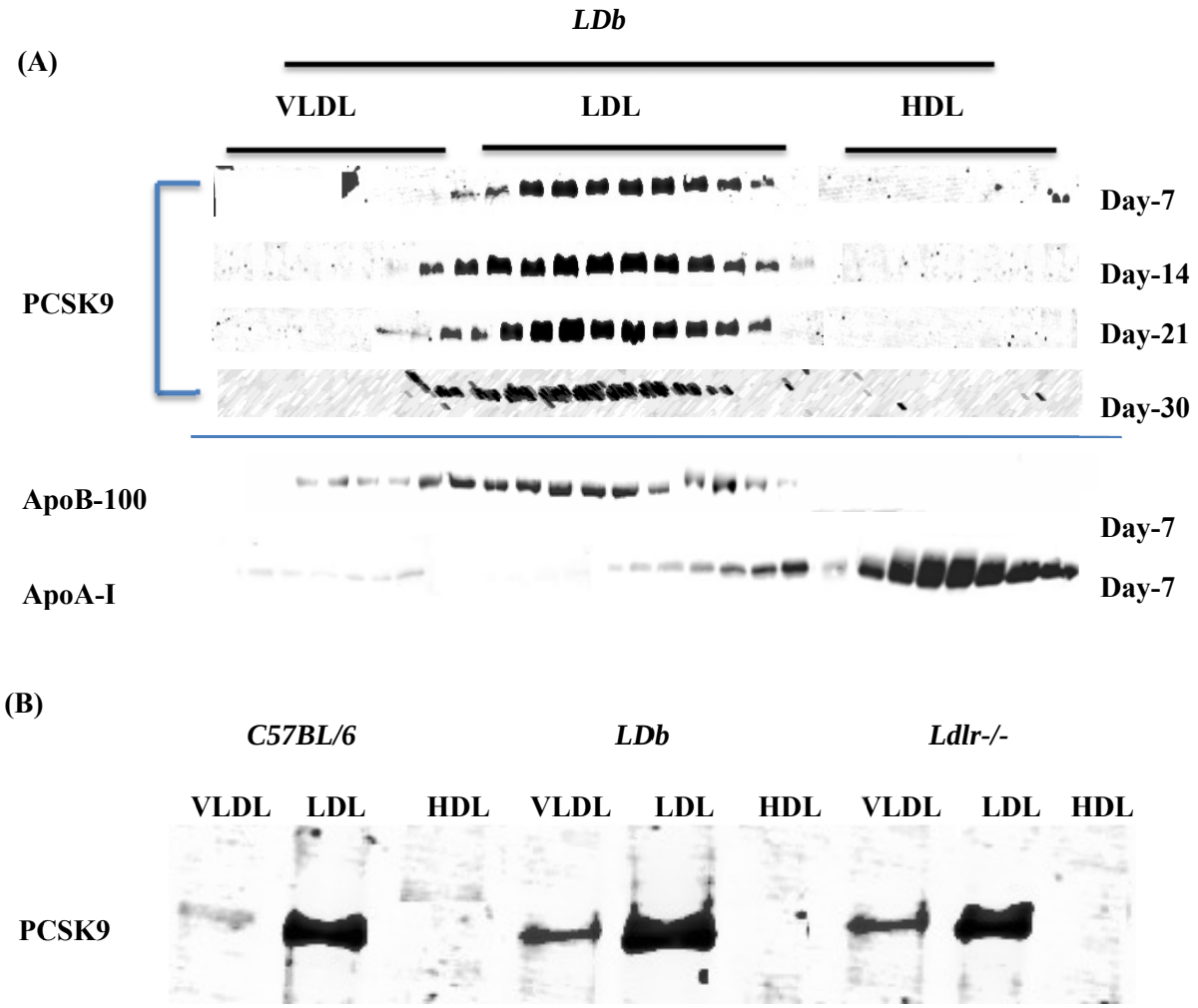

Figure 16. PCSK9 is associated with plasma LDL.

(A) Pooled plasma samples of *LDb* mice (n = 3 for each time point) on days 7, 14, 21, and 30 after transduction with adenovirus PCSK9 (Ad-PCSK9) were fractionated by FPLC. Each fraction was resolved by SDS-PAGE, followed by Western blot analysis using an anti-FLAG antibody to detect human PCSK9. The position of PCSK9 is marked. The corresponding fractions from day 7 were probed with anti-mouse apolipoprotein B (apoB) and anti-mouse apoA-I antibodies, respectively. The positions of apoB100 and apoA-I are marked.

(B) Pooled/concentrated FPLC-fractionated VLDL, LDL, and high-density lipoprotein (HDL) of *C57BL/6, Ldlr −/−,* and *LDb* mice on day 7 after Ad-PCSK9 transduction were resolved by SDS-PAGE, followed by Western blot analysis using an anti-FLAG antibody to detect human PCSK9. The position of PCSK9 is marked.

12. PCSK9 interacts with apoB intracellularly.

Next, we asked the question whether PCSK9 interacts with apoB intracellularly. We used 3 different approaches to investigate the interaction of PCSK9 with apoB.

Co-immunoprecipitation of PCSK9 with apoB: We obtained 2 McA-RH7777 cell lines that stably expressed apoB-18 and apoB-48 from Dr. Zemin Yao at University of Ottawa, Canada. Human apoB-18 and apoB-48 cell lines express the N-terminal 18% and 48% of the full-length apoB-100, respectively. The cells were plated onto a 6-well plate, followed by infection with either Ad-PCSK9 or Ad-Null overnight. On the next day, cell media and cell lysates were collected. We used either M2-anti-FLAG antibody or anti-apoB monoclonal 1D1 antibody to immunoprecipitate the PCSK9/apoB complex. As shown in Figure 17, apoB-18 and apoB-48 co-immunoprecipitated with PCSK9 in both cell lysates and cell media by using either anti-Flag antibody or anti-apoB-1D1 antibody. ApoB was not detected in the precipitates from the control cells transduced with Ad-Null. These results suggested that PCSK9 could bind to amino acid sequences within the N-terminal region of apoB, namely, apoB-18. In addition, the association of PCSK9 with apoB occurred both intracellularly and in the media. We failed to co-immunoprecipitate apoB100 with PCSK9. The reason for the failure was unclear.

Mammalian two-hybrid system: We used a mammalian two-hybrid system which expresses secreted alkaline phosphatase (SEAP) as the reporter (107) to determine the interaction of apoB and PCSK9 proteins. We cloned apoB-18 to pM vector and PCSK9 to pVP-16 vector. We used pM vector containing Apobec1 as the negative control and pM vector containing LDL receptor as the positive control. We co-transfected 293 cells and COS-1 cells with the following combinations of plasmid vectors and the reporter vector pG5SEAP is present in all the experiments; pVP16-PCSK9/pM-apoB18, pM-ApoB18/pVP16, pVP16-PCSK9/pM, pM-Apobec1/pVP16-PCSK9, and pM-LDLR/pVP16-PCSK9, pM-LDLR/pVP16, pM/pVP16-PCSK9, and non-transfected. The cells expressed both ApoB-18 and PCSK9 resulted in >10-fold SEAP activity as measured by ELISA,

compared to the controls (i.e., transfected with pVP16-PCSK9/pM, pM-apoB18/pVP-16, pM-Apobec1/pVP16-PCSK9, or pM/pVP16) (Figures 18A and 18B). The interaction of PCSK9/apoB-18 in 293 cells was even stronger than that of PCSK9/LDLR (Figure 18C). These results suggest that PCSK9 binds to apoB intracellularly.

In situ proximity ligation assay (PLA): The *in situ* proximity ligation assay, termed Duolink *in situ* PLA, detects endogenous protein–protein interaction (within 40 nm) at physiological concentrations with a very high specificity (108). To optimize the conditions of the assay, we first performed immunofluorescence assay to make sure the antibody can detect the intracellular proteins such as PCSK9, apoB, or LDLR in cells. In HepG2 cells, apoB and PCSK9 were detected in the cytoplasm, whereas the LDLR was localized on the cell membrane (Figure 19A). In HepG2 cells stably expressing Apobec1, Apobec1 and PCSK9 were also detected in the cytoplasm (Figure 19A).

The endogenous apoB-100 interacts with PCSK9 in the cytoplasm of HepG2 cells (αApoB/αPCSK9), as demonstrated by Duolink *in situ* PLA shown as red dot signals (Figure 19B). As expected, there was also a detectable interaction between PCSK9 and LDLR (αLDLR/αPCSK9). In HepG2 stably expressing Apobec1 cells, the Apobec1 did not interact with PCSK9 (αApobec1/αPCSK9), but there was a strong interaction between apoB and PCSK9 (αApoB/αPCSK9) again in the cytoplasm of these cells (Figure 19B). The following control experiments were performed, which are shown in Figure 19C. There was no interaction between PCSK9 and GAPDH, nor apoB and GAPDH. The experiments of anti-apoB only, or anti-PCSK9 only, or no antibody control are also shown in Figure 19C. Collectively, these 3 different approaches confirmed a physical interaction between PCSK9 and apoB within the hepatocytes.

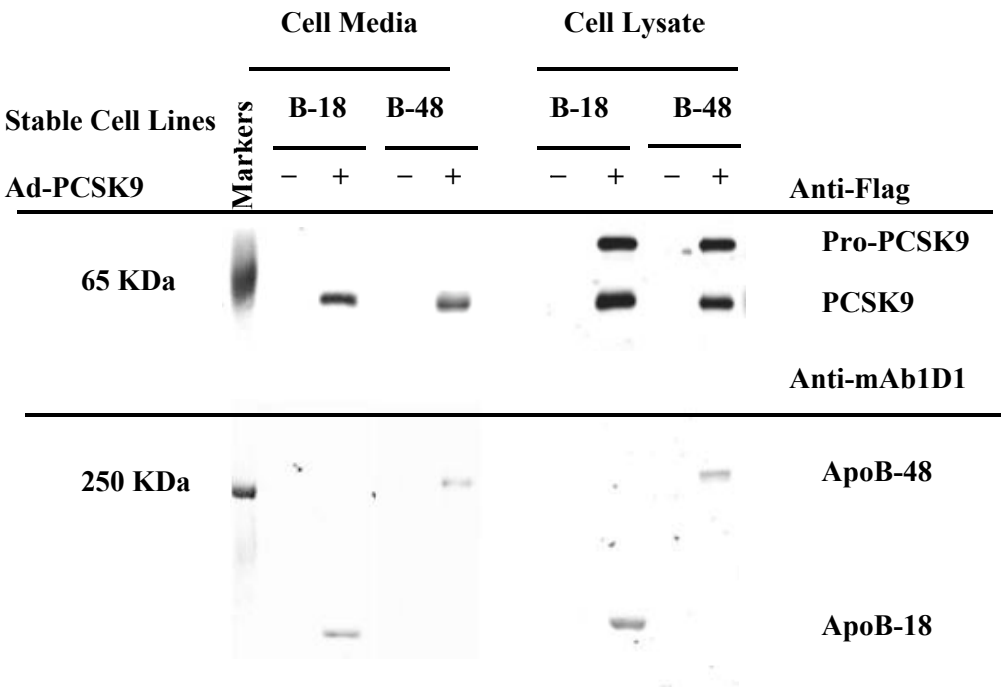

Figure 17. Co-immunoprecipitation of PCSK9 with apoB.

McA-RH7777 stable cell lines expressing human apoB18 or apoB48 were plated onto 6-well plates. The cells were infected with adenovirus PCSK9 (Ad-PCSK9)-FLAG (+) or Ad-Null (−) for 24 h. The immune complexes precipitated by anti-FLAG from cell lysates and cell media were resolved by SDS-PAGE and subjected to Western blot analysis using monoclonal antibody (mAb) 1D1 to detect apoB18 and apoB48 and anti-FLAG antibody to detect human PCSK9. The experiment was performed 4 times, and the representative results are shown here. The positions of PCSK9, apoB18, and apoB48 are marked.

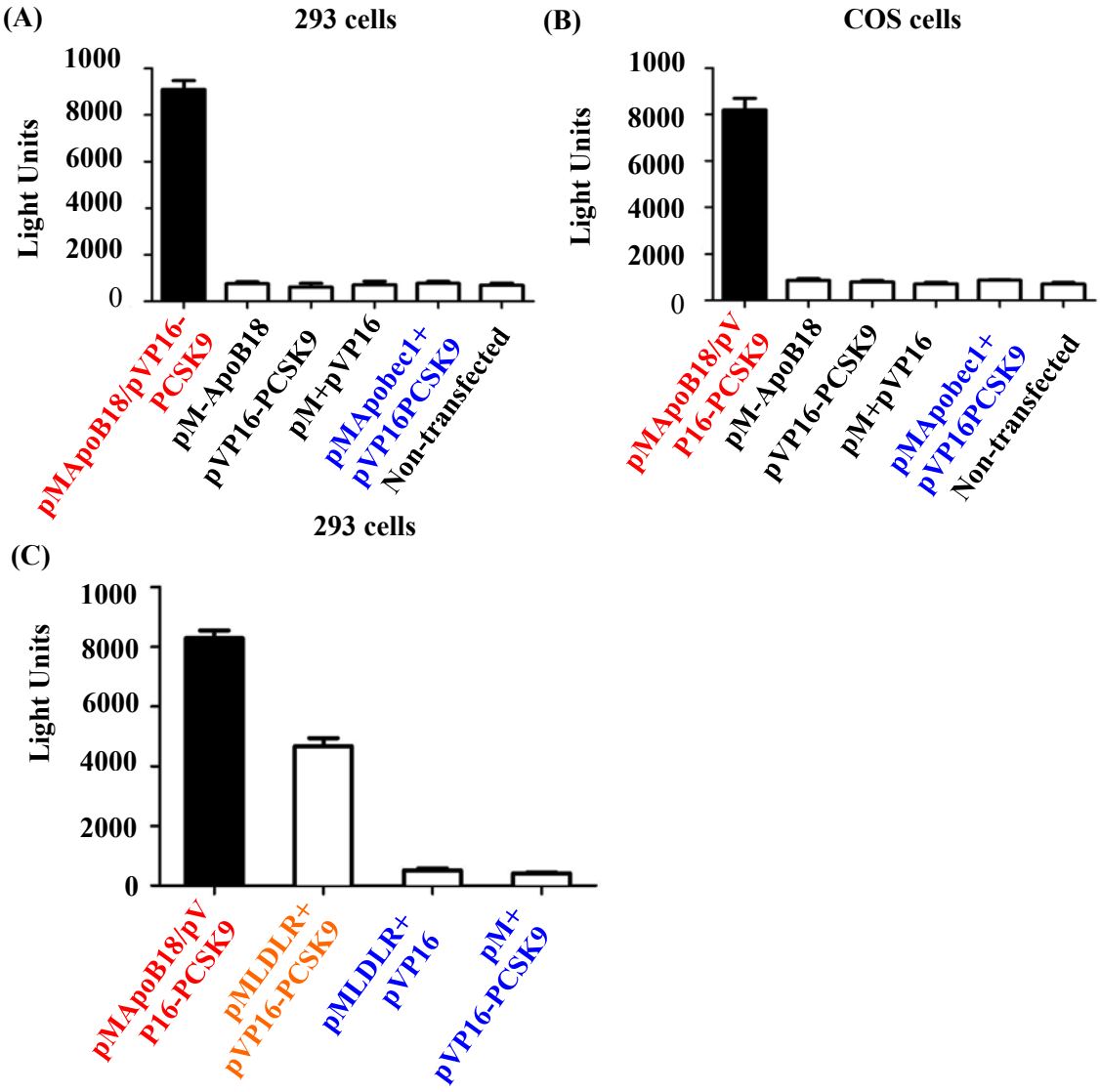

Figure 18. The protein–protein interaction between PCSK9 and apoB18 was observed with a mammalian matchmaker two-hybrid system.

The 293 and COS-1 cells were transfected with the indicated plasmids. At 48 h after transfection, the secreted alkaline phosphatase (SEAP) activities in the cell media were assayed. The results are expressed as light unit (mean ± SD). Control assays included pM-apoB18/pG5SEAP, pVP16-PCSK9/pG5SEAP, pM/pVP16/pG5SEAP, pM-Apobec1/pVP16-PCSK9/pG5SEAP, and pG5SEAP. The pM-LDLR/pVP16-PCSK9 pair in 293 cells was used as a positive control. The assay was carried out 3 times with duplicate samples.

(A)

Immunofluorenscence Staining in HepG2

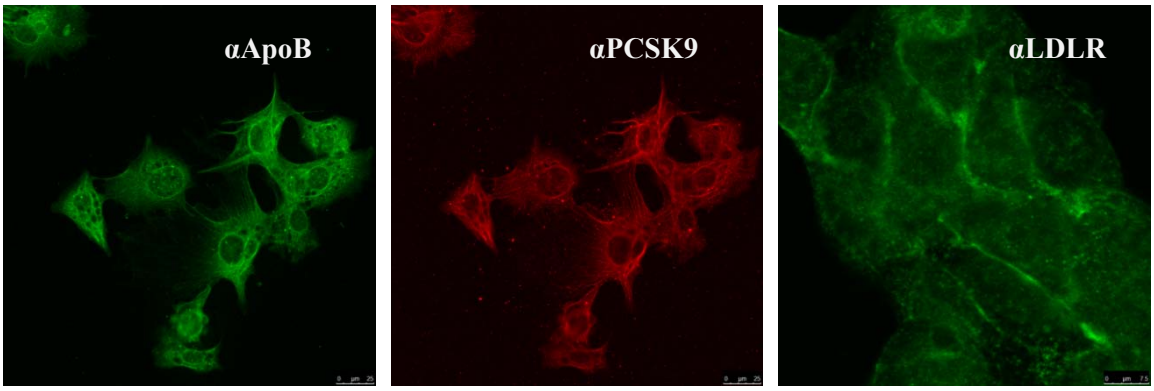

in HepG2 stably expressing Apobec1

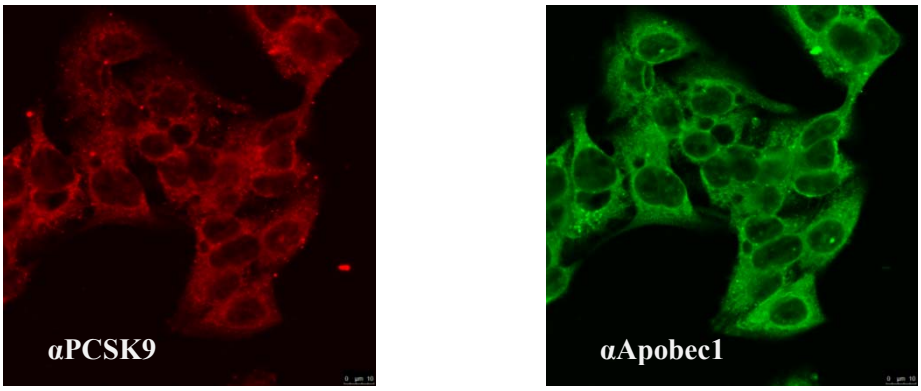

(B)

Duolink in situ PLA (αApoB/αPCSK9) in HepG2 cells

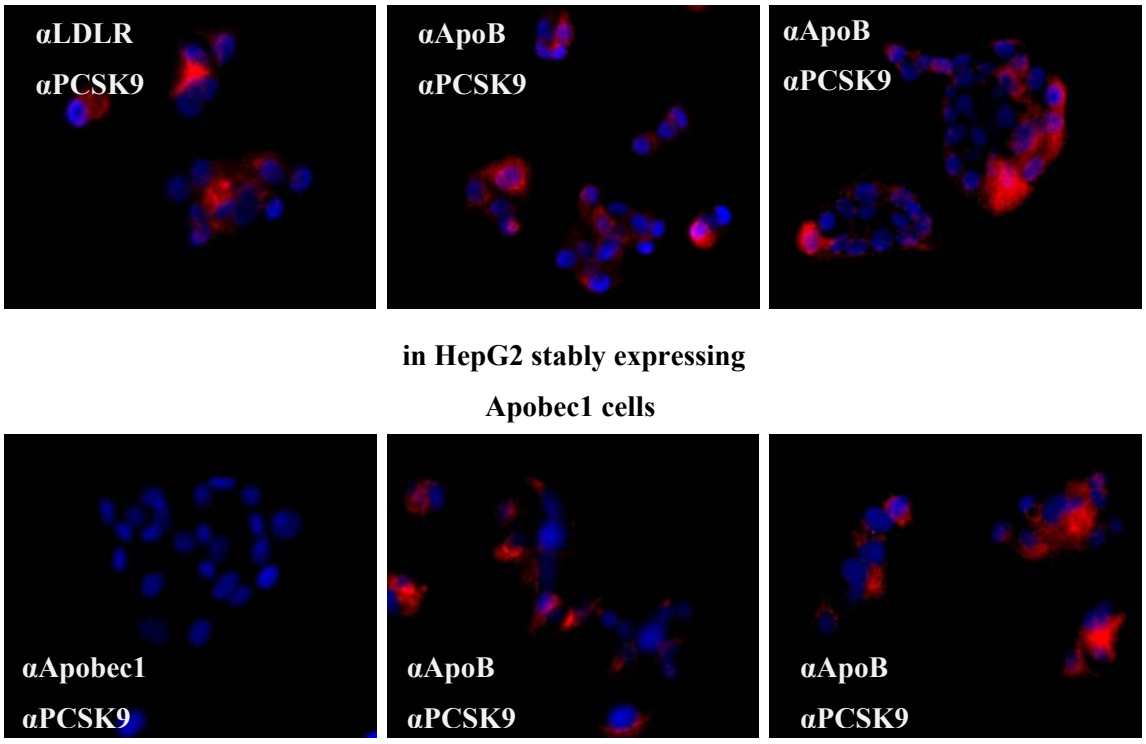

(C)

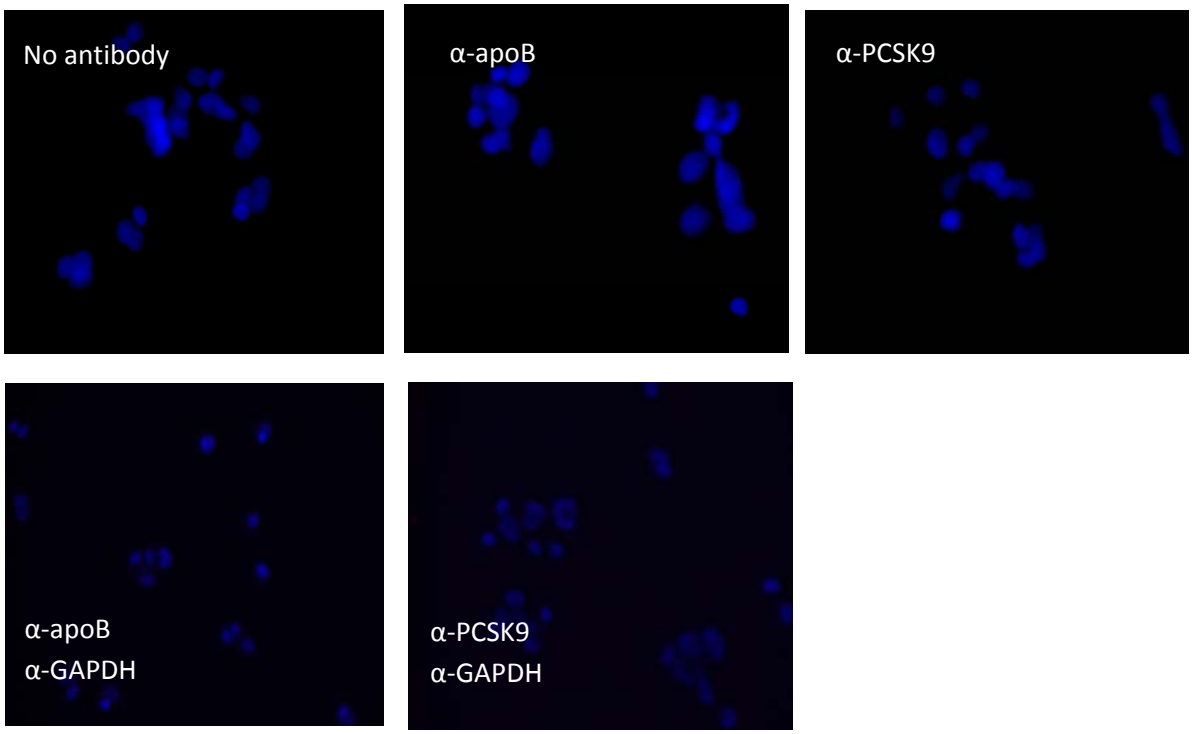

Figure 19. Immunostaining and Duolink *in situ* proximity ligation assay analysis of PCSK9 and apoB.

(A) **Immunofluorescence staining** of endogenous apoB, PCSK9, and LDLR in liver hepatocellular cells (HepG2 cells; top), and those plus Apobec1 in HepG2 stably expressing Apobec1 cells (bottom). The images were captured using a Leica DM 600B confocal microscope with 488 nm, 594 nm, and 633 nm filters. The experiments were performed in triplicate.

(B) **Protein–protein interaction of endogenous PCSK9 and apoB using Duolink *in situ* proximity ligation assay (PLA) in HepG2 cells (top) and HepG2 stably expressing Apobec1 cells (bottom**). The *in situ* PLA was performed using primary antibodies, including anti-apoB (α-ApoB), anti-PCSK9 (α-PCSK9), anti-LDLR (α-LDLR), and anti-Apobec1 (α-Apobec1).

(C) Controls for the PLA in HepG2 cells. The *in situ* PLA was performed using primary antibodies, including anti-apoB (α-ApoB), anti-PCSK9 (α-PCSK9), anti-GADPH.

The images were captured using a Zeiss Axio Observer D1m fluorescence microscope with 4',6-diamidino-2-phenylindole (DAPI), fluorescein isothiocyanate (FITC), and Texas Red filters. The red dots represent the positive protein–protein interaction of apoB with PCSK9 (α-ApoB/α-PCSK9) and LDLR with PCSK9 (α-LDLR/α-PCSK9). The blue nuclear staining is DAPI. Each experiment was performed in triplicate.

13. The interaction of PCSK9 with apoB increases apoB biosynthesis, irrespective of LDL receptor.

We next performed pulse-chase experiments to determine the impact of the PCSK9/apoB interaction on apoB biosynthesis by using primary hepatocytes isolated from *C57BL/6, Ldlr-/-,* and *LDb* (Ldlr-/-Apobec1-/-) mice. The hepatocytes were transduced with either Ad-PCSK9 or Ad-Null vectors overnight. The hepatocytes were then pulsed with ^{35}S-methionine/cysteine for 15 min, and chased for 30, 60, 120, 180, and 240 min. PCSK9 expression in the hepatocytes of *C57BL/6* mice significantly increased the incorporation of ^{35}S-methionine/cysteine into apoB-100 and apoB-48 in cell lysates, as compared to Ad-Null transduced cells (Figure 20A). Similarly, primary hepatocytes of *Ldlr-/-* mice expressing PCSK9 had significantly increased incorporation of ^{35}S-methionine/cysteine into apoB-100 and apoB48 in both cell lysates and media (Figure 20B), and the incorporation of methionine into apoB-100 in *LDb* mice was approximately 3-fold higher than that in either *C57BL/6* or *Ldlr-/-* mice (Figure 20C). The effect of PCSK9 expression on apoB synthesis is specific, because no effect was observed for albumin synthesis (Figure 20D). Thus, our results demonstrated that PCSK9 increased apoB biosynthesis in *C57BL/6* mice containing the LDL receptor and in *Ldlr-/-* and *LDb* mice deficient for the LDL receptor. The increased production of apoB in PCSK9-transduced hepatocytes could not be attributed to the increase of ApoB gene expression, because quantification of the apoB mRNA in the liver showed no difference between animals treated with Ad-PCSK9 and Ad-Null (Figure 14).

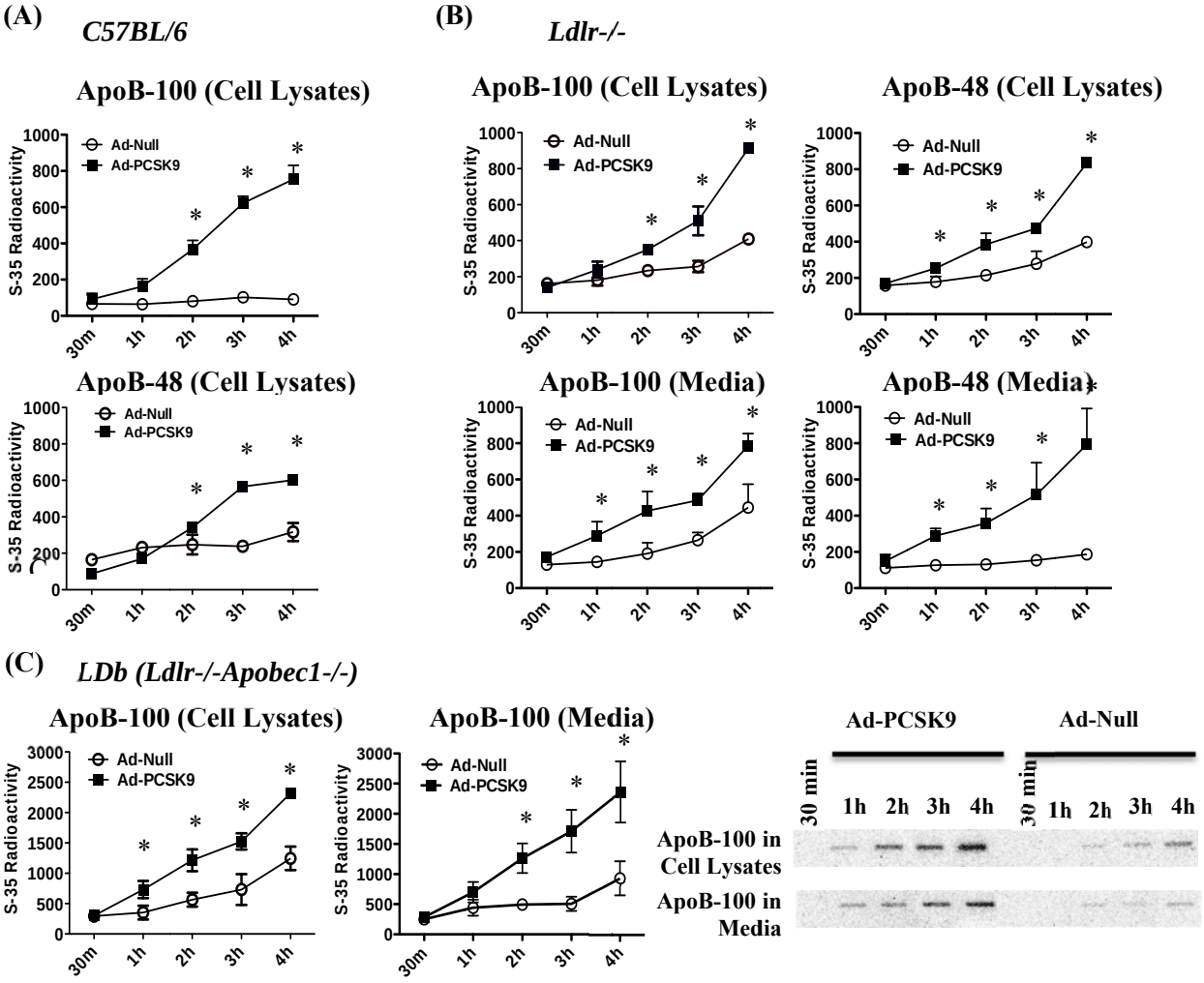
(A)
C57BL/6
ApoB-100 (Cell Lysates)
ApoB-48 (Cell Lysates)
(B)
Ldlr-/-
ApoB-100 (Cell Lysates)
ApoB-48 (Cell Lysates)
ApoB-100 (Media)
ApoB-48 (Media)
(C)
LDb (Ldlr-/-Apobec1-/-)
ApoB-100 (Cell Lysates)
ApoB-100 (Media)
Ad-Null
Ad-PCSK9
S-35 Radioactivity
30m
1h
2h
3h
4h
Ad-PCSK9
Ad-Null
30 min
ApoB-100 in Cell Lysates
ApoB-100 in Media

(D)

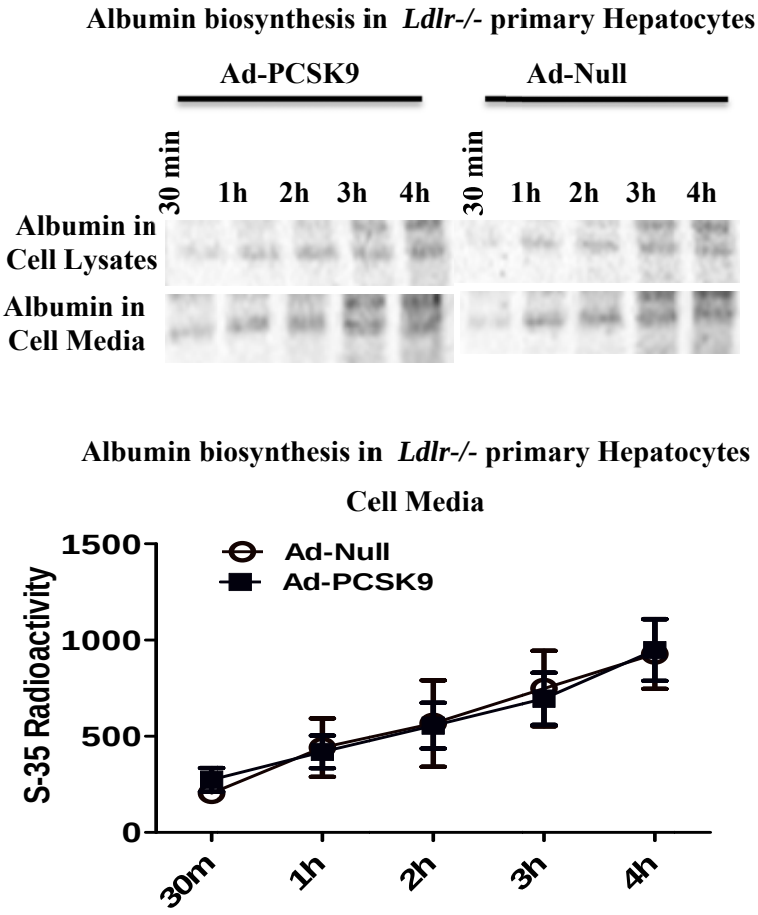

Figure 20. Apolipoprotein B (apoB) biosynthesis is increased in Ad-PCSK9 transduced mouse primary hepatocytes.

Primary hepatocytes were isolated from *C57BL/6* (A), *Ldlr-/-,* and *LDb* (C) mice. Cells were plated onto a 6-well plate coated with mouse type IV collagen, followed by overnight incubation with either Ad-Null or Ad-PCSK9. On the next day, the cells were labeled with ^{35}S-methionine/cysteine (^{35}S-Met/-Cys) for 30 minutes, and chased for 30, 60, 120, 180, and 240 minutes. Cell media and cell lysates were immunoprecipitated with anti-mouse apoB antibody and protein A agarose beads, followed by SDS-PAGE. Albumin (D) were immunoprecipitated with anti-mouse albumin antibody and protein A beads. The bands of apoB100, apoB48, and albumin were scanned by PhosphorImager and quantified using Quantity One software. The results are expressed as total radioactivity of each band (mean ± SD). *$p < 0.05$, comparing the Ad-PCSK9 group to the Ad-Null group. Representative gel images are shown. The experiments were performed 3 times with duplicate samples for each time point.

14. The interaction of PCSK9 and apoB hindered apoB degradation pathway via autophagosome

We next determined whether the interaction of PCSK9/apoB has any effect on intracellular degradation of apoB. The newly synthesized apoB can be degraded either through ubiquitin-mediated proteasomal degradation (82) or by non-proteasomal degradation, the latter of which involves autophagosomes. (109) Autophagosomes are membrane structures that enclose intracellular substrates and deliver them to lysosomes for disposal, a process termed autophagy. (110) The apoB protein has been shown to accumulate in this structure, which is in close proximity to cytosolic lipid droplets. (109) It is suggested that autophagy may represent an alternative pathway for the disposal of apoB. (111) Here, we investigated whether PCSK9 regulates apoB levels via autophagy.

Initially, we did the experiment of the autophagic apoB degradation in McA-RH7777 cell lysates. We transfected McA-RH7777 cells with pcDNA3-PCSK9 vector. At 48 h after transfection, we collected cell lysates and analyzed molecules involved in autophagy pathway including Beclin-1, Atg5, Atg7, LC3-I, and LC3-II by Western blot analysis. As shown in Figure 21A, there was no obvious difference between cells that overexpressed PCSK9 and the control cells. We thought the crude cell lysates might not be a good source for autophagy analysis. We then decided to purify autophagosomes from cells to analyze the effect of PCSK9 on apoB degradation.

We transfected pcDNA-PCSK9 and pcDNA3 into McA-RH7777 cells and we then purified autophagosomes to determine the concentration of apoB and LC3-II in isolated autophagosomes. As shown in Figure 21B, the ratios of apoB-100:LC3-II and apoB-48:LC3-II were significantly lower in cells expressing PCSK9 than in the control cells transfected with pcDNA3 vector. Thus, expression of PCSK9 in McA-RH7777 cells resulted in decreased apoB (apoB-100 and apoB-48) levels in autophagosomes.

To investigate the effect of endogenous PCSK9 on apoB levels, we compared the apoB levels in hepatic autophagosomes isolated from *C57BL/6* and *Pcsk9-/-* mice. As shown in Figure 21C, mice lacking Pcsk9 (Pcsk9-/-) had significantly increased ratio of apoB-100:LC3-II and apoB-48:LC3-II in autophagosomes, compared to *C57BL/6* mice.

Finally, we determined whether the effect of PCSK9 on apoB degradation was dependent upon the LDLR. We compared the effect on autophagosomes from LDb mice and triple knockout mice *LDbPcsk9-/-* (LDb = Ldlr-/-Apobec1-/-Pcsk9+/+ mice and *LDbPcsk9-/-* = Ldlr-/-Apobec1-/-Pcsk9-/- mice). Similar to what was observed in McA-RH7777 cells and *C57BL/6* versus *Pcsk9-/-* mice, the ratio of apoB-100:LC3-II was significantly lower in *LDb* mice (Ldlr-/-Apobec1-/-Pcsk9+/+), compared to that in *LDbPcsk9-/-* triple knockout mice (Ldlr-/-Apobec1-/-Pcsk9-/-) (Figure 21D). Thus, there was less apoB in the autophagosomes in Pcsk9-positive mice (*LDb*), which suggested that decreased amount of apoB was shunted to autophagosomes for degradation. These results together suggest that PCSK9 expression in the mouse liver protects/inhibits apoB from autophagic degradation, and the protection of apoB by PCSK9 is independent of the LDLR.

(A)

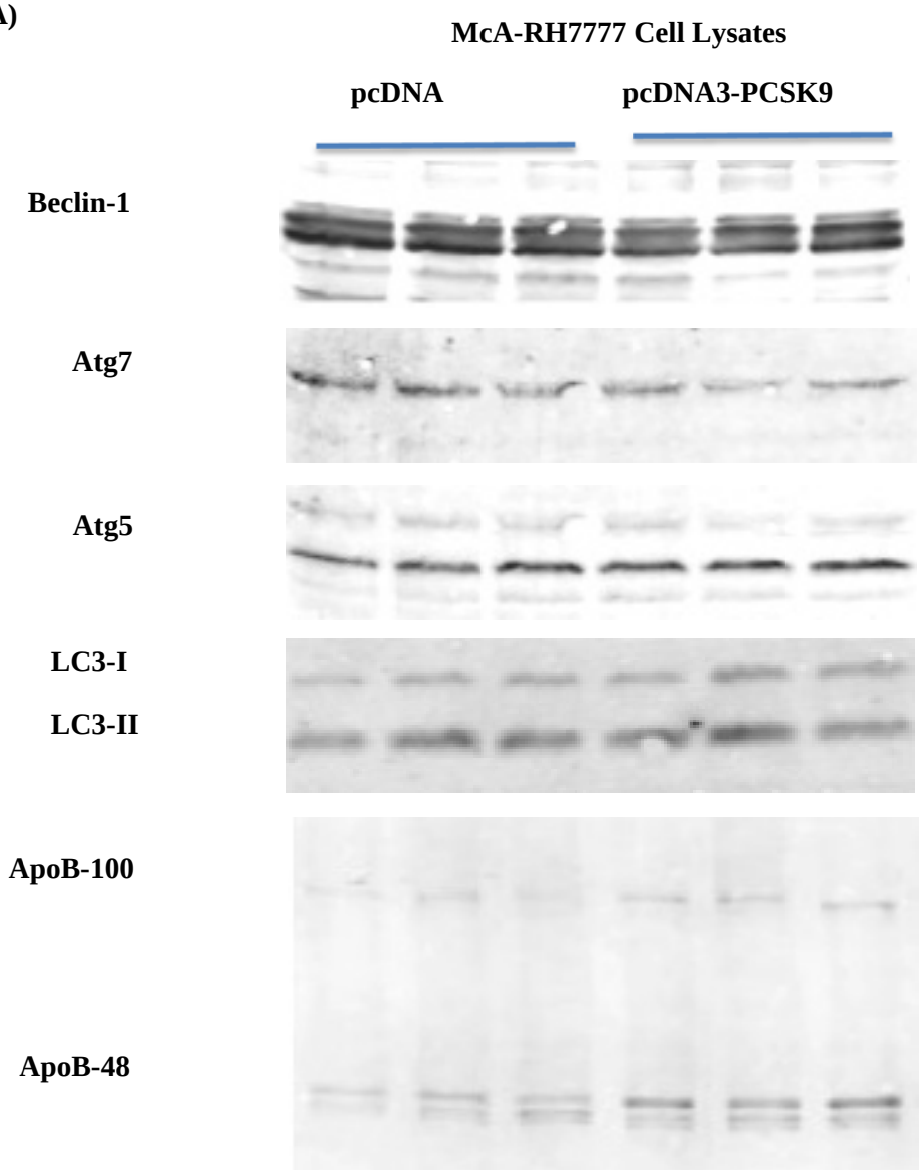
McA-RH7777 Cell Lysates
pcDNA
pcDNA3-PCSK9
Beclin-1
Atg7
Atg5
LC3-I
LC3-II
ApoB-100
ApoB-48

(B)

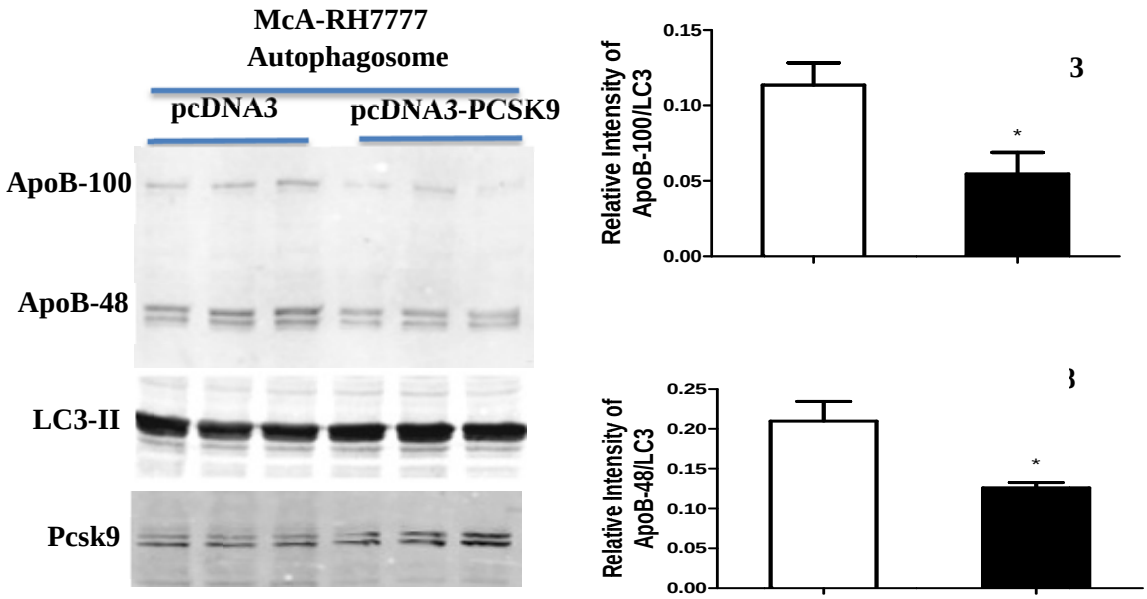
McA-RH7777
Autophagosome
pcDNA3
pcDNA3-PCSK9
ApoB-100
ApoB-48
LC3-II
Pcsk9
Relative Intensity of ApoB-100/LC3
0.15
0.10
0.05
0.00
*
Relative Intensity of ApoB-48/LC3
0.25
0.20
0.15
0.10
0.05
0.00
*

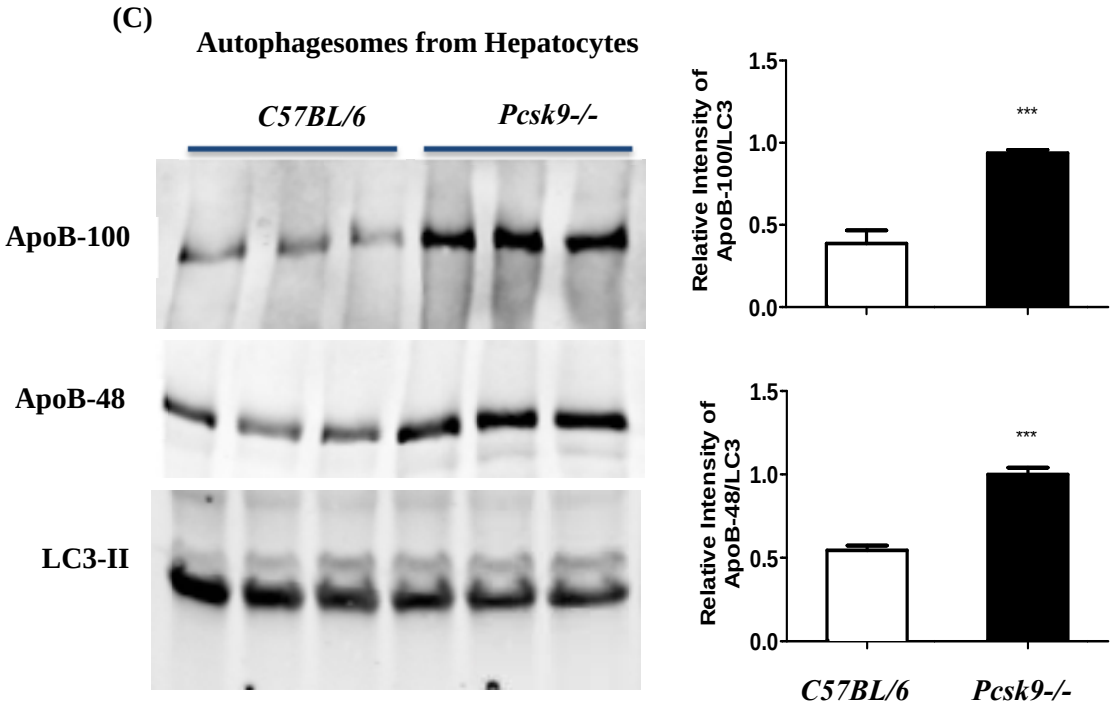
(C)
Autophagesomes from Hepatocytes
C57BL/6
Pcsk9-/-
ApoB-100
ApoB-48
LC3-II
Relative Intensity of ApoB-100/LC3
1.5
1.0
0.5
0.0
***
Relative Intensity of ApoB-48/LC3
1.5
1.0
0.5
0.0
***
C57BL/6
Pcsk9-/-

(D)

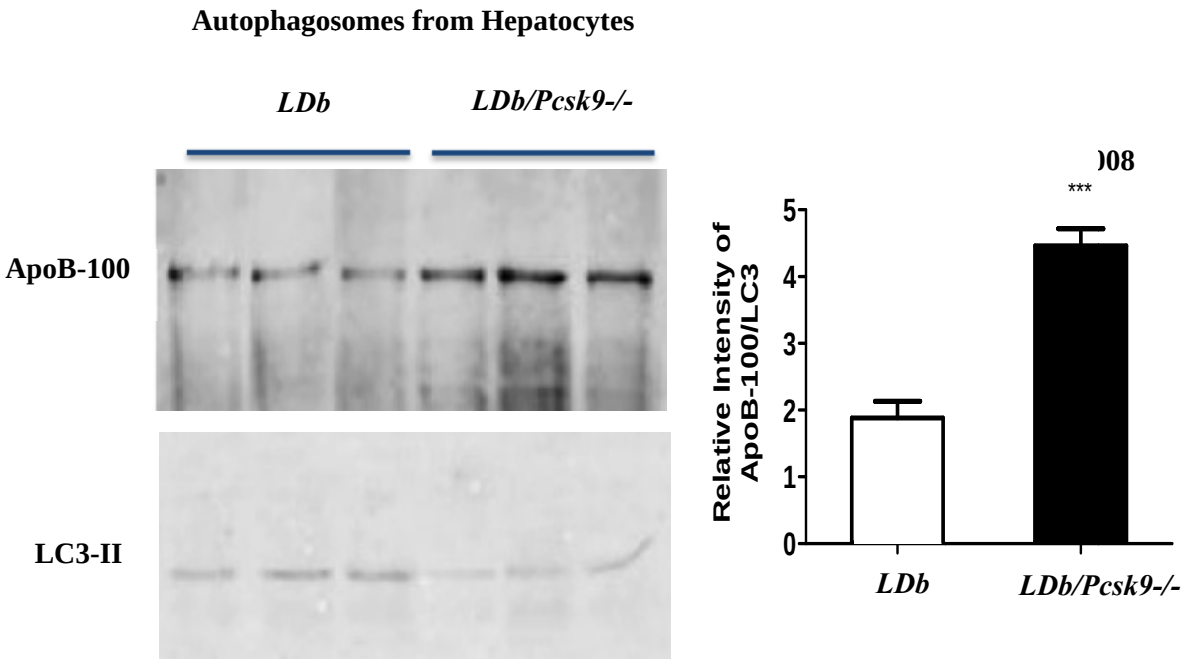

Figure 21. The effects of PCSK9 on autophagosomal apoB.

(A) Overexpressing PCSK9 does not change autophagy process in McARH7777 cells. McARH7777 cells were transfected with pcDNA3 or pcDNA3-PCSK9. Forty-eight hours after transfection, cells were collected and lysed by RIPA buffer. Total 50 μg protein were subjected to SDS-PAGE and then transferred onto PVDF membrane. Autophagy protein Beclin-1, Atg5, Atg7, LC3-I, and II were detected by specific antibodies as well as apoB100 and 48.

(B), PCSK9 expression decreases the levels of apoB100 and apoB48 in hepatic autophagosomes. Autophagosomes were isolated from McA-RH7777 cells transfected with either pcDNA3 vector or pcDNA3-PCSK9 vector.

(C) Hepatic autophagosomes were isolated from *LDb* and *LDbPcsk9−/−* mice.

(D) Hepatic autophagosomes were isolated from *C57BL/6* and *Pcsk9−/−* mice. In B, C, and D, the lysed autophagosomes (30 μg) were subjected to Western blot analysis to detect apoB100, apoB48, PCSK9, and LC3-II. Each protein was detected and quantified using an Odyssey Infrared Imaging System (LICOR, Lincoln, NE). The results are expressed as a ratio of the intensities of apoB100:LC3-II and apoB48:LC3-II and are shown as mean ± SD. $*p < 0.05$ compared with the corresponding samples. The assays were performed 3 times with duplicate samples.

15. *LDbPCSK9-/-* mice have decreased cholesterol, TAG, and apoB levels, compare to LDb mice.

Our study has demonstrated an important new role of PCSK9 that interacts with apoB, which inhibits intracellular degradation of apoB via the autophagosome/lysosome pathway, and this, in turn, results in increased secretion of apoB-containing lipoproteins, leading to increased cholesterol and triglyceride levels. This process is irrespective of the presence of LDLR. To confirm the role of PCSK9 in regulating apoB production, we crossbred *LDb* mice with *Pcsk9-/-* mice to generate a triple knockout mouse model (*Ldlr-/-Apobec1-/-Pcsk9-/-*).

As shown in Figure 22, in comparison of *LDbPcsk9-/-* triple knockout mice with *LDb* mice there was no significance difference in body weight or the lean and fat ratio of these 2 group mice at 4 months of age. Importantly, deleting of the Pcsk9 from LDb mice (*LDbPcsk9-/-*) resulted in significant decrease of plasma cholesterol (decreased 25%), TAG (decreased 33%), and apoB (decreased 38%) levels (Figure 23), when compared to LDb mice. FPLC analysis showed that the levels of cholesterol and triglyceride in VLDL and LDL were markedly decreased (Figure 23). Thus, our results corroborated that PCSK9 is an important molecule that regulates apoB production in the absence of LDL receptor.

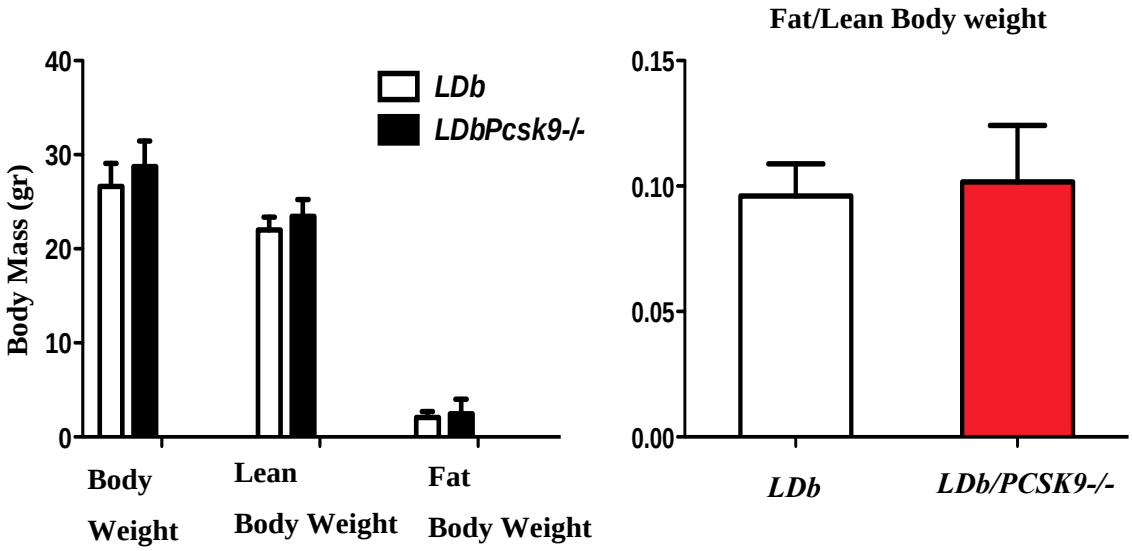

Figure 22. The comparisons of body weight of *LDbPcsk9-/-* triple knockout mice and *LDb* mice.

LDbPcsk9-/- triple knockout mice and *LDb* mice have similar body weight or the lean and fat ratio at 4 months of age. The *LDbPcsk9-/-* and *LDb* were measured for total, fat, and lean body weights by Eco-MIR. The data are presented as mean ± SD. *p* value of <0.05 is considered significant difference.

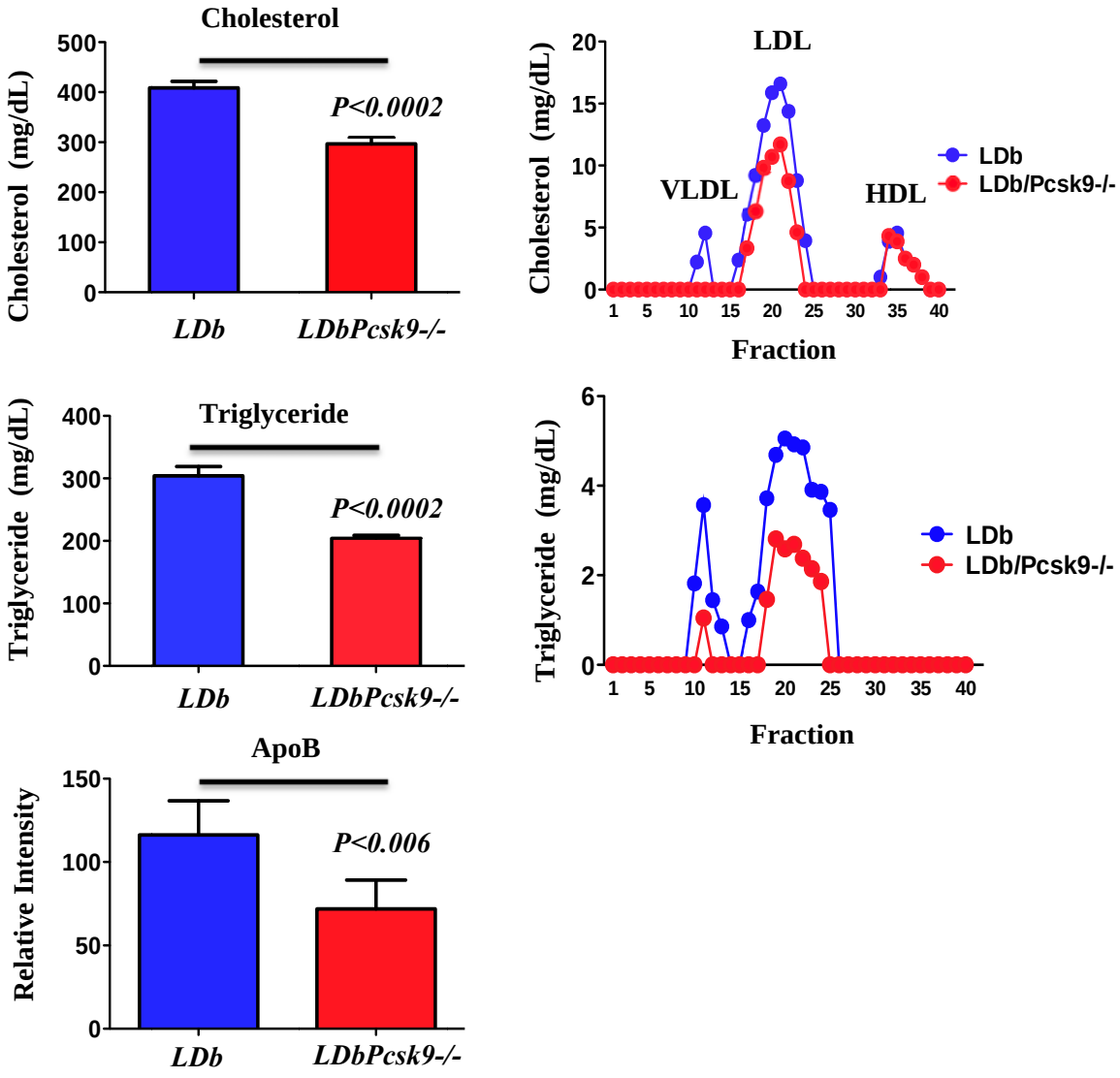

Figure 23. *LDbPCSK9-/-* mice have lower plasma cholesterol and TAG.

LDbPCSK-/- mice were bred and genotyped in our lab. Mice at 3 months old were bled through post-orbital sinus/plexus. The plasmas were subjected to total cholesterol and TAG measurement. The levels of total cholesterol and TAG are presented as mean ± SD. A *p* value of <0.05 is considered significant difference. The plasmas were also fractionated by FPLC as described before. All the fractions were subjected to cholesterol and TAG measurement. The *LDb* mice served as control.

DISCUSSION

The current study demonstrates that long-term overexpression of PCSK9 in mice increases plasma cholesterol, TAG, and apoB levels, irrespective of the presence of the LDLR. PCSK9 interacts with apoB to prevent/inhibit/decrease the mobilization of apoB towards autophagosomes for degradation via autophagosome/lysosome pathway. This, in turn, results in increased production and secretion of apoB and apoB-containing lipoprotein. Significantly, mice deficient of Pcsk9 in the background without the LDLR had lower levels of plasma cholesterol, TAG, and apoB, which indicate PCSK9 regulates apoB production independent of LDLR. Most importantly, our study demonstrates a direct protein–protein interaction of PCSK9 and apoB in cells under physiological conditions. This interaction also exists in the circulation. Taken together, these data established that PCSK9 regulates lipoprotein and apoB metabolism independent of the LDLR. This study provides a new concept that PCSK9 interacts with apoB and regulates apoB degradation, which implicates the therapeutic importance of lower PCSK9 levels to reduce the production/secretion of apoB-containing lipoproteins.

The new role of PCSK9 regulates apoB production, irrespective of LDL receptor

Early investigations in cells (27), mice, (103) and humans (97) have suggested that PCSK9 might play a role in regulating apoB production, but some other studies failed to observe the effects of PCSK9 on apoB production (98, 99). Studies in mice using first-generation adenoviral vector expressing PCSK9 for 3–6 days did not see any significant change in apoB- containing lipoprotein levels, whereas one study extended to 7 days observed the increase of apoB levels in *Ldlr-/-* mice. To circumvent this problem, we used a 2nd generation adenoviral vector system to express PCSK9 in a longer term. This vector can express transgene for more than one month with a very low toxicity (94). Our study demonstrated the long-term gene expression ability of this 2nd generation vector system.

By doing so, we observed a consistent increase of the VLDL and LDL cholesterol levels in wild-type *C57BL/6* mice and LDLR deficient mouse models of *Ldlr-/-* and *LDb* mice. Our result demonstrated that PCSK9 increases the VLDL and LDL levels, independent of LDLR. The most interesting finding is that the TAG and cholesterol levels in VLDL increased more dramatically than those of LDL, which indicated an enhanced VLDL production. So far, enhanced apoB and VLDL productions were only reported in 2 gain-of-function mutations: D374Y and S127R (27, 97). Our results, for the first time, showed that wild-type PCSK9 increases VLDL production, irrespective of LDLR. This finding is further supported by our work that deletion of PCSK9 from LDb mice (*LDb/PCSK9-/-* mice), resulting in decreased plasma levels of apoB, TAG, and cholesterol as well as the decreased levels of VLDL and LDL particles. Thus, our study demonstrated the role of PCSK9 on apoB production is independent of LDLR. *Pcsk-/-* mice have been shown to have a reduction in lymphatic apoB secretion, compared with *Pcsk+/+* mice (93), which suggested PCSK9 affected apoB production in small intestine. Taken together, a new role of PCSK9 in apoB production is defined.

The potential impact of this study

The PCSK9/LDLR interaction is a well-established mechanism, which elucidates how PCSK9 regulates LDL cholesterol levels. Based on this concept, different therapeutics was developed to block the PCSK/LDLR interaction, mainly, in the circulation or on the cell surface of hepatocytes. Recently REGN727, a PCSK9-specific monoclonal antibody product (Regeneron and Sanofi) has been shown to reduce LDL cholesterol ranging from 30% to more than 65% in a 12-week Phase II trial involving 75 patients with heterozygous familial hypercholesterolemia exhibiting elevated LDL-C levels despite of statin therapy (112). Amegen also announced their Phase I clinical study of AMG 145, another PCSK9 monoclonal antibody, in patients with hypercholesterolemia (American College of Cardiology Scientific Session in Chicago; Abstract # 923-4). The study shows

that multiple doses of AMG 145 significantly reduced LDL-C by up to 81% in patients treated with statins versus placebo controls.

With the emerging results of monoclonal antibody clinical trials, the ability of PCSK9 to lower LDL cholesterol in patients not compatible with statin treatment appears very hopeful. However, although monoclonal antibody is shown to be an effective way to blocking the PCSK9/LDLR interaction to lower LDL cholesterol, antibody regiment is very costly for a long-term usage. In our study, we demonstrated a new role of how PCSK9 regulates apoB production, thus, new therapeutic strategies targeting at both intra- and extracellular PCSK9 levels are warranted.

The proposed mechanism of PCSK9/apoB interaction

Zhang et al. (23) have demonstrated that PCSK9 selectively interacts with the EGF-A repeat of the LDLR (and not with other members of the LDLR family) in a calcium-dependent manner. Moreover, they have shown that the PCSK9-mediated degradation of the LDLR requires the ligand-binding domain and the β-propeller domain of LDLR and the prodomain, the catalytic domain, and the C-terminal domain of PCSK9 for PCSK9-mediated degradation of the LDLR.

In our study, we showed that there is a direct protein–protein interaction between PCSK9 and apoB. We have shown that PCSK9 interacts with apoB-18 (18% of N-terminal of apoB), but we did not know the minimal sequences requirement of apoB that is needed to interact with PCSK9. Moreover, apoB is a 550,000 Da protein, it contains a lipid-binding domain, a RNA editing region, and a LDL receptor binding domain; we wondered whether any of these regions was required for the interaction of apoB with PCSK9. We are setting up experiments to delineate these questions.

It was reported that the half-life of recombinant human PCSK9 in the circulation was 5 min (17). This raises the question whether the PCSK9 that was associated with LDL might have a longer half-life; or the PCSK9/LDL complex would have the same half-life as LDL, which is 3 days under normal physiological conditions, or, whether the PCSK9/LDL complex might bind to LDLR more

efficiently than free PCSK9. These are important questions to elucidate the function of PCSK9. We have shown that a substantial amount of PCSK9 (30–40%) was associated with LDL, and this PCSK9 could interact with apoB. Thus, PCSK9 could block the apoB-binding domain for LDLR, which leads to a consequence that PCSK9/LDL complex would not be able to bind to LDLR via apoB binding sites. All these questions will be our future study to delineate the structure/function relationship of PCSK9 and apoB.

In our study, we proposed that the impact of the interaction of PCSK9 with apoB was to inhibit the degradation of apoB via autophagosome/lysosome pathway, and this, in turn, results in increased secretion of apoB-containing lipoproteins to the circulation. We provided the evidence that animals or cells containing PCSK9 have less apoB in the autophagosomes, compared with those deficient of PCSK9. However, we did not propose a detailed mechanism on how the interaction of these 2 proteins might regulate autophagy, or whether this interaction would regulate autophagy process at all in the hepatocytes.

It is known that PI3 kinase type I and III, which help recruit autophagic proteins, initiates the autophagy process (113). Several autophagy-related genes (Atg) that are evolutionarily conserved mediate the elongation process to start the autophagosomes process. The Atg genes recruit microtubule light chain-3 (LC3) to form the mature autophagosome. LC3 undergoes proteolytic cleavage and lipidation to yield LC3-II, this is the protein that associates with autophagic membrane and represents the mature autophagosomes. At this stage, the outer membrane of the autophagosomes fuses with a lysosome to form autophagolysosome. Lysosomal contents subsequently degrade the cytosolic components inside the autophagosomes (114).

PI3 kinase type I is activated by growth factors such as insulin and inhibits autophagy through PDK1 and AKT, which regulates mammalian target of rapamycin (mTOR) (115). It is suggested that active PI3K/mTOR maintains autophagy at basal lower levels. It is still unclear how activation of mTOR inhibits autophagy, but the mechanism may involve phosphorylation of Atg13,

which is part of a protein complex with Atg1, a serine/threonine kinase (116). mTOR governs many downstream signaling pathways. Here, we propose that when mTOR was activated, it activated PKC δ, which activated HNF1alpha, SREBP2, and the production of PCSK9. The increased production of PCSK9 interacts with apoB to inhibit the degradation of apoB via autophagosome. At the same time, the activation of mTOR suppresses the autophagy. Thus, the activation of mTOR results in increased production of PCSK9 and decreased autophagy activity. This signaling pathway is a potential mechanism involving PCSK9, apoB, and autophagy (Figure D-1) in the hepatocytes.

PI3 kinase type III, which includes Atg6 in its complex, promotes the nucleation of autophagic vesicles (117). Expansion of autophagic vesicles or the elongation of autophagosome is mediated by 2 ubiquitin-like conjugation systems: (1) the Atg12 pathway involves Atg12 (ubiquitin-like), Atg7 (E1-like), Atg10 (E2-like), and Atg5. (2) The Atg8 pathway involves Atg8 (ubiquitin-like), Atg7 (E1-like), Atg3 (E2-like), and Atg5. In the Atg12 pathway, Atg12 is conjugated to Atg5, while in the Atg8 pathway, Atg8 is conjugated to phosphatidylethanolamine (118).

Autophagy is a dynamic process in biological and pathological process. Recent work by Razani et al. (119) demonstrated increased levels of p62 in atherosclerotic lesions, which suggested a dysfunctional autophagy process is associated with atherosclerosis development. Oxidized-LDL has been shown to be removed through autophagosome/lysosome pathway in human vascular endothelial cells (119). Also, engulfed LDL may be broken down in activated macrophages via the autophagy process (120). Thus, there are a lot of examples implicating autophagy with the atherosclerosis process. In our preliminary results, we detected PCSK9 in the atherosclerotic plaque in LDb mice. It would be interesting to determine whether the association of PCSK9 with LDL via apoB would inhibit the uptake of LDL via macrophages and in turn, hinder the removal of lipids via autophagy-mediated efflux process. Our study, thus, has raised many unexpected questions related to PCSK9/apoB/LDL, which remain to be answered.

The ubiquitin proteasome pathway also plays a role in the quality control of apoB production. (121) The translated apoB is accompanied by the process of lipidation. If the lipidation does not perform well, nascent apoB cannot fold properly. Therefore, poorly lipidated and misfolded apoB will be detected by specialized factors within the ER and delivered to a ubiquitination machinery for degradation. This process is proteasomal apoB degradation pathway (121). Although the detailed mechanism remains to be defined, it is suggested that many chaperon molecules such as HSP70, 90, BiP/GRP78, GRP94, and ERp57 participate in this process (87, 88). In our study, we could not exclude the possibility that the interaction between PCSK9 and apoB might inhibit the ubiquitin-proteasome degradation system. Further study will be needed to distinguish the influence of the interaction of PCSK9 with apoB on both of the apoB degradation pathways.

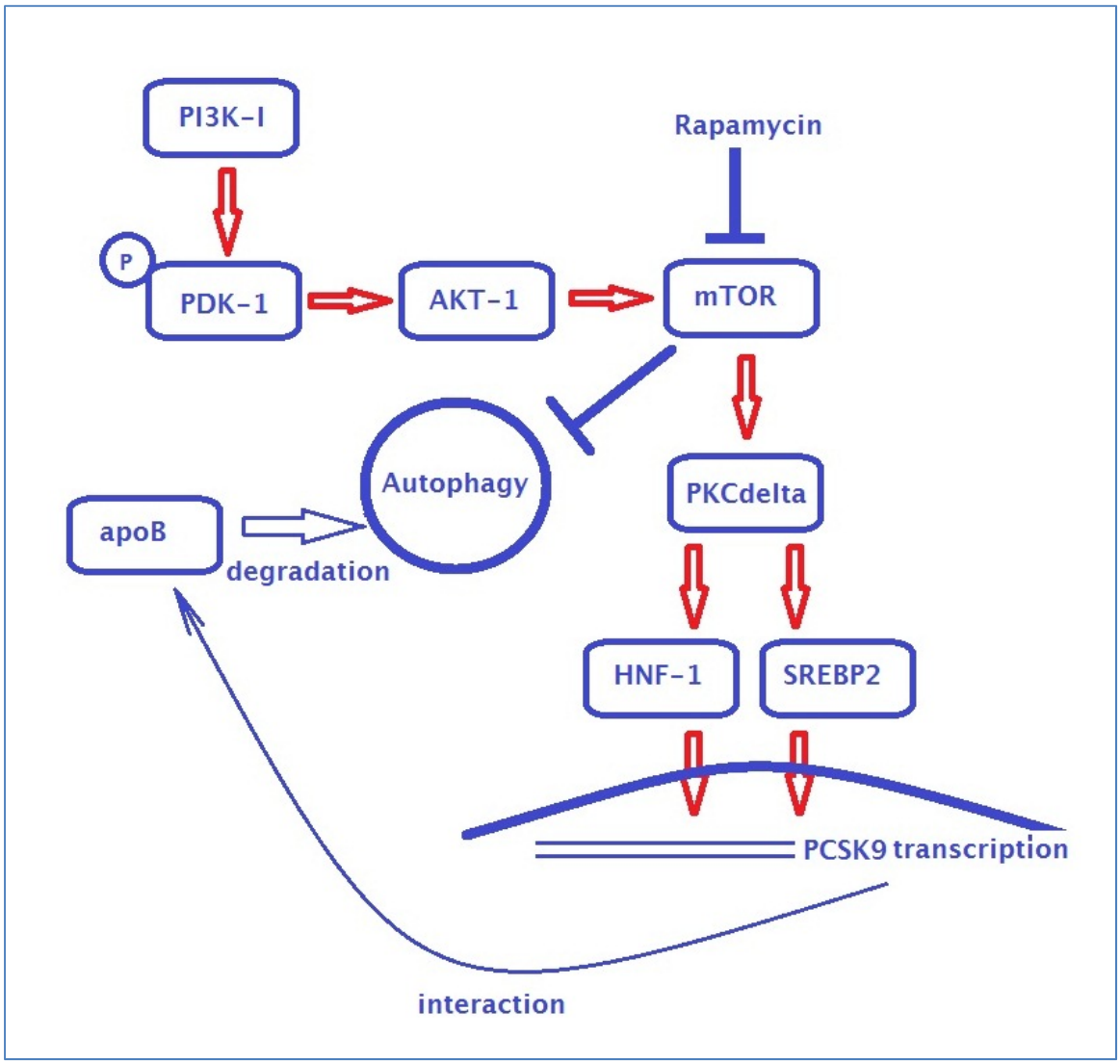

Figure D-1. The proposed signaling pathway involving PCSK9 and apoB interaction. After being activated by growth factor such as VEGF or insulin, PI3 kinase activates PDK-1, which then activates its downstream signaling molecule AKT-1. AKT-1 activates mTOR, the key molecule that inhibits autophagy. mTOR activates two important transcriptional factors, HNF-1 and SREBP2. Both of these two transcriptional factors can up-regulate PCSK9 transcription. Increased PCSK9 interacts with apoB and inhibits its degradation through autophagy, which has been inhibited by activated mTOR. The overall outcome of this pathway is increased hepatic apoB production.

The role of PCSK9/apoB/LDLR: a proposed model.

The mechanism that PCSK9 binds to LDLR and leads it to degradation has been well established. Here, we have demonstrated an important mechanism that PCSK9 interacts with apoB, and the consequence of this interaction leads to decreased degradation of apoB via the autophagosome/lysosome pathway. Thus, PCSK9 is a molecule that shuttles between apoB and LDLR. PCSK9 is the main regulator of apoB and LDLR production.

In summary, the study provides evidence on how overexpressing PCSK9 increased cholesterol, TAG, and apoB levels independent of LDLR. Our study also opens up a proposed mechanism of how PCSK9 might regulate the autophagy process in lipid metabolism. Taken together, our results suggest that decreasing intracellular PCSK9 levels may be a promising therapeutic approach to regulate the production of atherogenic apoB-containing lipoproteins and thus prevent the development of atherosclerosis.

5. The future study.

Based on our findings, many questions have been proposed.

5.1. The structure/functional relationship of PCSK9 and apoB.

ApoB: To determine the minimal length of apoB that is required to interact with PCSK9. We will use the mammalian two-hybrid system to investigate this minimal apoB length requirement for the interaction of PCSK9 with apoB. We will also construct clones deficient of apoB lipid binding domain, editing region, or LDL receptor binding domain to study if any of this domain is required for the interaction.

PCSK9: We will make gain-of-function mutations such as D374Y and S127R and loss-of-function mutations such as Y142L to investigate whether these mutations have influence on the interaction of PCSK9 with apoB.

5.2. To investigate the effect of PCSK9 on atherogenesis.

As described before, we have generated a triple knockout mouse model (Ldlr-/-Apobec1-/-Pcsk9-/-). Based on this mouse model, we will delineate the influence of PCSK9 on atherogenesis. The mechanism in atherogenesis may be different from that in the hepatocytes.

5.3. To delineate the molecular mechanism of the regulation of PCSK9 on apoB production in the liver.

As discussed above, we proposed a signaling pathway indicating mTOR inhibits autophagy process and activates PCSK9 transcription. We will proceed step by step to approve or disapprove of the pathway to understand the interrelationship of PCSK9, apoB, and autophagy. We will investigate

whether hyperlipidemia regulates the upstream signaling of mTOR. Moreover, we will delineate whether ubiquitin-proteasome pathway play a role in the regulation of PCSK9 on apoB production.

5.4. To define the miRNAs that regulate PCSK9.

PCSK9 plays an important function in lipoprotein metabolism. It also plays a role in atherogenesis, since I have detected PCSK9 in atherosclerotic plaques. I have identified hsa-miR-601 and hsa-miR-632 miRNAs that targeted PCSK9 to elucidate the mechanism of how miRNAs regulate PCSK9.

5.5. To develop therapeutics to decrease PCSK9 levels.

5.5.1 To block the interaction between PCSK9 and LDLR:

Our laboratory is using a novel disulfide scrambling technique to generate vaccine to block the interaction between PCSK9 and LDLR.

5.5.2 To design siRNA to inhibit the production of PCSK9:

We have designed a couple of siRNAs targeted at human and mouse PCSK9 mRNA. PCSK9-specific siRNA would decrease the production of PCSK9 intracellularly.

5.5.3. To design RNA or DNA specific aptamer to target at PCSK9 to block the interaction of PCSK9 and apoB: T

This strategy would be a better approach than using small molecules to block the protein–protein interaction.

Finally, with the understanding of how PCSK9 regulates apoB, new PCSK9 intracellular inhibitory strategies appear more promising. Intracellular inhibition of PCSK9 by siRNA, anti-sense RNA,

intracellular antibodies, and kinase inhibitors can achieve this goal more efficiently than by only inhibiting free PCSK9 in the circulation. With the rapid development in the cancer therapy area, more and more safe and effective kinase inhibitors have entered the clinical trials. It is possible one of the current kinase inhibitors will have a very bright and promising future in lower PCSK9 levels.

REFERENCES

1. Davignon, J., Dubuc, G., and Seidah, N.G. 2010. The influence of PCSK9 polymorphisms on serum low-density lipoprotein cholesterol and risk of atherosclerosis. *Curr Atheroscler Rep* 12:308-315.
2. Seidah, N.G., Benjannet, S., Wickham, L., Marcinkiewicz, J., Jasmin, S.B., Stifani, S., Basak, A., Prat, A., and Chretien, M. 2003. The secretory proprotein convertase neural apoptosis-regulated convertase 1 (NARC-1): liver regeneration and neuronal differentiation. *Proc Natl Acad Sci U S A* 100:928-933.
3. Varret, M., Rabes, J.P., Saint-Jore, B., Cenarro, A., Marinoni, J.C., Civeira, F., Devillers, M., Krempf, M., Coulon, M., Thiart, R., et al. 1999. A third major locus for autosomal dominant hypercholesterolemia maps to 1p34.1-p32. *Am J Hum Genet* 64:1378-1387.
4. Abifadel, M., Varret, M., Rabes, J.P., Allard, D., Ouguerram, K., Devillers, M., Cruaud, C., Benjannet, S., Wickham, L., Erlich, D., et al. 2003. Mutations in PCSK9 cause autosomal dominant hypercholesterolemia. *Nat Genet* 34:154-156.
5. Timms, K.M., Wagner, S., Samuels, M.E., Forbey, K., Goldfine, H., Jammulapati, S., Skolnick, M.H., Hopkins, P.N., Hunt, S.C., and Shattuck, D.M. 2004. A mutation in PCSK9 causing autosomal-dominant hypercholesterolemia in a Utah pedigree. *Hum Genet* 114:349-353.
6. Abifadel, M., Rabes, J.P., Devillers, M., Munnich, A., Erlich, D., Junien, C., Varret, M., and Boileau, C. 2009. Mutations and polymorphisms in the proprotein convertase subtilisin kexin 9 (PCSK9) gene in cholesterol metabolism and disease. *Hum Mutat* 30:520-529.
7. Leren, T.P. 2004. Mutations in the PCSK9 gene in Norwegian subjects with autosomal dominant hypercholesterolemia. *Clin Genet* 65:419-422.
8. Pisciotta, L., Priore Oliva, C., Cefalu, A.B., Noto, D., Bellocchio, A., Fresa, R., Cantafora, A., Patel, D., Averna, M., Tarugi, P., et al. 2006. Additive effect of mutations in LDLR and

PCSK9 genes on the phenotype of familial hypercholesterolemia. *Atherosclerosis* 186:433-440.

9. Bottomley, M.J., Cirillo, A., Orsatti, L., Ruggeri, L., Fisher, T.S., Santoro, J.C., Cummings, R.T., Cubbon, R.M., Lo Surdo, P., Calzetta, A., et al. 2009. Structural and biochemical characterization of the wild type PCSK9-EGF(AB) complex and natural familial hypercholesterolemia mutants. *J Biol Chem* 284:1313-1323.

10. Cohen, J.C., Boerwinkle, E., Mosley, T.H., Jr., and Hobbs, H.H. 2006. Sequence variations in PCSK9, low LDL, and protection against coronary heart disease. *N Engl J Med* 354:1264-1272.

11. Cohen, J., Pertsemlidis, A., Kotowski, I.K., Graham, R., Garcia, C.K., and Hobbs, H.H. 2005. Low LDL cholesterol in individuals of African descent resulting from frequent nonsense mutations in PCSK9. *Nat Genet* 37:161-165.

12. Hooper, A.J., Marais, A.D., Tanyanyiwa, D.M., and Burnett, J.R. 2007. The C679X mutation in PCSK9 is present and lowers blood cholesterol in a Southern African population. *Atherosclerosis* 193:445-448.

13. Kotowski, I.K., Pertsemlidis, A., Luke, A., Cooper, R.S., Vega, G.L., Cohen, J.C., and Hobbs, H.H. 2006. A spectrum of PCSK9 alleles contributes to plasma levels of low-density lipoprotein cholesterol. *Am J Hum Genet* 78:410-422.

14. Tibolla, G., Norata, G.D., Artali, R., Meneghetti, F., and Catapano, A.L. 2011. Proprotein convertase subtilisin/kexin type 9 (PCSK9): from structure-function relation to therapeutic inhibition. *Nutr Metab Cardiovasc Dis* 21:835-843.

15. Maxwell, K.N., and Breslow, J.L. 2004. Adenoviral-mediated expression of Pcsk9 in mice results in a low-density lipoprotein receptor knockout phenotype. *Proc Natl Acad Sci U S A* 101:7100-7105.

16. Lagace, T.A., Curtis, D.E., Garuti, R., McNutt, M.C., Park, S.W., Prather, H.B., Anderson, N.N., Ho, Y.K., Hammer, R.E., and Horton, J.D. 2006. Secreted PCSK9 decreases the

number of LDL receptors in hepatocytes and in livers of parabiotic mice. *J Clin Invest* 116:2995-3005.

17. Grefhorst, A., McNutt, M.C., Lagace, T.A., and Horton, J.D. 2008. Plasma PCSK9 preferentially reduces liver LDL receptors in mice. *J Lipid Res* 49:1303-1311.

18. Schmidt, R.J., Beyer, T.P., Bensch, W.R., Qian, Y.W., Lin, A., Kowala, M., Alborn, W.E., Konrad, R.J., and Cao, G. 2008. Secreted proprotein convertase subtilisin/kexin type 9 reduces both hepatic and extrahepatic low-density lipoprotein receptors in vivo. *Biochem Biophys Res Commun* 370:634-640.

19. Rashid, S., Curtis, D.E., Garuti, R., Anderson, N.N., Bashmakov, Y., Ho, Y.K., Hammer, R.E., Moon, Y.A., and Horton, J.D. 2005. Decreased plasma cholesterol and hypersensitivity to statins in mice lacking Pcsk9. *Proc Natl Acad Sci U S A* 102:5374-5379.

20. Benjannet, S., Rhainds, D., Essalmani, R., Mayne, J., Wickham, L., Jin, W., Asselin, M.C., Hamelin, J., Varret, M., Allard, D., et al. 2004. NARC-1/PCSK9 and its natural mutants: zymogen cleavage and effects on the low density lipoprotein (LDL) receptor and LDL cholesterol. *J Biol Chem* 279:48865-48875.

21. Cunningham, D., Danley, D.E., Geoghegan, K.F., Griffor, M.C., Hawkins, J.L., Subashi, T.A., Varghese, A.H., Ammirati, M.J., Culp, J.S., Hoth, L.R., et al. 2007. Structural and biophysical studies of PCSK9 and its mutants linked to familial hypercholesterolemia. *Nat Struct Mol Biol* 14:413-419.

22. Zhang, D.W., Lagace, T.A., Garuti, R., Zhao, Z., McDonald, M., Horton, J.D., Cohen, J.C., and Hobbs, H.H. 2007. Binding of proprotein convertase subtilisin/kexin type 9 to epidermal growth factor-like repeat A of low density lipoprotein receptor decreases receptor recycling and increases degradation. *J Biol Chem* 282:18602-18612.

23. Zhang, D.W., Garuti, R., Tang, W.J., Cohen, J.C., and Hobbs, H.H. 2008. Structural requirements for PCSK9-mediated degradation of the low-density lipoprotein receptor. *Proc Natl Acad Sci U S A* 105:13045-13050.

24. Piper, D.E., Jackson, S., Liu, Q., Romanow, W.G., Shetterly, S., Thibault, S.T., Shan, B., and Walker, N.P. 2007. The crystal structure of PCSK9: a regulator of plasma LDL-cholesterol. *Structure* 15:545-552.

25. Horton, J.D., Cohen, J.C., and Hobbs, H.H. 2007. Molecular biology of PCSK9: its role in LDL metabolism. *Trends Biochem Sci* 32:71-77.

26. McNutt, M.C., Lagace, T.A., and Horton, J.D. 2007. Catalytic activity is not required for secreted PCSK9 to reduce low density lipoprotein receptors in HepG2 cells. *J Biol Chem* 282:20799-20803.

27. Sun, X.M., Eden, E.R., Tosi, I., Neuwirth, C.K., Wile, D., Naoumova, R.P., and Soutar, A.K. 2005. Evidence for effect of mutant PCSK9 on apolipoprotein B secretion as the cause of unusually severe dominant hypercholesterolaemia. *Hum Mol Genet* 14:1161-1169.

28. Nassoury, N., Blasiole, D.A., Tebon Oler, A., Benjannet, S., Hamelin, J., Poupon, V., McPherson, P.S., Attie, A.D., Prat, A., and Seidah, N.G. 2007. The cellular trafficking of the secretory proprotein convertase PCSK9 and its dependence on the LDLR. *Traffic* 8:718-732.

29. Kwon, H.J., Lagace, T.A., McNutt, M.C., Horton, J.D., and Deisenhofer, J. 2008. Molecular basis for LDL receptor recognition by PCSK9. *Proc Natl Acad Sci U S A* 105:1820-1825.

30. Surdo, P.L., Bottomley, M.J., Calzetta, A., Settembre, E.C., Cirillo, A., Pandit, S., Ni, Y.G., Hubbard, B., Sitlani, A., and Carfi, A. 2011. Mechanistic implications for LDL receptor degradation from the PCSK9/LDLR structure at neutral pH. *EMBO Rep* 12:1300-1305.

31. Dong, B., Wu, M., Li, H., Kraemer, F.B., Adeli, K., Seidah, N.G., Park, S.W., and Liu, J. 2010. Strong induction of PCSK9 gene expression through HNF1alpha and SREBP2: mechanism for the resistance to LDL-cholesterol lowering effect of statins in dyslipidemic hamsters. *J Lipid Res* 51:1486-1495.

32. Horton, J.D., Shah, N.A., Warrington, J.A., Anderson, N.N., Park, S.W., Brown, M.S., and Goldstein, J.L. 2003. Combined analysis of oligonucleotide microarray data from transgenic

and knockout mice identifies direct SREBP target genes. *Proc Natl Acad Sci U S A* 100:12027-12032.

33. Maxwell, K.N., Soccio, R.E., Duncan, E.M., Sehayek, E., and Breslow, J.L. 2003. Novel putative SREBP and LXR target genes identified by microarray analysis in liver of cholesterol-fed mice. *J Lipid Res* 44:2109-2119.

34. Jeong, H.J., Lee, H.S., Kim, K.S., Kim, Y.K., Yoon, D., and Park, S.W. 2008. Sterol-dependent regulation of proprotein convertase subtilisin/kexin type 9 expression by sterol-regulatory element binding protein-2. *J Lipid Res* 49:399-409.

35. Dubuc, G., Chamberland, A., Wassef, H., Davignon, J., Seidah, N.G., Bernier, L., and Prat, A. 2004. Statins upregulate PCSK9, the gene encoding the proprotein convertase neural apoptosis-regulated convertase-1 implicated in familial hypercholesterolemia. *Arterioscler Thromb Vasc Biol* 24:1454-1459.

36. Persson, L., Galman, C., Angelin, B., and Rudling, M. 2009. Importance of proprotein convertase subtilisin/kexin type 9 in the hormonal and dietary regulation of rat liver low-density lipoprotein receptors. *Endocrinology* 150:1140-1146.

37. Cameron, J., Ranheim, T., Kulseth, M.A., Leren, T.P., and Berge, K.E. 2008. Berberine decreases PCSK9 expression in HepG2 cells. *Atherosclerosis* 201:266-273.

38. Naoumova, R.P., Tosi, I., Patel, D., Neuwirth, C., Horswell, S.D., Marais, A.D., van Heyningen, C., and Soutar, A.K. 2005. Severe hypercholesterolemia in four British families with the D374Y mutation in the PCSK9 gene: long-term follow-up and treatment response. *Arterioscler Thromb Vasc Biol* 25:2654-2660.

39. Berge, K.E., Ose, L., and Leren, T.P. 2006. Missense mutations in the PCSK9 gene are associated with hypocholesterolemia and possibly increased response to statin therapy. *Arterioscler Thromb Vasc Biol* 26:1094-1100.

40. Zhao, Z., Tuakli-Wosornu, Y., Lagace, T.A., Kinch, L., Grishin, N.V., Horton, J.D., Cohen, J.C., and Hobbs, H.H. 2006. Molecular characterization of loss-of-function mutations in PCSK9 and identification of a compound heterozygote. *Am J Hum Genet* 79:514-523.

41. Stein, E.A., Mellis, S., Yancopoulos, G.D., Stahl, N., Logan, D., Smith, W.B., Lisbon, E., Gutierrez, M., Webb, C., Wu, R., et al. 2012. Effect of a monoclonal antibody to PCSK9 on LDL cholesterol. *N Engl J Med* 366:1108-1118.

42. Chan, J.C., Piper, D.E., Cao, Q., Liu, D., King, C., Wang, W., Tang, J., Liu, Q., Higbee, J., Xia, Z., et al. 2009. A proprotein convertase subtilisin/kexin type 9 neutralizing antibody reduces serum cholesterol in mice and nonhuman primates. *Proc Natl Acad Sci U S A* 106:9820-9825.

43. Graham, M.J., Lemonidis, K.M., Whipple, C.P., Subramaniam, A., Monia, B.P., Crooke, S.T., and Crooke, R.M. 2007. Antisense inhibition of proprotein convertase subtilisin/kexin type 9 reduces serum LDL in hyperlipidemic mice. *J Lipid Res* 48:763-767.

44. Lindholm, M.W., Elmen, J., Fisker, N., Hansen, H.F., Persson, R., Moller, M.R., Rosenbohm, C., Orum, H., Straarup, E.M., and Koch, T. 2012. PCSK9 LNA Antisense Oligonucleotides Induce Sustained Reduction of LDL Cholesterol in Nonhuman Primates. *Mol Ther* 20:376-381.

45. Frank-Kamenetsky, M., Grefhorst, A., Anderson, N.N., Racie, T.S., Bramlage, B., Akinc, A., Butler, D., Charisse, K., Dorkin, R., Fan, Y., et al. 2008. Therapeutic RNAi targeting PCSK9 acutely lowers plasma cholesterol in rodents and LDL cholesterol in nonhuman primates. *Proc Natl Acad Sci U S A* 105:11915-11920.

46. Goldstein, J.L., and Brown, M.S. 2001. Molecular medicine. The cholesterol quartet. *Science* 292:1310-1312.

47. Yokoyama, S. 2006. ABCA1 and biogenesis of HDL. *J Atheroscler Thromb* 13:1-15.

48. Schmitz, G., Langmann, T., and Heimerl, S. 2001. Role of ABCG1 and other ABCG family members in lipid metabolism. *J Lipid Res* 42:1513-1520.

49. Jiang, X.C. 2002. The effect of phospholipid transfer protein on lipoprotein metabolism and atherosclerosis. *Front Biosci* 7:d1634-1641.

50. Dobiasova, M., and Frohlich, J.J. 1999. Advances in understanding of the role of lecithin cholesterol acyltransferase (LCAT) in cholesterol transport. *Clin Chim Acta* 286:257-271.

51. Barter, P.J., Brewer, H.B., Jr., Chapman, M.J., Hennekens, C.H., Rader, D.J., and Tall, A.R. 2003. Cholesteryl ester transfer protein: a novel target for raising HDL and inhibiting atherosclerosis. *Arterioscler Thromb Vasc Biol* 23:160-167.

52. Kastelein, J.J., van Leuven, S.I., Burgess, L., Evans, G.W., Kuivenhoven, J.A., Barter, P.J., Revkin, J.H., Grobbee, D.E., Riley, W.A., Shear, C.L., et al. 2007. Effect of torcetrapib on carotid atherosclerosis in familial hypercholesterolemia. *N Engl J Med* 356:1620-1630.

53. de Grooth, G.J., Kuivenhoven, J.A., Stalenhoef, A.F., de Graaf, J., Zwinderman, A.H., Posma, J.L., van Tol, A., and Kastelein, J.J. 2002. Efficacy and safety of a novel cholesteryl ester transfer protein inhibitor, JTT-705, in humans: a randomized phase II dose-response study. *Circulation* 105:2159-2165.

54. Ma, P.T., Gil, G., Sudhof, T.C., Bilheimer, D.W., Goldstein, J.L., and Brown, M.S. 1986. Mevinolin, an inhibitor of cholesterol synthesis, induces mRNA for low density lipoprotein receptor in livers of hamsters and rabbits. *Proc Natl Acad Sci U S A* 83:8370-8374.

55. Ma, P.T., Yamamoto, T., Goldstein, J.L., and Brown, M.S. 1986. Increased mRNA for low density lipoprotein receptor in livers of rabbits treated with 17 alpha-ethinyl estradiol. *Proc Natl Acad Sci U S A* 83:792-796.

56. Brunzell, J.D., Davidson, M., Furberg, C.D., Goldberg, R.B., Howard, B.V., Stein, J.H., and Witztum, J.L. 2008. Lipoprotein management in patients with cardiometabolic risk: consensus conference report from the American Diabetes Association and the American College of Cardiology Foundation. *J Am Coll Cardiol* 51:1512-1524.

57. Brown, M.S., and Goldstein, J.L. 1979. Receptor-mediated endocytosis: insights from the lipoprotein receptor system. *Proc Natl Acad Sci U S A* 76:3330-3337.

58. Pullinger, C.R., North, J.D., Teng, B.B., Rifici, V.A., Ronhild de Brito, A.E., and Scott, J. 1989. The apolipoprotein B gene is constitutively expressed in HepG2 cells: regulation of secretion by oleic acid, albumin, and insulin, and measurement of the mRNA half-life. *J Lipid Res* 30:1065-1077.

59. Powell, L.M., Wallis, S.C., Pease, R.J., Edwards, Y.H., Knott, T.J., and Scott, J. 1987. A novel form of tissue-specific RNA processing produces apolipoprotein-B48 in intestine. *Cell* 50:831-840.

60. Teng, B., Burant, C.F., and Davidson, N.O. 1993. Molecular cloning of an apolipoprotein B messenger RNA editing protein. *Science* 260:1816-1819.

61. Dutta, R., Singh, U., Li, T.B., Fornage, M., and Teng, B.B. 2003. Hepatic gene expression profiling reveals perturbed calcium signaling in a mouse model lacking both LDL receptor and Apobec1 genes. *Atherosclerosis* 169:51-62.

62. Mak, S., Sun, H., Acevedo, F., Shimmin, L.C., Zhao, L., Teng, B.B., and Hixson, J.E. 2010. Differential expression of genes in the calcium-signaling pathway underlies lesion development in the LDb mouse model of atherosclerosis. *Atherosclerosis* 213:40-51.

63. Singh, U., Zhong, S., Xiong, M., Li, T.B., Sniderman, A., and Teng, B.B. 2004. Increased plasma non-esterified fatty acids and platelet-activating factor acetylhydrolase are associated with susceptibility to atherosclerosis in mice. *Clin Sci (Lond)* 106:421-432.

64. Hoenig, M.R. 2008. Implications of the obesity epidemic for lipid-lowering therapy: non-HDL cholesterol should replace LDL cholesterol as the primary therapeutic target. *Vasc Health Risk Manag* 4:143-156.

65. Cui, Y., Blumenthal, R.S., Flaws, J.A., Whiteman, M.K., Langenberg, P., Bachorik, P.S., and Bush, T.L. 2001. Non-high-density lipoprotein cholesterol level as a predictor of cardiovascular disease mortality. *Arch Intern Med* 161:1413-1419.

66. Scharnagl, H., Nauck, M., Wieland, H., and Marz, W. 2001. The Friedewald formula underestimates LDL cholesterol at low concentrations. *Clin Chem Lab Med* 39:426-431.

67. Contois, J.H., McConnell, J.P., Sethi, A.A., Csako, G., Devaraj, S., Hoefner, D.M., and Warnick, G.R. 2009. Apolipoprotein B and cardiovascular disease risk: position statement from the AACC Lipoproteins and Vascular Diseases Division Working Group on Best Practices. *Clin Chem* 55:407-419.

68. Lamarche, B., Moorjani, S., Cantin, B., Dagenais, G.R., Lupien, P.J., and Despres, J.P. 1995. [Cardiovascular study in Quebec: importance of apolipoprotein B and insulinemia in the risk evaluation for myocardial ischemia]. *Union Med Can* 124:17-21.

69. van Lennep, J.E., Westerveld, H.T., van Lennep, H.W., Zwinderman, A.H., Erkelens, D.W., and van der Wall, E.E. 2000. Apolipoprotein concentrations during treatment and recurrent coronary artery disease events. *Arterioscler Thromb Vasc Biol* 20:2408-2413.

70. Pischon, T., Girman, C.J., Sacks, F.M., Rifai, N., Stampfer, M.J., and Rimm, E.B. 2005. Non-high-density lipoprotein cholesterol and apolipoprotein B in the prediction of coronary heart disease in men. *Circulation* 112:3375-3383.

71. Gotto, A.M., Jr., Whitney, E., Stein, E.A., Shapiro, D.R., Clearfield, M., Weis, S., Jou, J.Y., Langendorfer, A., Beere, P.A., Watson, D.J., et al. 2000. Relation between baseline and on-treatment lipid parameters and first acute major coronary events in the Air Force/Texas Coronary Atherosclerosis Prevention Study (AFCAPS/TexCAPS). *Circulation* 101:477-484.

72. Pontrelli, L., Sidiropoulos, K.G., and Adeli, K. 2004. Translational control of apolipoprotein B mRNA: regulation via cis elements in the 5' and 3' untranslated regions. *Biochemistry* 43:6734-6744.

73. Sidiropoulos, K.G., Meshkani, R., Avramoglu-Kohen, R., and Adeli, K. 2007. Insulin inhibition of apolipoprotein B mRNA translation is mediated via the PI-3 kinase/mTOR signaling cascade but does not involve internal ribosomal entry site (IRES) initiation. *Arch Biochem Biophys* 465:380-388.

74. Sidiropoulos, K.G., Pontrelli, L., and Adeli, K. 2005. Insulin-mediated suppression of apolipoprotein B mRNA translation requires the 5' UTR and is characterized by decreased

binding of an insulin-sensitive 110-kDa 5' UTR RNA-binding protein. *Biochemistry* 44:12572-12581.

75. Berriot-Varoqueaux, N., Dannoura, A.H., Moreau, A., Verthier, N., Sassolas, A., Cadiot, G., Lachaux, A., Munck, A., Schmitz, J., Aggerbeck, L.P., et al. 2001. Apolipoprotein B48 glycosylation in abetalipoproteinemia and Anderson's disease. *Gastroenterology* 121:1101-1108.

76. Segrest, J.P., Jones, M.K., and Dashti, N. 1999. N-terminal domain of apolipoprotein B has structural homology to lipovitellin and microsomal triglyceride transfer protein: a "lipid pocket" model for self-assembly of apob-containing lipoprotein particles. *J Lipid Res* 40:1401-1416.

77. Hussain, M.M., Bakillah, A., Nayak, N., and Shelness, G.S. 1998. Amino acids 430-570 in apolipoprotein B are critical for its binding to microsomal triglyceride transfer protein. *J Biol Chem* 273:25612-25615.

78. Rava, P., Ojakian, G.K., Shelness, G.S., and Hussain, M.M. 2006. Phospholipid transfer activity of microsomal triacylglycerol transfer protein is sufficient for the assembly and secretion of apolipoprotein B lipoproteins. *J Biol Chem* 281:11019-11027.

79. Borchardt, R.A., and Davis, R.A. 1987. Intrahepatic assembly of very low density lipoproteins. Rate of transport out of the endoplasmic reticulum determines rate of secretion. *J Biol Chem* 262:16394-16402.

80. Bostrom, K., Wettesten, M., Boren, J., Bondjers, G., Wiklund, O., and Olofsson, S.O. 1986. Pulse-chase studies of the synthesis and intracellular transport of apolipoprotein B-100 in Hep G2 cells. *J Biol Chem* 261:13800-13806.

81. Yeung, S.J., Chen, S.H., and Chan, L. 1996. Ubiquitin-proteasome pathway mediates intracellular degradation of apolipoprotein B. *Biochemistry* 35:13843-13848.

82. Fisher, E.A., Zhou, M., Mitchell, D.M., Wu, X., Omura, S., Wang, H., Goldberg, A.L., and Ginsberg, H.N. 1997. The degradation of apolipoprotein B100 is mediated by the ubiquitin-proteasome pathway and involves heat shock protein 70. *J Biol Chem* 272:20427-20434.

83. Gusarova, V., Caplan, A.J., Brodsky, J.L., and Fisher, E.A. 2001. Apoprotein B degradation is promoted by the molecular chaperones hsp90 and hsp70. *J Biol Chem* 276:24891-24900.

84. Oyadomari, S., Yun, C., Fisher, E.A., Kreglinger, N., Kreibich, G., Oyadomari, M., Harding, H.P., Goodman, A.G., Harant, H., Garrison, J.L., et al. 2006. Cotranslocational degradation protects the stressed endoplasmic reticulum from protein overload. *Cell* 126:727-739.

85. Hrizo, S.L., Gusarova, V., Habiel, D.M., Goeckeler, J.L., Fisher, E.A., and Brodsky, J.L. 2007. The Hsp110 molecular chaperone stabilizes apolipoprotein B from endoplasmic reticulum-associated degradation (ERAD). *J Biol Chem* 282:32665-32675.

86. Fisher, E.A., and Williams, K.J. 2008. Autophagy of an oxidized, aggregated protein beyond the ER: a pathway for remarkably late-stage quality control. *Autophagy* 4:721-723.

87. Rutledge, A.C., Su, Q., and Adeli, K. 2010. Apolipoprotein B100 biogenesis: a complex array of intracellular mechanisms regulating folding, stability, and lipoprotein assembly. *Biochem Cell Biol* 88:251-267.

88. Rutledge, A.C., Qiu, W., Zhang, R., Kohen-Avramoglu, R., Nemat-Gorgani, N., and Adeli, K. 2009. Mechanisms targeting apolipoprotein B100 to proteasomal degradation: evidence that degradation is initiated by BiP binding at the N terminus and the formation of a p97 complex at the C terminus. *Arterioscler Thromb Vasc Biol* 29:579-585.

89. Fisher, E.A. 2012. The degradation of apolipoprotein B100: Multiple opportunities to regulate VLDL triglyceride production by different proteolytic pathways. *Biochim Biophys Acta*.

90. Ohsaki, Y., Cheng, J., Fujita, A., Tokumoto, T., and Fujimoto, T. 2006. Cytoplasmic lipid droplets are sites of convergence of proteasomal and autophagic degradation of apolipoprotein B. *Mol Biol Cell* 17:2674-2683.

91. Ohsaki, Y., Cheng, J., Suzuki, M., Fujita, A., and Fujimoto, T. 2008. Lipid droplets are arrested in the ER membrane by tight binding of lipidated apolipoprotein B-100. *J Cell Sci* 121:2415-2422.

92. Qiu, W., Zhang, J., Dekker, M.J., Wang, H., Huang, J., Brumell, J.H., and Adeli, K. 2011. Hepatic autophagy mediates endoplasmic reticulum stress-induced degradation of misfolded apolipoprotein B. *Hepatology* 53:1515-1525.

93. Le May, C., Kourimate, S., Langhi, C., Chetiveaux, M., Jarry, A., Comera, C., Collet, X., Kuipers, F., Krempf, M., Cariou, B., et al. 2009. Proprotein convertase subtilisin kexin type 9 null mice are protected from postprandial triglyceridemia. *Arterioscler Thromb Vasc Biol* 29:684-690.

94. Amalfitano, A., Hauser, M.A., Hu, H., Serra, D., Begy, C.R., and Chamberlain, J.S. 1998. Production and characterization of improved adenovirus vectors with the E1, E2b, and E3 genes deleted. *J Virol* 72:926-933.

95. Teng, B.B., Ochsner, S., Zhang, Q., Soman, K.V., Lau, P.P., and Chan, L. 1999. Mutational analysis of apolipoprotein B mRNA editing enzyme (APOBEC1). structure-function relationships of RNA editing and dimerization. *J Lipid Res* 40:623-635.

96. Sniderman, A.D., and Marcovina, S.M. 2006. Apolipoprotein A1 and B. *Clin Lab Med* 26:733-750.

97. Ouguerram, K., Chetiveaux, M., Zair, Y., Costet, P., Abifadel, M., Varret, M., Boileau, C., Magot, T., and Krempf, M. 2004. Apolipoprotein B100 metabolism in autosomal-dominant hypercholesterolemia related to mutations in PCSK9. *Arterioscler Thromb Vasc Biol* 24:1448-1453.

98. Lalanne, F., Lambert, G., Amar, M.J., Chetiveaux, M., Zair, Y., Jarnoux, A.L., Ouguerram, K., Friburg, J., Seidah, N.G., Brewer, H.B., Jr., et al. 2005. Wild-type PCSK9 inhibits LDL clearance but does not affect apoB-containing lipoprotein production in mouse and cultured cells. *J Lipid Res* 46:1312-1319.

99. Lambert, G., Jarnoux, A.L., Pineau, T., Pape, O., Chetiveaux, M., Laboisse, C., Krempf, M., and Costet, P. 2006. Fasting induces hyperlipidemia in mice overexpressing proprotein convertase subtilisin kexin type 9: lack of modulation of very-low-density lipoprotein hepatic output by the low-density lipoprotein receptor. *Endocrinology* 147:4985-4995.

100. Everett, R.S., Hodges, B.L., Ding, E.Y., Xu, F., Serra, D., and Amalfitano, A. 2003. Liver toxicities typically induced by first-generation adenoviral vectors can be reduced by use of E1, E2b-deleted adenoviral vectors. *Hum Gene Ther* 14:1715-1726.

101. Zaid, A., Roubtsova, A., Essalmani, R., Marcinkiewicz, J., Chamberland, A., Hamelin, J., Tremblay, M., Jacques, H., Jin, W., Davignon, J., et al. 2008. Proprotein convertase subtilisin/kexin type 9 (PCSK9): hepatocyte-specific low-density lipoprotein receptor degradation and critical role in mouse liver regeneration. *Hepatology* 48:646-654.

102. Seiradake, E., Henaff, D., Wodrich, H., Billet, O., Perreau, M., Hippert, C., Mennechet, F., Schoehn, G., Lortat-Jacob, H., Dreja, H., et al. 2009. The cell adhesion molecule "CAR" and sialic acid on human erythrocytes influence adenovirus in vivo biodistribution. *PLoS Pathog* 5:e1000277.

103. Benjannet, S., Rhainds, D., Hamelin, J., Nassoury, N., and Seidah, N.G. 2006. The proprotein convertase (PC) PCSK9 is inactivated by furin and/or PC5/6A: functional consequences of natural mutations and post-translational modifications. *J Biol Chem* 281:30561-30572.

104. Lagace, T.A., Curtis, D.E., Garuti, R., McNutt, M.C., Park, S.W., Prather, H.B., Anderson, N.N., Ho, Y.K., Hammer, R.E., and Horton, J.D. 2006. Secreted PCSK9 decreases the number of LDL receptors in hepatocytes and in livers of parabiotic mice. *The Journal of clinical investigation* 116:2995-3005.

105. Maxwell, K.N., Fisher, E.A., and Breslow, J.L. 2005. Overexpression of PCSK9 accelerates the degradation of the LDLR in a post-endoplasmic reticulum compartment. *Proc Natl Acad Sci U S A* 102:2069-2074.

106. Park, S.W., Moon, Y.A., and Horton, J.D. 2004. Post-transcriptional regulation of low density lipoprotein receptor protein by proprotein convertase subtilisin/kexin type 9a in mouse liver. *J Biol Chem* 279:50630-50638.

107. Teng, B.-B., Song, L.-Z., and Chan, L. 1995. Mutations in the leucine-rich motif in apolipoprotein mRNA editing enzyme catalytic polypeptide 1 eliminate apoB mRNA editing activity. *Circulation Suppl.* 92:I-165.

108. Soderberg, O., Gullberg, M., Jarvius, M., Ridderstrale, K., Leuchowius, K.J., Jarvius, J., Wester, K., Hydbring, P., Bahram, F., Larsson, L.G., et al. 2006. Direct observation of individual endogenous protein complexes in situ by proximity ligation. *Nature methods* 3:995-1000.

109. Ohsaki, Y., Cheng, J., Fujita, A., Tokumoto, T., and Fujimoto, T. 2006. Cytoplasmic lipid droplets are sites of convergence of proteasomal and autophagic degradation of apolipoprotein B. *Molecular biology of the cell* 17:2674-2683.

110. Glick, D., Barth, S., and Macleod, K.F. 2010. Autophagy: cellular and molecular mechanisms. *The Journal of pathology* 221:3-12.

111. Pan, M., Maitin, V., Parathath, S., Andreo, U., Lin, S.X., St Germain, C., Yao, Z., Maxfield, F.R., Williams, K.J., and Fisher, E.A. 2008. Presecretory oxidation, aggregation, and autophagic destruction of apoprotein-B: a pathway for late-stage quality control. *Proceedings of the National Academy of Sciences of the United States of America* 105:5862-5867.

112. Crunkhorn, S. 2012. Trial watch: PCSK9 antibody reduces LDL cholesterol. *Nat Rev Drug Discov* 11:11.

113. Burman, C., and Ktistakis, N.T. 2010. Regulation of autophagy by phosphatidylinositol 3-phosphate. *FEBS Lett* 584:1302-1312.

114. Rabinowitz, J.D., and White, E. 2010. Autophagy and metabolism. *Science* 330:1344-1348.

115. Baehrecke, E.H. 2005. Autophagy: dual roles in life and death? *Nat Rev Mol Cell Biol* 6:505-510.

116. Chang, Y.Y., and Neufeld, T.P. 2010. Autophagy takes flight in Drosophila. *FEBS Lett* 584:1342-1349.

117. Cao, Y., and Klionsky, D.J. 2007. Physiological functions of Atg6/Beclin 1: a unique autophagy-related protein. *Cell Res* 17:839-849.

118. Chen, Y., and Klionsky, D.J. 2011. The regulation of autophagy - unanswered questions. *J Cell Sci* 124:161-170.

119. Razani, B., Feng, C., Coleman, T., Emanuel, R., Wen, H., Hwang, S., Ting, J.P., Virgin, H.W., Kastan, M.B., and Semenkovich, C.F. 2012. Autophagy links inflammasomes to atherosclerotic progression. *Cell Metab* 15:534-544.

120. Ouimet, M., Franklin, V., Mak, E., Liao, X., Tabas, I., and Marcel, Y.L. 2011. Autophagy regulates cholesterol efflux from macrophage foam cells via lysosomal acid lipase. *Cell Metab* 13:655-667.

121. Shelness, G.S., and Ledford, A.S. 2005. Evolution and mechanism of apolipoprotein B-containing lipoprotein assembly. *Curr Opin Lipidol* 16:325-332.

VITA

Hua Sun, the son of Youshou Sun and Qiuyun Hua, was born on March 10th, 1978 in Nanjing, the capital city of Jiangsu Province, People's Republic of China. In 1996, he graduated from Nanjing No. 9 High School in Nanjing. In the fall of that year, he entered Nanjing Medical University. He received the degree of Bachelor of Medicine from Nanjing Medical University in July of 2001. After that he, he received his degree of Master of Science from the same university in 2004. Then, Hua worked as a microbiologist in Nanjing Center for Diseases Control and Prevention for 2 years. In August 2006, Hua entered the University of Texas Health Science Center at Houston, Graduate School of Biomedical Sciences where he conducted her research project in the Brown Foundation of Molecular Medicine, at the University of Texas Health Science Center at Houston.